Defining and Characterizing Mesaverde and Mancos Sandstone Reservoirs Based on Interpretation of Image Logs, Eastern Uinta Basin

by Mark W. Longman and Randy J. Koepsell

OPEN-FILE REPORT 458 September 2005
Utah Geological Survey
a division of
Utah Department of Natural Resources

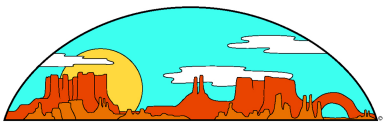

DEFINING AND CHARACTERIZING MESAVERDE AND MANCOS SANDSTONE RESERVOIRS BASED ON INTERPRETATION OF IMAGE LOGS, EASTERN UINTA BASIN, UTAH

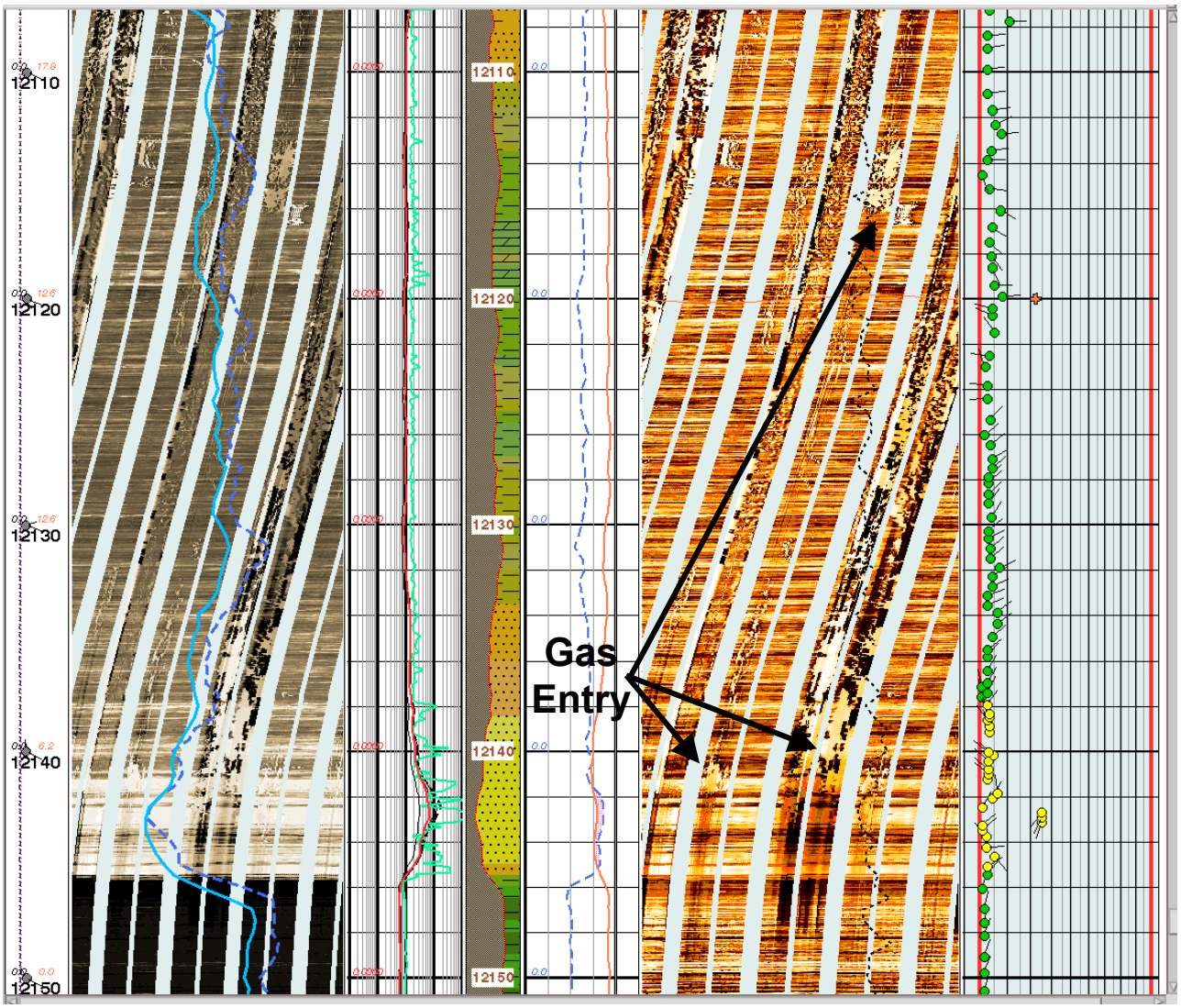

Mark W. Longman
Consulting Geologist
Lakewood, Colorado

Randy J. Koepsell
Schlumberger Oilfield Services
Greenwood Village, Colorado

DEFINING AND CHARACTERIZING MESAVERDE AND MANCOS SANDSTONE RESERVOIRS BASED ON INTERPRETATION OF IMAGE LOGS, EASTERN UINTA BASIN, UTAH

A RESEARCH STUDY
for the
Utah Geological Survey

by

Mark W. Longman and **Randolph J. Koepsell**
Consulting Geologist — Schlumberger Oilfield Services
Lakewood, Colorado — Greenwood Village, Colorado

On the Cover: Portion of an image log across the deepest of three Mancos "B" sandstones in the El Paso Production (now Kerr McGee) #3-181 Pawwinnee well (NW NW Sec. 3, T9S, R21E) showing common entry of gas (bright yellow) into the well bore. The sandstone beds (orangy-yellow) appear to be turbidites with graded bedding (not obvious in this image). Planar beds of shale are visible above and below the sandstone interval, which is about 7 ft thick. The image log indicates that there are no natural fractures in these sandstones, but they were completed for over 2 MMCFGPD after fracture stimulation with 607,000 pounds of sand. The Mancos "B" sandstones produced 343 MMCFG during their first 26 months on production.

May, 2005

Disclaimers

This open-file report was prepared on a contract basis with the author(s) and the Utah Department of Natural Resources, Utah Geological Survey, contract number 51897. The report has not been reviewed for technical quality by professional scientists and is being made available to the public as submitted to the Utah Geological Survey.

This open-file report makes information available to the public, which may not conform to Utah Department of Natural Resources, Utah Geological Survey policy, editorial, or technical standards. Therefore, it may be premature for an individual or group to take action based on its content.

Although this product represents the work of professional scientists, the Utah Department of Natural Resources, Utah Geological Survey, makes no warranty, expressed or implied, regarding its suitability for a particular use. The Utah Department of Natural Resources, Utah Geological Survey, shall not be liable under any circumstances for any direct, indirect, special, incidental, or consequential damages with respect to claims by users of this product.

Defining and Characterizing Mesaverde and Mancos Sandstone Reservoirs Based on Interpretation of Image Logs, Eastern Uinta Basin, Utah

TABLE OF CONTENTS

Defining and Characterizing Mesaverde and Mancos Sandstone Reservoirs Based on Interpretation of Image Logs, Eastern Uinta Basin, Utah

EXECUTIVE SUMMARY

Image logs provide a useful tool for identifying, interpreting, and evaluating Upper Cretaceous Mancos and Mesaverde low-permeability gas reservoirs in the northeast Uinta Basin and elsewhere. These high-resolution logs work by measuring the resistivity at 1/10th inch intervals on each of 192 electrodes distributed on pads circumferentially around the well bore. Data from each electrode is then converted into a micro-resistivity log and merged with the neighboring electrode's logs to create a "picture" of the walls of the well bore. Image logs clearly reveal bedding, sedimentary and tectonic structures, burrowing, and fractures with apertures as small as a few microns.

A primary objective of this study was to use the image logs obtained in 10 wells during the past 5 years across large intervals of the Mesaverde Group in and around Natural Buttes Field to assess the depositional environments and reservoir characteristics of both producing and non-producing sandstones. The ability to continuously quantify changes in sedimentary dip directions and dip angles in sedimentary structures less than an inch thick greatly aids in interpreting sandstone depositional environments and defining paleocurrent flow directions.

The major sandstone depositional environments recognized in this study include fluvial channels ranging in thickness from a few feet to more than 25 ft, splays generally <10 ft thick, braided stream packages up to 100 ft thick with anastomosing small channel sandstones and relatively low shale content (although shale rip-up clasts are locally common), distal, middle, and upper marine shoreface with a variety of bed and burrow types, lagoonal shoreline and washover fans, and relatively deep-water turbidites, which occur locally in the Mancos Shale.

All of the various sandstone facies in the Mesaverde and Mancos produce gas in at least some of the study wells. Overall, the fluvial channel sandstones in the Mesaverde above the Sego Sandstone appear to offer the majority of Cretaceous gas production in the study area, probably due in part to their proximity with and position above the coal source beds in the Lower Mesaverde and their abundance of stratigraphic traps. However, the turbiditic sandstones in the Mancos "B" form good gas reservoirs in the 3-181 Pawwinnee well, and both middle and upper shoreface sandstones in the Blackhawk are prolific reservoirs locally.

In general, the poorest producing sandstones in the Mesaverde are the relatively laterally continuous shoreline sandstones of the upper Castlegate and upper Sego, and the Braided Stream Interval in the Middle Mesaverde. These sandstones are generally water bearing, apparently because they lack adequate lateral seals to trap gas. However, some braided stream sandstones do produce gas locally, particularly in the Upper Mesaverde Interval.

Based on interpretation of vector plots, the image logs support previous interpretations that the shoreline during deposition of the regressive Sego Sandstone was oriented generally north-south, but they reveal that there were embayments and lagoons that created a complex depositional package. They also show that the major flow direction for the rivers and braided streams in the Middle and Upper Mesaverde was generally eastward, although again with common exceptions.

Image logs are excellent at revealing open and healed natural fractures. Because image logs are directionally oriented, the strike of these fractures is easily determined along with the dip direction and amount. Image logs also reveal wellbore breakout, which is generally oriented perpendicular to the natural fractures and can be used to confirm the directions that artificially induced fractures will follow. The similar orientation of the natural and induced fractures confirms that the far field stress of the past is identical to the orientation today. Most of the natural fractures in the Mesaverde in the study wells are oriented about N80˚W and dip at >70˚, although exceptions occur locally in some intervals. Image logs can define fractures with apertures as small as a few microns, and total fracture porosity over specific intervals can be quantified by measuring the length, orientation, and apertures of the fractures. In general, natural fractures play a decreasingly important role in production upward through the Mesaverde.

One of the most interesting aspects of image logs is that they can reveal sites of gas entry into the well bore, particularly if the well is logged underbalanced with a mud weight less than reservoir pressure. About half the image logs used in this study reveal sandstones that yielded good gas entry into the well bore. These images reveal that gas generally does not enter the well bore uniformly from all sides, even in the most porous sandstones, but only from a few points around the well bore. They also reveal surprising amounts of gas entry from shale facies, particularly in the Mancos Shale and shales associated with coals in the Lower Mesaverde. Somewhat surprising is that less than 10% of the natural fractures seen on the image logs have associated gas entry, although this may be partly because strong gas entry can conceal the natural fractures.

An unusually diffuse and weak type of gas entry on the image logs, herein referred to as “regurgitated gas,” can be seen coming out of wet, underpressured, low-resistivity sandstones that have been invaded by drilling mud and natural gas derived from deeper reservoir zones. This “regurgitated gas” could fool a novice interpreter into believing there are gas reservoirs where none exist.

Finally, image logs run across the unconformity at the top of the Mesaverde where it lies in contact with the Paleocene to Eocene Wasatch shales reveal no evidence of an angular unconformity. Considering that the whole Laramide Orogeny occurred during the unconformity between these two formations, the absence of any angular discordance is enigmatic. However, a slightly irregular, probably erosional surface with possible calcified roots is present locally at the top of the Mesaverde along with a dolomitic caliche cap.

Defining and Characterizing Mesaverde and Mancos Sandstone Reservoirs Based on Interpretation of Image Logs, Eastern Uinta Basin, Utah

INTRODUCTION

The Upper Cretaceous Mesaverde Group and underlying Mancos Shale in the eastern Uinta Basin consist of more than 4000 ft of interbedded sandstones, siltstones, shales, and coals. Sandstones in these intervals have become a major exploration target for gas over the past decade. The productive sandstones range in thickness from 3 ft to more than 50 ft and occur at depths of 6,000 to 13,000 ft. They were deposited in a variety of environments including marine upper and lower shoreface, washover fans, fluvial channels and point bars, splays, and braided streams. Reservoir quality of the sandstones is strongly influenced by the environment of deposition. Furthermore, certain facies, particularly the widespread upper shoreface sandstones of the Sego, tend to be wet through most of the study area, in part because they lack adequate lateral seals.

This study was undertaken to identify and interpret gas-bearing sandstones in the Mesaverde and Mancos intervals with a special emphasis on using image logs. Three companies (Questar, Kerr McGee, and EOG Resources) provided a database with access to 10 Formation MicroImager logs (aka FMI® logs; FMI is a registered trademark of Schlumberger Logging Services) run through thick sections of the Mesaverde Group in the area of Natural Buttes Field centered on T9S, R23E, Uintah County, Utah. Characteristics of this field have been discussed by Osmond (1992). Data on thickness, porosity, and depositional features of each sandstone interval were compiled in spreadsheets for each of the study wells. The image logs for each sandstone more than about 4 ft thick were captured in digital form including dip azimuth correlation "vector plots" through the interval. Approximately 400 of these images and vector captures provide the main source of data for defining characteristics of each major type of reservoir sandstone. The digital images are included on a CD's for each well enclosed as Appendix 1 at the end of this report.

Image logs are particularly useful for characterizing sandstone reservoirs for a variety of reasons including their ability to display sedimentary structures such as planar bedding, trough crossbeds, bioturbation, root traces, soft-sediment deformation features, bed boundaries including basal erosional scour contacts, and shale rip-up clasts. In the low-permeability sandstones that form the Mesaverde and Mancos gas reservoirs, image logs clearly reveal natural fractures with apertures as small as a few microns. Furthermore, because an image log is a directionally oriented logging tool, the orientation, abundance, and dip of the fractures can be quantified. Although the focus of this study is on the use of image logs to define and characterize the depositional facies of the reservoir sandstones in the Mesaverde and Mancos, a portion of the report discusses the distribution and orientation of natural fractures in the study wells.

Image logs can also provide direct indications of gas seeping into the well bore, particularly if they are run when the mud weight in the well is sufficiently low to allow gas entry. Sites of gas entry include fractures, permeable sandstones, shales, and coals, and are more diverse than one might expect looking at standard wireline logs. Equally interesting is that certain beds that are quite clearly wet based on resistivity logs and calculated water saturation values can be seen to give up "regurgitated" gas -- i.e., gas that entered a wet bed from overpressured underlying reservoirs and then subsequently logged with gas seeping back into the well bore. Once the existence and appearance of "regurgitated" gas is recognized, it is fairly easily identified on image logs as a diffuse, weak entry contrasts with true gas “jetting” entry. In addition, invasion of barite-rich drilling mud into the permeable "wet" sandstones revealed by a high photo-electric (Pe) curve generally accompanies the “regurgitated” gas.

ACKNOWLEDGMENTS

This study would not have been possible without the generous support of three oil and gas companies that provided access to image logs run in selected wells in the area of Natural Buttes Field. These companies, Questar Exploration and Production, Kerr McGee Corporation, and EOG Resources, also supplied detailed information on which sandstone intervals were completed in the wells and the completion techniques including fracture stimulation. Cumulative production figures for the wells through December, 2004, were obtained from the Utah Oil and Gas Division of Oil, Gas, and Mining’s website at “http://dogm.nr.state.ut.us/oilgas/PUBLICATIONS/Reports/PROD_book_list.htm”.

This study also benefited greatly from the support of Schlumberger Oilfield Services in Denver, which provided access to the digital files for the image logs along with technical and computer support. Because image logs record data from 192 electrodes to create microresistivity logs with data at 0.1-inch intervals, the data files for these logs are huge, especially when the logs are run over intervals of several thousand feet. It would have been difficult or impossible to work with these logs independently of Schlumberger.

The work of quantifying fracture abundance, orientation, and distribution on the image logs was done by Tom Becker, and is much appreciated. Barbara Luneau’s assistance in mapping the distribution of fractures and generating the maps of vector plots of specific intervals using *Petral* software is also greatly appreciated.

Finally, both the impetus for this study and the financial support to the senior author that made it possible were provided by the Utah Geological Survey under its program to improve understanding of gas reservoirs throughout the Uinta Basin. The Survey's funding of such a research study was the key incentive that led Questar, Kerr McGee, and EOG Resources to release their FMI logs, which initially cost tens of thousands of dollars to run and process, into a public forum for review and scientific use. The willingness of the Utah Geological Survey to support and fund such research studies is greatly appreciated.

STUDY METHODS AND MATERIALS

The 10 image logs used in this study were first retrieved from the archives at Schlumberger Oilfield Services. All older files were updated and brought up to the processing standards of the recent 2004 wells (processing and interpretation of image logs have improved tremendously over the past five years since the first image log used in this study was run). Printed copies of the image logs at scales of 1 inch = 20 ft (highly compressed for an image log), 1 inch = 5 ft (very useful for working with features tens of feet thick), and 1 inch = 1 ft (highest resolution with best detail for individual beds, but requiring large amounts of paper) were printed for the senior author. In a few cases, beds and fractures had to be repicked from those generated in the original processing to make the log set consistent with the more recent logs for mapping of sedimentary features and fractures.

LAS files for the gamma-ray, resistivity, neutron, and density logs for the 10 study wells were imported into *Petra*® software and used to generate cross-sections tying all the study wells. These cross-sections allowed recognition of intervals within the Mesaverde Group, and correlation of such well-known units as the Sego Sandstone, Buck Tongue Shale, Castlegate Sandstone, Blackhawk sandstones, and Mancos Shale including the "Mancos B" Sandstone interval, which is the deepest stratigraphic interval examined for this study and which was reached in only one of the study wells. Following the precedent set by Osmond (1992), the top of the Mesaverde Group is picked at the top of the shallowest blocky sandstone below the red and green shales (and thin fluvial channels sandstones) of the Paleocene Wasatch Formation. Three of the image logs contain data across the contact between the Wasatch and Mesaverde, which is commonly interpreted as an unconformity representing 10 to 20 million years of time. Surprisingly, though, none of these image logs shows any hint of an angular unconformity between the Wasatch and Mesaverde.

Working with the image logs and the cross-sections, quantitative data was compiled in a set of Excel spreadsheets for all porous (>6%) sandstone intervals more than 4 ft thick. Depending on how much of the Mesaverde Group was covered by the image log, anywhere from 20 to 50 potential reservoir sandstones were identified and quantified. Data on the spreadsheets, which are presented in Appendix 2, include the top and bottom of each sandstone, gamma-ray response, average density and neutron porosity values, amount of crossover or separation of the neutron and density logs, sedimentary features seen on the image logs, abundance of fractures, breakout, and gas entry, and whether or not the interval was completed.

THE STUDY WELLS

Key information on each of the ten study wells is summarized below. Included is information on when the well was drilled, the interval over which the image log was run, a comment on image log quality, and production information for the well.

1. Questar NBE 7ML-17-9-23, located in SW NW Sec. 17, T9S, R23E (API: 43-047-35464) with image log data from 7460 ft about 860 ft below the top of the Mesaverde to 9104 ft near the top of the Castlegate Sandstone. The image log, run on July 20, 2004, is of excellent quality and covers 27 Mesaverde sandstones. This well was completed in August, 2004, for 1.1 MMCFGPD from 3 fluvial channel sandstones in the Wasatch and 15 Mesaverde sandstones that range in depth from 7620 to 8950 ft. Gas entry can be seen on the image log from 7620 to 8601 ft. Mud weight during logging was 9.5 lbs/gallon. In part because this well had 50 sidewall cores cut for petrographic study, it serves as a "type well" for defining intervals within the Mesaverde Group. This well produced 86.6 million cubic feet of gas (MMCFG) and 2588 barrels of condensate (BC) during its first 5 months on production.

2. Questar NBE 3ML-17-9-23, located in NE NW Sec. 17, T9S, R23E (API: 43-047-35465) with image log data from 6866 ft about 100 ft below the top of the Mesaverde to 9230 ft in the Buck Tongue Shale. The image log, run on August 23, 2004, is of excellent quality and covers 40 Mesaverde sandstones. Four Wasatch channel sandstones from 5716 to 6674 ft were completed along with 27 Mesaverde sandstones that range in depth from 6900 to 9102 ft. Sandstones with obvious gas entry on the image log occur from 6900 to 9100 ft, and closely match the completed sandstones. Mud weight during logging was 9.5 lbs/gallon. This well produced 24 MMCFG and 1472 BC during its first 4 months on production. The relatively low amount of production was due in part to problems with barite scale plugging the well bore in the Lower Mesaverde section.

3. Questar WRU EIH 9ML-23-8-22, located in NE SE Sec. 23, T8S, R22E (API 43-047-35189) with image log data from 7697 in the lower Wasatch Formation to 10,325 ft near the top of the Sego Sandstone. The image log, run on December 7, 2004, is of excellent quality and covers 27 Mesaverde sandstones. The well was completed from 6 sandstones at depths of 6122 to 7758 ft in the Wasatch, and 15 Mesaverde sandstones that range in depth from 8026 to 10,204 ft. Mud weight during logging was 9.9 lbs/gallon and gas entry can be seen on the image log from 8198 to 10,213 ft. Production data on this well was not available as of December 31, 2004.

4. Questar NBE 11ML-26-9-23 well, located in NE SW Sec. 26, T9S, R23E (API: 43-047-35665) with image log data from 5795 ft in the lower Wasatch Formation to 8493 ft in the Buck Tongue Shale interval of the lower Mesaverde Group. This log, run on October 30, 2004, is of excellent quality and contains approximately 50 Mesaverde sandstones representing depositional environments ranging from marine lower shoreface in the Sego Sandstone to braided stream packages and classic fining-upward fluvial channel sandstones in the upper part of the Mesaverde Group. Perforated sandstones in this well range in depth from 6702 to 8113 ft, all in the Mesaverde. All Wasatch sandstones appear to be wet. Mud weight during logging was 11.7 lbs/gallon, and sandstones with gas entry on the image log occur from to 5832 to 8300 ft. This well produced 21.8 MMCFG and 577 BC during its first month of production in December, 2004.

5. Coastal's Natural Buttes Unit (NBU) #222, located in the SW NE Sec. 11, T10S, R22E, and now operated by Kerr McGee (API: 43-047-32509), was initially drilled to 6900 ft in 1994. The well was deepened in 2000 and an image log was run from 6908 about 800 ft below the top of the Mesaverde to 9599 ft in the Blackhawk Sandstone. This is the oldest of our image logs, having been run in February, 2000, and it is also the poorest quality because it was run in such a small hole that the flaps on the logging tool couldn't deploy properly. The data on sedimentary structures and fractures is only marginally useful, and the image log was run with 12.8-pound mud in the hole so there is virtually no gas entry. This well produced 798 MMCFG and 11,877 BC from the Wasatch and Mesaverde through December, 2004.

6. Coastal's Kennedy Wash (KWFU) 16-1, located in the NW NW NW Sec. 16, T8S, R23E and now operated by Kerr McGee (API 43-047-33589), has image log data from 8490 near the top of the Mesaverde to 10,960 ft in the Desert Interval. This image log was run in October, 2000, and is of significantly better quality than that run in the NBU #222 well 6 months earlier. The log covers 37 sandstones including perforated sandstones from 8490 to 10,557 ft. Mud weight during logging was 9.8 lbs/gallon, and gas entry can be seen on the image log from 10,297 to 10,840 ft. The well was a poor producer from numerous sandstones in both the Wasatch and Mesaverde, yielding just 62.7 MMCFG and 4,045 BC before being shut in in mid-2003. This is the poorest producing well among the 10 study wells.

7. Westport Bonanza #4-6, located in the SE NE SW Sec. 4, T10S, R23E (API 43-047-34751) and now operated by Kerr McGee. An image log was run from 6800 about 800 ft below the top of the Mesaverde to 8510 ft in the upper Castlegate Sandstone. The image log was run September 7, 2003, and is of good quality. It covers 38 sandstones including perforated sandstones from 7258 to 8263 ft. Mud weight during logging was 12 lbs/gallon, and good gas entry can be seen from sandstones at depths of 6833 to 8154 ft. The abundance of gas entry is somewhat surprising considering the 12-pound mud in the hole when logging occurred. This well was completed in sandstones of the Lower Mesaverde in September, 2003, and had produced 136.5 MMCFG with just 634 BC through December, 2004. A completion attempt in the Middle Mesaverde yielded no gas.

8. El Paso Pawwinnee 3-181, located in the NW NW NW Sec. 3, T9S, R21E (API 43-047-34019), was initially completed in April, 2002, from 3 sandstones of the Mancos "B" at depths of 12,049 to 12,141 ft. Surprisingly, the image log reveals no natural fractures in these relatively thin (<10 ft), deep-water sandstones. The Mancos "B" produced 343 MMCFG and 1,106 BC in 26 months. In June, 2004, Kerr McGee, the well's new operator, added perforations in two sandstones in the Blackhawk from 11,260 to 11,338 ft, in 14 sandstones in the Mesaverde from 8762 to 10,622 ft, and 3 sandstones in the Wasatch from 7766 to 8230 ft. These sandstones produced 156 MMCFG and 2,039 BC in just 6 months through December, 2004. The image log was run on March 27, 2002, from 9,470 in a package of braided stream deposits near the middle of the Mesaverde Group to 12,222 ft in shales below the Mancos "B" Sandstone. The log covers 42 sandstones including perforated sandstones from 9810 to 12,145 ft that show good gas entry. Mud weight during logging was 11.6 lbs/gallon.

9. EOG Resources #71-8FX Stagecoach Unit, located in NW NW Sec. 8, T9S, R22E (API: 43-047-34620) with image log data from 8450 ft in the middle of the Mesaverde to 10,750 ft in the Blackhawk Sandstone. This image log was run July 22, 2002, and is of good quality. The log covers 32 sandstones including 20 perforated sandstones in the Mesaverde from 8479 to 9,449 ft and 7 perforated intervals in the Blackhawk from 10,555 to 10,714 ft. Good gas entry can be seen in places on the image log from 8400 to 10,580 ft. Mud weight during logging was 11.2 lbs/gallon. This well, completed in August, 2002, had produced 487.8 MMCFG and 13,311 BC through December, 2004.

10. EOG #807-10 Chapita Wells Unit, located in NW SW SW Sec. 10, T9S, R22E (API: 43-047-34508) with image log data from 6890 ft in the lower Wasatch Formation to 8400 ft in the middle of the Mesaverde, and from 9900 ft in the Castlegate to 10,488 ft below the Mancos B Sandstone. This image log was run October 16, 2002, and is of good quality. The two sections of the log cover 21 Mesaverde and 4 Blackhawk sandstones. The well was initially completed for 906 MCFGPD and 20 BCPD by fracture stimulating three naturally fractured, highly burrowed, lower shoreface Blackhawk sandstones from 10,300 to 10,402 ft. The well was subsequently recompleted in 29 sandstone intervals in the Mesaverde, and had produced 283.7 MMCFG and 12,384 BC through December, 2004. Of special note is that the Blackhawk was cored in this well. EOG provided the opportunity to examine this core along with the image log, which provided a great opportunity to compare the two. Only about half of the fractures identified on the image log could actually be seen in the core, partly because some were drilling induced and perhaps because the others were too small to see with the naked eye. A trace of gas entry can be seen on the image log from some of the various productive sandstones, but most yielded no sign of gas entry on the log, probably because the mud weight during logging was a fairly high 11.7 lbs/gallon.

FEATURES OF AN IMAGE LOG

Tools for logging oil and gas wells have evolved tremendously over the past 70 years. Image logs evolved from four-armed resistivity dipmeter logs and the 4-pad Formation MicroScanner (FMS) log developed by Schlumberger during the 1970s and 1980s (Safinya et al., 1991). A photo of Schlumberger's Formation MicroImager (FMI) logging tool is shown in Figure 1. In order to improve resolution of features in the borehole over the FMS logging tool, Schlumberger added a movable "flap" to each of the four "pads" that were originally used, and increased the number of sensor electrodes on each pad and flap to 24 in two staggered rows of 12 buttons each. In a standard bore hole 7 and 7/8ths inches in diameter, these pads and flaps provide 78% coverage of the well bore wall as compared to the roughly 40% coverage provided by the 4-pad Formation MicroScanner logging tool.

A combination of springs and hydraulic power push the pads and flaps firmly against the sides of the well bore to assure reliable measurement of the resistivity at each electrode button. Resolution in the image log was also improved by increasing the rate of data capture

on each sensor electrode to one-tenth of an inch. Thus, with 192 sensors recording resistivity data every 1/10th of an inch, each foot of an FMI log has over 23,000 data points assigned a resistivity value and used to generate the image of the well bore wall. Each electrode essentially provides a continuous microresistivity log that is then merged with its neighboring microresistivity logs to create the image log. Resolution of an image log is about 0.2 inches, which is sufficient to see burrow traces, root marks, and a variety of other features including ripple marks and mineral nodules such as pyrite or calcite a fraction of an inch in diameter.

The image log is also directionally oriented so that the direction and angle of dip of beds, sedimentary structures such as planar bedding and troughs, and fractures can be determined. Collecting so much resistivity and directional data over thousands of feet of section requires major computer arrays to sort and archive the data. In addition, guidance packages and electronics processing devices are housed above the data-collecting pads and flaps in a pipe about 25 ft long. The image logging tool can be run alone or in combination with other logging tools, and can be run in horizontal wells.

Factors affecting the quality of the image log include well bore size (7 and 7/8ths inches is ideal, but the tool can be used in holes ranging from 6 to 21 inches in diameter), fluid in the hole (fresh water makes for relatively poor image quality; oil-based mud offers fair resolution with advanced technologies; normal water-based drilling mud is generally ideal), the amount of gas entry (too much can obscure the image log data for tens or hundreds of feet), washout (which prevents the sensor electrodes from measuring the resistivity of the well bore wall), and the amount of electrical current introduced into the formation during logging. In rare cases, bit marks and scrapes on the well bore can also obscure sedimentary structures and fractures.

Relatively few papers have been published to date on the use and application of image logs in interpreting oil and gas reservoirs of the western US. Grace and Newberry (1998) presented a very useful overview of geologic applications of image logs, but their report is now out of print. Luthi (1990) and Thompson (2000) also offer useful overviews of image logs with examples of how they can be used to interpret various sedimentary facies and reservoir characteristics. However, no one has previously published information on the use of image logs in evaluating reservoirs in the Uinta Basin.

An example of Schlumberger's processed image log is shown in Figure 2. Like the image logging tool itself, this display has evolved greatly over the past 5 years. From left to right, the FMI log consists of seven tracks. Track 1 includes caliper logs recorded by both the FMI tool and the density logs, a depth track, and a borehole deviation and azimuth tadpole. Track 2 contains a scaled black and white image using 16 color shades for the image data with thin white bands separating the merged 24 microresistivity logs collected on each pad and flap, gamma-ray curves from the image log and Platform Express, and fracture traces color-coded to show fracture aperture. Track 3 has resistivity logs with mean fracture aperture points. Track 4 is a generalized lithology column calculated based on the gamma-ray, density, neutron, and photo electric (Pe) log traces. Track 5 contains the compensated neutron and density logs, induced fracture traces, and breakout trace length. Track 6 is a dynamic 42-

shade color image of the resistivity data (often used more than the scaled black and white image for interpreting sedimentary structures and bedding) with bedding and fracture sinusoids showing apparent dip. Finally, track 7 is a “tadpole plot” that shows the direction and degree of dip of beds in the formation along with “tadpoles” for any fractures or breakout that may be present. The tadpoles in this column are color coded to show standard depositional bed dip (green), sedimentary dips in sandstone beds from troughs and planar beds (yellow), scour surfaces (orange), and fractures (generally red and blue, but also other colors depending on the origin and nature of the feature).

Although the first view of an image log may seem a bit overwhelming because of the amount of data displayed, with a little practice it becomes easy to recognize a wide variety of features including patterns in the sedimentary tadpoles that provide clues to the depositional environments of the sandstones. Breakout is also easily recognized and is important because it is generally oriented perpendicular to the direction of any drilling induced fractures that may be present. Natural fractures that can be identified with an image log include continuous fractures that enter and exit the well bore as a complete sinusoid, lithologically bound fractures (those restricted to a certain type of sedimentary bed), partially healed fractures, healed fractures filled with resistive cement, and discontinuous “fracture pieces” that are locally contribute to production. Considerable research has also been done to document the width or aperture of open fractures. Calculated aperture width for open fractures is plotted on the resistivity log track, and shown with color coded traces on the static black and white image.

INTRODUCTION TO STRATIGRAPHY OF THE MESAVERDE GROUP

Before starting our review and discussion of selected image logs, a brief discussion of the stratigraphy of the Mesaverde and Mancos intervals seems appropriate. Although these rocks have been the focus of numerous studies where they crop out on the flanks of the Uinta Basin (e.g., Fisher, 1936; Franczyk, 1989; Van Wagoner, 1995; Kirschbaum and Hettinger, 2004), relatively few detailed studies of the Upper Cretaceous stratigraphy in the subsurface have been published (e.g., Keighin and Fouch, 1981; Pitman et al., 1987; Fouch et al., 1992; USGS Uinta-Piceance Assessment Team, 2003).

In simplest terms, the Mancos Shale can be thought of as a black marine shale deposited in the Western Interior Seaway during the Turonian to Santonian about 90 to 70 million years ago, and the Mesaverde can be thought of as coastal marine sandstones grading up into nonmarine shales and sandstones that were deposited during the Campanian and Maastrichtian about 70 to 65 million years ago (Lindberg, 1988). The real story, however, is much more complex as there were numerous regressions and transgressions creating a diffuse, interfingering boundary between the Mancos Shale and Mesaverde Group.

Van Wagoner (1995) nicely summarizes some of the complex stratigraphic terminology for the transitional section above the Mancos in the eastern Uinta Basin. In ascending

sequence above the Mancos east of the Green River, he recognizes the Blackhawk Formation (which includes the Sunnyside, Desert, and Grassy members), Castlegate Sandstone, Buck Tongue Shale member of the Mancos (deposited during the last major marine transgression in the eastern Uinta Basin area), Sego Sandstone (a shallowing-upward marine shoreline sandstone), Neslen Formation (containing common coal beds deposited in coastal plains and flood plain swamps), and undifferentiated non-marine Farrer and Tuscher formations.

For this study, we basically follow the terminology of Van Wagoner (1995), but we have subdivided the section equivalent to his Farrer and Tuscher formations. Key components for subdividing the Mesaverde are the presence of thick sandstone packages with a blocky gamma-ray signature versus thinner, more traditional fining-upward fluvial channel sandstones, and the presence or absence of coal beds and carbonaceous shales. Coal beds occur only in the lower part of the Mesaverde Group. The intervals we recognize and correlate in the Mesaverde Group and Mancos Shale are as follows:

1) Upper Mesaverde, which is typically 450 to 550 ft thick and distinguished from the deeper parts of the Mesaverde by the presence of several (generally 5 to 7) braided stream deposits with a "blocky" gamma-ray signature. These braided stream deposits occur in packages about 15 to 50 ft thick with thick intervening shale packages. Classic fining-upward fluvial channel sands are rare in the Upper Mesaverde Interval, although 2 or 3 channels less than 15 ft thick may occur between the blocky braided stream sandstones.

2) Upper Fluvial Interval of the Middle Mesaverde, which is typically 500 to 600 ft thick and contains common (5 to 12) fining-upward fluvial channel sandstones with thick intervening floodplain shale deposits and sparse blocky sandstones. No coal is present in this interval.

3) Middle Mesaverde Braided Stream Interval, which is typically about 300 ft thick and composed mainly of thick sandstones with blocky gamma-ray signatures and relatively thin intervening shale beds. This is the most sand-rich part of the Mesaverde above the Sego.

4) Lower Fluvial Interval of the Middle Mesaverde, which is typically about 140 ft thick and contains 2 to 5 fining-upward fluvial channel sandstones with no blocky braided stream sandstones.

5) Upper Coal-Bearing Interval of the Lower Mesaverde (note that coal is rare or absent in the Upper and Middle Mesaverde intervals, so the shallowest good coal or carbonaceous shale in the Mesaverde marks the top of the Lower Mesaverde). This interval is typically about 350 ft thick and contains 10 to 20 distinct coal beds typically only 1 to 4 ft thick, but locally up to 10 ft in thickness. These coals are interbedded with shales and fluvial channel sandstones that form some of the best reservoirs in the Lower Mesaverde Group.

6) Neslen Interval, which is a distinctive, relatively homogenous, non-coaly package of sandstones and shales about 300 ft thick with a consistent, relatively low, non-spiky

resistivity response. This interval contains 4 to 10 fluvial channel sandstones typically less than 15 ft thick that form good reservoirs locally in the Lower Mesaverde.

7) Lower Neslen Interval, which is another coal-bearing package of shales about 100 ft thick with rare, thin sandstones. This interval represents mainly coastal plain deposition.

8) Upper Sego Transitional Interval, which is a package of shales and washover sandstones representing lagoonal deposits and lying between the Blocky Sego Sandstone and the deepest coal bed in the Lower Neslen Interval. This transitional package is typically 50 to 80 ft thick, but is quite variable across distances of a few miles.

9) Blocky Sego Sandstone, which is a widespread, easily recognized package from 60 to 90 ft thick of relatively shaly lower shoreface sandstones that grade up into clean marine shoreline and upper shoreface sandstones. In the study wells, it actually consists of two shallowing-upward, regressive shoreline packages that have fairly good reservoir characteristics for gas (>10% porosity, >0.1 md permeability), but are wet across most of the study area.

10) Buck Tongue Shale Member of the Mancos Shale, which thins northwestward across the study area from more than 60 ft to less than 10 ft. This shale was deposited during the last major marine transgression of the Western Interior Seaway about 68 million years ago.

11) Castlegate Sandstone, which is generally a clean, well-sorted, very fine to fine-grained sandstone representing shallow marine and braided stream deposits. Like the Sego, it is generally wet across the study area because of a lack of lateral seals.

12) Blackhawk Sandstone, which actually contains up to 4 separate sandstone intervals. In the study area. Each of these sandstones represents a regressive marine shoreline sequence that prograded eastward into the Western Interior Seaway. These Blackhawk sandstones are commonly productive in the study area, but become more shaly and offer poorer reservoir quality eastward.

13) Mancos Shale, consisting of a thick (hundreds of feet) section of dark gray to black marine shale with some thin silty and sandy beds. This interval offers fair to good gas source potential and yields surprisingly common indications of gas entry on the image logs.

14) The Mancos “B” Interval, a laterally extensive package of thin, relatively clean, very fine grained sandstones encased in the Mancos Shale. This is the deepest interval examined for this study, and it has proven to be a good reservoir zone locally, most notably in the El Paso Pawwinnee 3-181 well (NW NW Sec. 3, T9S, R21E).

A TOUR OF MESAVERDE SANDSTONES IN THE QUESTAR 7ML-17-9-23 WELL

A good way to introduce the variety of data revealed by an image log is to pick a "type well" and peruse images for the different types of sandstones including some that are wet and some that are productive. We have selected Questar's 7ML-17-9-23 well for the role of "type well" for three reasons. First, it has an excellent suite of wireline logs including an excellent image log. Second, two production tests were run in the well within the first few months after production began so there is information on which sandstones produced what amount of gas initially. Third, 50 rotary sidewall cores were cut in the well and provide useful data for defining the nature of the various sandstone intervals, although discussion of this petrographic work is beyond the scope of the present study.

The 7ML-17 well (SW NE Sec. 17, T9S, R23E) was logged on July 20, 2004, when the mud weight was 9.5 pounds per gallon (this is fairly low for a 9100-ft well in an area known for being gas charged and somewhat overpressured). The image log was run from near total depth at 9104 ft up to 7460 ft in the lower part of the Upper Fluvial Interval of the Middle Mesaverde. The well was initially completed for 1.1 MMCFGPD from 15 sandstone intervals in the Lower and Middle Mesaverde, and from 3 sandstones in the lower Wasatch. The top of the Mesaverde is picked at 6600 ft some 860 ft above the top of the interval on the image log. Examples of sandstones in the various intervals of the Mesaverde are discussed in descending stratigraphic sequence below.

Middle Mesaverde: Upper Fluvial Interval

The Upper Fluvial Interval extends from 7040 to 7670 ft in the 7ML-17-9-23 well, and the top of the image log is at 7460 ft two-thirds of the way down through the interval. Four of the 9 fining-upward fluvial channel sandstones in the Upper Fluvial Interval are covered by the image log along with several thin (<5-ft) splay sandstones. The channel sands have an average gross thickness of 14.9 ft, and an average net pay thickness (>6% porosity) of 11.4 ft. These channel sandstones form 18.9% of the total thickness of the Upper Fluvial Interval, which indicates a moderate amount of sand in the system, but less than half as much as is present in the Upper Mesaverde interval with its 5 to 7 packages of braided stream deposits.

Figure 3 shows the shallowest channel sandstone captured on the image log. This is a relatively thin channel about 8 ft thick from 7502 to 7510 ft and, as shown in the tadpole plot on the right side of the image log, it is characterized by planar beds dipping northward at about 5 degrees (note that structural dip has been removed from the tadpole plot so what is shown is true depositional dip independent of present-day structure). Furthermore, it is clear from the "vector plot" in the lower right corner of Figure 3, which is created by sequentially connecting the dip azimuth tadpoles head to tail through a specific interval, in this case from 7502 to 7508 ft, that the dip is remarkably unidirectional and trends consistently to the north. In a fluvial channel system, such low-angle planar beds indicate that deposition occurred in accreting planar beds in a point bar on the inside of a channel meander. Flow direction,

indicated by the blue arrow in the vector plot, was perpendicular to the accretion direction and must have been from west to east in this setting. It is also clear from the image log that a second thin point-bar deposit is stacked on the first, extending from 7497 to 7501.5 ft, but this sandstone package has less than 5% porosity and offers no reservoir potential.

This uppermost channel sand on the image log had 9% density log porosity near the base and decreases to 5% as the amount of detrital shale in the point bar deposit increases upward. With 30 ohm-m deep resistivity, this sandstone approaches the boundary of possible pay, but the image log revealed no natural fractures in the interval, nor any sign of gas entry. Consequently, this thin, shaly point bar deposit was not completed.

A useful piece of information that can be inferred from the thickness of a fining-upward fluvial channel sand is the width of the channel. Work by Leeder (1973) and Lorenz (1983, 1985) on very fine-grained channels in low-gradient settings led Lorenz to the conclusion that channel width and meander width in the Mesaverde Group in the eastern Piceance Basin of northwest Colorado could be calculated from channel thickness using the following equations:

$$\text{Channel Width } (w) = 6.8 \times h^{1.54} \qquad \text{Meander Width} = 7.44 \times w^{1.01}$$

Applying these equations yields the following results:

Channel Thickness (h in ft)	Channel Width (ft)	Meander Width (ft)
5	81	603
10	236	1754
15	440	3275
20	686	5101
25	968	7193

As a comparison, Cole and Cumella (2003, 2005) studied fluvial channels in a beautifully exposed outcrop of the Upper Cretaceous Williams Fork Formation (part of the Mesaverde Group) in the southern Piceance Basin. They defined five types of channel sands and provided average thickness and width numbers for each as follows:

Channel Type	Average Thickness (ft)	Average Width (ft)
Type A (narrow channel)	9.2	98.5
Type B (wide, single story)	8.8	505
Type C (multi-story)	13.8	815
Type D (poorly channelized)	5.4	235
Type E (broad lenticular)	2.8	276

It is clear from comparing these two data sets that channel geometry is highly variable, and that Lorenz's (1985) equation for quantifying width from thickness is probably a great

over-simplification. This is partly because it does not account for any internal or truncational erosion of the sands. However, it provides a starting point for estimating minimum channel width and we have used his equation to calculate the width presented in Figure 3 and subsequent figures.

Figure 4 shows a closer view of the same channel sandstone shown in Figure 3 taken from the image log printed at a scale of 1" = 1 ft. This is the scale (or an even larger view) used to pick individual beds (indicated by the yellow sinusoids on the dynamic color image) and fractures (although no fractures are present in this interval). At this scale, the individual tadpoles are more easily resolved, and the consistent nearly unidirectional dip of the beds in the point bar at just over 10 degrees is apparent. Also clearly seen are the breakout of the well bore wall, which is oriented almost north-south perpendicular to the natural fracture set in the area, and ripple marks in thin beds near the top of the image.

Figure 5 shows a portion of the image log across another fluvial channel, but this one is about twice as thick as the first example (16 ft vs. 8 ft). This channel sand has a basal scour, as indicated by the orange tadpole and sinusoid, and then a fairly uniform package of planar accretion beds dipping generally to the southeast at 10 to 15 degrees from 7581 to 7590 ft. Flow direction is interpreted to be perpendicular to these beds to the northeast (blue arrow in Figure 5). The interval from 7575 to 7581 ft is characterized by contorted beds, which are shown at a scale of 1 inch = 1 ft in Figure 6. Disruption of the beds masks the depositional stratification of individual beds. As a result, there are no correlated tadpoles in this interval. Deposition was clearly rapid to create such a "soupy" sand that could contort so readily.

Another feature of interest in Figure 5 is the relatively broad color bands near the top of the image log segment. Although it is not obvious from an image at this scale, these long straight line patches and the alternating yellow and orange colors in the different tracks are a result of tool pull (the logging tool got stuck on a lip of hard sandstone or other lithologic boundary and then sprung loose creating the tool pull). These artifacts of logging are much more apparent in some later figures (e.g., Figure 7). Image and accelerometer-based speed corrections have been applied, but typically do not remove all of these artifacts.

The channel sandstone shown in Figures 5 and 6 had fair porosity (~6%) and a deep resistivity of 45 ohm-m, but the image log revealed no natural fractures or any sign of gas entry. Thus, no attempt was made to complete this bed.

The shallowest producing sandstone in the Upper Fluvial Interval of the Middle Mesaverde, which extends from 7620 to 7631 ft, is shown in Figures 7 and 8. This sandstone yielded 94 mcf/d in the production test run on August 20, 2004, roughly 10% of the well's total gas production at that time. Unfortunately, the imaging tool suffered from significant tool pull below, within, and above this reservoir sandstone, but one can identify multidirectional trough crossbeds dipping at up to 18 degrees in the channel, which is 11 ft thick. The top few feet of the channel from 7620 to 7622 ft show planar accretion beds (point bar deposits) dipping to the west-northwest. The main channel sandstone had 10% porosity with minor cross-over of the neutron and density logs in some beds, and a deep resistivity of 40 ohm-m,

which led to the decision to complete it. Again, the image log shows no signs of natural fractures or gas entry from this productive sandstone.

Figure 8, a close-up view of part of the same channel sand shown in Figure 7, reveals a mix of trough crossbeds and minor contorted bedding. Of special interest is the black hole visible at the right center part of the image. This is the place where a 1-inch diameter rotary sidewall core was cut, reportedly at a depth of 7624 ft. It is about 3/4^{ths} of a foot off depth. The sidewall core had 9.45% porosity, which matches the porosity indicated by the compensated density log, and 0.0485 md Klinkenberg permeability at 2100 psi confining pressure.

An image log with a stacked set of two, possibly three fining-upward fluvial channel sandstones is shown in Figure 9. Equivalent to the "Type C" multi-storied channels described by Cole and Cumella (2003, 2005), this package is 22 ft thick. The bases of the channels tend to contain multi-directional crossbeds deposited in the thalweg of the channel as seen in the beds from 7646 to 7650 ft. The upper parts of the channel sands are dominated by planar lateral accretion beds deposited in point bars. The model for deposition of these lateral accretion beds is presented in Figure 10. The general flow direction of the river seems to have been to the southeast. These sandstones show minor gas entry on the image log (near vertical yellow stripes) and have up to 14% density porosity at the base of the deeper channel. However, the deep resistivity is under 10 ohm-m and there is no cross-over of the neutron and density logs. These characteristics suggest the sandstone is wet and completion was not attempted.

Middle Mesaverde: Braided Stream Complex

Underlying the Upper Fluvial Interval of the Middle Mesaverde is a 350-ft-thick package of thick (commonly >50 ft), "blocky" sandstones herein interpreted as braided stream deposits. These sandstones, which extend from 7670 to 8028 ft in the 7ML-17 well, have a distinctive tadpole pattern on the image log with stacked intervals typically 2 to 4 ft thick having dips in different, commonly opposed directions (Figure 11). Plotting these diverse dips in a vector plot (lower right, Figure 11) reveals a "spaghetti-like trail" with different sets representing the opposed accretions of small meandering channels. Overall flow direction is inferred to be perpendicular to the channel walls. In the case of the interval from 7762 to 7777 ft (Figure 11), current flow was apparently to the east-southeast.

Significantly, this 350-ft-thick package of "blocky" sandstones can be correlated quite easily from well to well across the study area, changing in thickness by only 50 ft. This interval consists of more than 70% sandstone with just 15 to 25% shale and some siltstones. Normal fining-upward fluvial channels are sparse or completely absent in most wells. It is the most sand-rich part of the Middle and Upper Mesaverde intervals so something must have changed in the source terrain (climate and runoff?, uplift?) to deposit this abundance of very fine grained sand in a broad "sheet" across the study area.

Braided stream sandstones commonly contain shale rip-up clasts that show up clearly on image logs (Figure 12). Highly cemented nodules, which appear bright yellow in the dynamic color track, are also present locally. Borehole breakout is also common in these sandstones and suggests a significant difference between maximum and minimum stress fields. Some of these braided stream sands also show gas entry into the well bore on the image logs, suggesting possible pay, and the interval shown in Figures 11 and 12 was perforated and fracture stimulated. However, it yielded no significant gas entry on the production tests. Many of the braided stream sandstones have less than 8% porosity, and some have just 2 to 4% porosity, which is too low to form a commercial reservoir. These problems, combined with the lack of lateral seals in the sand-rich package, probably explain why the sandstones in the Braided Stream Complex form poorer reservoirs than the normal fluvial channel sandstones occurring above and below this interval.

Another example of a braided stream deposit is shown in Figure 13. Here again, packages of tadpoles dipping in different directions probably represent the margins of small, anastomosing channels with an overall flow direction to the southeast. This interval was also completed, but had little or no gas production.

Modern analogs for the braided stream complex in the Mesaverde include parts of the Colville River channel on Alaska's North Slope (Figure 14; see also Bridge and Tye, 2000), and the Arkansas River channel where it flows through Tulsa, Oklahoma. In both areas, if one were to walk laterally across the broad river channel, he would cross dozens of small channels less than 100 ft wide and up to about 3 ft deep separated by lateral sandstone bars extending above normal river flow level. The whole system of braided channels is very sand rich with limited amounts of shale, except where mud accumulates in small abandoned channels. The common shale clasts in this depositional system come from shale beds reworked when the river system again becomes flooded.

Braided stream systems vary tremendously in width depending on the source terrain and climate, but all share one thing in common: An abundance of sand with relatively minor amounts of clays. We envision the Braided Stream Complex in the middle of the Middle Mesaverde as extending laterally for tens of miles because the package of thick, "blocky" sandstones can be correlated across several townships.

Middle Mesaverde: Lower Fluvial Interval

The lower part of the Middle Mesaverde interval in the 7ML-17 well is picked on wireline logs from 8028 to 8158 ft. The top is picked at the base of the deepest "blocky" braided stream sandstone with the base at the shallowest coaly bed in the "Upper Coal-Bearing Interval" of the Lower Mesaverde. This interval is only 130 ft thick, but it contains three fining-upward fluvial channel sands, two of which are shown in Figure 14, and several thin (<5 ft) splay sandstones. The total gross thickness of the sandstones in the Lower Fluvial Interval is about 45 ft, which is 35.7% of the interval's total thickness. Average net pay with >6% porosity in these sandstones is about 30 ft, or two-thirds of the gross sandstone thickness. Because the

channel sands in the Lower Fluvial Interval lie just above an interval containing common coals, they commonly contain gas and are productive in most of the study wells including the 7ML-17-9-23 well.

As shown by the gamma-ray and lithology tracks in Figure 15, two fining-upward channel sandstones are present at depths of 8070 to 8100 ft. The greater detail of the image log, however, suggests that the lower of these contains two separate channel sands as indicated by the change in dip direction of the tadpoles and the vector plot at 8096 ft. Opposed lateral accretion beds dipping to the northeast mark the upper part of both channel sands whereas troughs dipping to the west mark the base of the upper channel sand. Flow in the channel was probably to the east-southeast. These sandstones were perforated and fracture stimulated in the 7ML-17 well, but apparently yielded only minor amounts of gas.

A close-up view of the top of the channel sand at 8088 ft (Figure 16) reveals major breakout in a north-south direction, and major washout of the shale just above the channel sandstone at 8088 ft.

Lower Mesaverde: Upper Coal-Bearing Interval

The Lower Mesaverde is distinguished from the Middle Mesaverde by its common intervals of carbonaceous shale and coal. In the 7ML-17 well, the shallowest coal marking the top of the Lower Mesaverde occurs at 8158 ft. This coal-bearing interval extends down to 8518 ft and is 360 ft thick. It is called the “Upper Coal-Bearing Interval” (aka Upper Coaly Interval). A package of relatively low resistivity shales and sandstones without coal and herein called the Middle Neslen Interval extends from 8518 to 8797 in the 7ML-17 well. The Middle Neslen conformably overlies another coal-bearing interval in the Lower Mesaverde called the Lower Nelsen Coal-Bearing Interval.

In part because of their close association with gas-prone source rocks, the sandstones in the Upper Coal-Bearing Interval commonly contain gas and offer fair to good reservoir potential. This is true for the 7ML-17 well where a15-ft-thick fluvial channel sandstone extending from 8384 to 8395 ft (Figure 17) directly above a 4-ft-thick coal forms the best Mesaverde producing zone in the well. This sandstone also had up to 15% porosity according to the density log, and 4 to 6 units of cross-over on the neutron and density curves. Its porosity is higher than normal (generally 8 to 12%) for sandstones in this interval. Three other fluvial channel sands in the Upper Coal-Bearing Interval also had sufficient porosity and resistivity to merit completion, but their combined gas production was less than the volume of this “best” sandstone.

Much to our disappointment, the image log across the good producing sandstone was mostly lost due to sticking of the logging tool near the base of the channel sandstone. However, the top 6 feet of the channel sand from 8380 to 8385 ft was imaged fairly well and reveals southwest-dipping planar accretion beds and two scour surfaces (Figures 17 and 18). Surprisingly, this interval contains common natural fractures dipping at 70 to 80° and trending in a west-northwest direction. This swarm of natural fractures was undoubtedly

reached during the artificial fracture stimulation of the underlying channel sandstone. It is probably at least partly responsible for the relatively high rate of production (287 mcf/d during the production test on August 20th).

Along with the fining-upward fluvial channel sandstone in the Upper Coal-Bearing Interval are approximately a dozen thin (<8 ft thick) splay sands that can be recognized by their cleaning-upward response on the gamma-ray log, and their low-angle planar dip in the tadpole plot on the image log (Figures 19 and 20). This splay sand was perforated and fractured, and contributed a small portion of the well's production. Breakout of the well bore is obvious on the image. The sidewall core cut near 8506 ft (supposed to be at 8505 ft) had 8.91% porosity and 0.014 md Klinkenberg permeability at 2450 psi.

Lower Mesaverde: Middle Neslen Interval

Lying between the Upper and Lower coal-bearing intervals of the Lower Mesaverde is an interval containing fining-upward fluvial channel sandstones and non-carbonaceous floodplain shales. This interval, called the Middle Neslen, lacks the coals that characterize the adjacent intervals, and tends to have a relatively uniform, fairly low resistivity on logs. It extends from 8518 to 8797 ft in the 7ML-17 well and is 279 ft thick. This interval is easily correlated into wells throughout the study area due to its lack of coal beds and distinctive relatively smooth (non-spiky), low resistivity signature when plotted on a linear rather than logarithmic scale.

Not counting stacked channel sandstones individually, there are six fining-upward fluvial channel sandstone complexes in the 7ML-17 well and five of these were completed. The thickest of these sandstones is shown in Figures 21 and 22. It is a stacked channel sand-stone with a mix of trough crossbed sets dipping up to 25°, and a general accretion direction to the southeast. An interesting feature for this channel is that it contains a basal shale clast conglomerate about 4 ft thick (Figure 22). The cut bank of this channel collapsed into the channel creating the abundant shale clasts. With a relatively consistent porosity of 10%, a deep resistivity of 30 ohm-m, and sparse natural fractures, the whole channel sand-stone was completed and yielded some gas. Surprisingly, though, very little gas entry is visible on the image log. The mud program evidently had sealed the relatively permeable sandstones.

Lower Mesaverde: Lower Neslen Coal-Bearing Interval

Lying below the non-coaly Middle Neslen is the Lower Neslen Interval, which contains a few thin coal beds and carbonaceous shales. It extends from 8798 to 8901 ft in the 7ML-17 well and is 103 ft thick (it is consistently about 100 ft thick through the study area). The amount of coal in this interval varies significantly, but it typically offers some gas source potential. The coal beds were deposited in coastal plain swamps and commonly correlate across distances of several miles, particularly along a north-northeast to south-southwest direction that probably represents the paleo-shoreline.

The Lower Neslen Interval is dominated by shales and coals, and contains few fluvial channel sandstones. No reservoir-quality channel sandstones are present in the 7ML-17 well, so no image data for this interval were captured on the CD in Appendix 1.

Lower Mesaverde: Upper Sego Transitional Interval

Below the coaly Lower Neslen Interval and lithologically quite similar to it lies a package of thin sandstones with interbedded shales with minor amounts of coal. Herein called the Upper Sego Transitional Interval, this interval extends from the base of the deepest carbonaceous shale to the top of the "blocky" Sego Sandstone. In the 7ML-17 well, it extends from 8901 to 8970 ft. The interval contains 4 thin (<8 ft) sandstones interbedded with dark-gray shales. Sandstones with >8% porosity have a combined thickness of 20 ft and form 28.6% of the interval. Average net pay thickness, however, is just 4.75 ft. These sandstones were perforated at 8904 and 8922 ft. Their contribution to production is unknown.

An image log across three of these sandstones is shown in Figure 23, and a closer view of one of these sandstones is shown in Figure 24. The sandstones are moderately burrowed and have low angle (~5 degrees) westerly dipping planar bedding. Some oblique bit scars are also present as artifacts of drilling. The sidewall core cut at 8921.2 ft (requested to be cut at 8920 ft) had a measured porosity of 9.07%, which is significantly less than the 13% porosity indicated on the compensated density log. Measured Klinkenberg permeability at 2700 psi was 0.0137 md.

The sandstones shown in Figures 23 and 24 probably accreted along a lagoonal shoreline on the west side of a lagoon, and the shales probably accumulated under slightly deeper, quieter water conditions. The deepest sandstone in the Upper Sego Transitional Interval appears to have been deposited in a southwesterly dipping washover fan. A schematic depositional model for the Upper Sego Transitional Interval, and the "Blocky Sego Sandstone" is shown in Figure 25.

The upper two sandstones in the Upper Sego Transitional Interval had good to minor cross-over of the neutron and density logs, 65 ohm-m deep resistivity, >10% log porosity, and some natural fractures so they were perforated and fracture stimulated in the 7ML-17 well, but their contribution to production is unknown.

Blocky Sego Sandstone

The widespread Sego Sandstone is a generally coarsening-upward (regressive) package of marine shoreline sandstones about 50 to 70 ft thick that forms an easily correlated unit across much of the eastern Uinta Basin (Franczyk, 1989; Kirschbaum and Hettenger, 2004). In the 7ML-17 well, this interval extends from a sharp top at 8970 ft to a gradational base with the Buck Tongue Shale at 9038 ft. The gamma-ray log indicates the presence of two

sand bodies: 1) A lower one about 14 ft thick extending from 9010 to 9024 ft that caps a coarsening-upward (progradational) shoreface sequence with 14 ft of siltstones and shales in its lower part; and 2) A blocky sandstone 36 ft thick extending from 8970 to 9006 ft that becomes slightly cleaner and more porous in its top 10 ft.

An image log across the top of Blocky Sego Sandstone (Figure 26) shows a variety of crossbed sets near the top of the sandstone, and low-angle planar beds with common burrows below about 8982 ft. A closer view of the crossbed sets in the upper part of the Sego is shown in Figure 27, which reveals what may be hummocky cross stratification dipping at up to 10 degrees along with some low-angle (<5 degrees) planar bedding. The shales and siltstones immediately above the Blocky Sego also show planar bedding with very low dips (<5 degrees). The vector plot shows that the beds dip in a variety of directions, perhaps due to lateral migration of tidal channels through the upper shoreface and shoreline bar sands. It is probable that the lower part of the interval shown in the vector plot represents southeastward shoreline progradation, and that the rest of the section is an assortment of shallower depositional facies dipping in a variety of directions.

The image log for the lower part of the Sego Sandstone below about 9010 ft (Figure 28) reveals burrowed middle shoreface sandstones with beds dipping to the northeast at about 5 degrees. A closer view of the interval (Figure 29) more clearly shows the common burrows, and the common thin planar beds, many of which contain carbonate cement, in the lower to middle shoreface sandstones. This interval represents seaward progradation of the shoreface complex and a shoreline that trended roughly north-northwest to south-southeast.

The sandstones in the Sego typically have 7 to 11% porosity and 0.01 to 0.02 md klinkenberg permeability at 2700 psi confining pressure, although the sidewall core cut at 9015.8 ft (visible in Figure 29) had just 3.85% with 0.0032 md Klinkenberg permeability. Deep resistivities in the 7ML-17 well are 15 to 22 ohm-m and suggest the interval is wet. It was not tested in the 7ML-17 well, but appears to be wet throughout the study area. It was not completed in any of the 10 study wells. The absence of lateral seals in the blanket-like shoreface sandstones probably prevented gas from being trapped in the Sego Sandstone.

Buck Tongue Shale

One of the most distinctive marker beds for correlation in the lower Mesaverde is the Buck Tongue Shale. In the 7ML-17 well, this shale extends from 9038 to 9091 ft. It is characterized by a relatively high gamma-ray response (>90 API units) and <10 ohm-m resistivity. About 6 miles to the northwest of the 7ML-17 well, the Buck Tongue Shale thins to less than 20 ft thick but it still provides a useful marker bed between the Castlegate and Sego sandstones. As noted by Van Wagoner (1995) and others, the Buck Tongue represents the last major marine transgression of the Western Interior Seaway westward across what is now the eastern Uinta Basin.

Based in part on description of cuttings and distinctive planar bedding seen on the image

log (Figure 30), the Buck Tongue is interpreted as an open marine dark-gray to black shale, possibly with enough organic matter to offer some hydrocarbon source potential. However, the low resistivity of the Buck Tongue suggests that it is either thermally immature or does not contain much organic matter.

Castlegate Sandstone

The deepest sandstone penetrated in the 7ML-17 well is the Castlegate, the top of which occurs at 9091 ft. The Castlegate is generally a thick (>100 ft), clean (non-shaly), blocky, very fine-grained sandstone that produces water in most wells where it has been tested in the Uinta Basin. However, it forms an excellent reservoir zone for gas on the Douglas Creek Arch about 25 miles updip to the east. The Castlegate has an even more blanket-like distribution than the Sego Sandstone so it is not surprising that it lacks commercial amounts of gas in the eastern Uinta Basin. Van Wagoner (1995) presents a detailed sequence stratigraphic interpretation of the Castlegate and underlying sandstones in the Book Cliffs on the south side of the Uinta Basin and concludes that it represents a non-marine lowstand sequence at the base overlain by an increasingly marine transgressive systems tract at the top.

An image log across the top several feet of the Castlegate (Figures 30 and 31) confirms the marine depositional environment for the top of the sandstone because burrows are common. The parallel banding visible in the sandstone in Figure 30 is due mainly to bit marks on the well bore, but the burrows visible in Figure 31 are clearly part of the formation. Also present are two relatively large (aperture = 1/100th of an inch), open, lithology bound vertical fractures trending in a west-northwesterly direction, and some significant breakout trending in a north-south direction. If all of the Castlegate in the study area is as fractured as that in the 7ML-17 well, it is clear why the formation can yield significant amounts of water upon completion.

COMPARISON OF THE IMAGE LOG AND A CORE, EOG RESOURCES CWU 807-10 WELL

As part of their contribution to this study, EOG Resources made available a 120-ft-long core cut through part of the Mancos Shale and most of the Blackhawk Sandstone. Comparison of this core with the image log for the Chapita Wells Unit 807-10 well, located in the SW SW of Section 10, T9S, R22E, provides a great way to assess the quality of a Formation MicroImager log and its ability to detect various sedimentary features and fractures. The image log was run when the mud weight was 11.7 pounds per gallon and does not reveal much gas entry. However, EOG used the image log to define naturally fractured intervals in the Blackhawk, which they then artificially fractured. The well was initially completed for 906 MCFGPD and 20 BCPD from four intervals at 10,303-10,305 ft, 10,330-10,334 ft, 10,357-10,359 ft, and 10,393-10,395 ft in the Blackhawk. A year later, numerous perforations were added from 8681 ft in the Lower Fluvial Interval of the Middle

Mesaverde to 9714 ft in the Upper Sego Transitional interval (note that the Castlegate, Sego, and Middle Mesaverde Braided Stream sandstones were not tested in this well).

The core was cut in October, 2002, and was slabbed and photographed by Triple O Slabbing in Denver, which provided the core photos used in this report. The core is in excellent shape with most of the pieces fitting together and no significant missing intervals. There is a core to log correction of +8 ft such that the top of the Blackhawk "A" Sandstone occurs on the image log at 10,299 ft (Figures 32 and 33) and in the core just below 10,291 ft (Figure 34). The image log reveals a highly burrowed lower to middle shoreface sandstone with gently dipping planar beds. The tadpoles and vector plot suggest that the interval from 10,298 to 10,314 ft was deposited during a progradation of the shoreline followed by backstepping and renewed seaward progradation (lower right, Figure 32).

The Blackhawk "A" Sandstone contains one drilling induced fracture. Not surprisingly, this fracture, which shows up clearly in Figure 33, could not be found in the core (Figure 34). However, the burrows on the image log show up clearly in the core. The contact with the overlying dark-gray shales of the Mancos is also obvious in both the core and image log.

The top of the Blackhawk "B" Sandstone on the image log (Figure 35) closely resembles the top of the "A" Sandstone with common burrowing in both. One difference between the two intervals, however, is that there is more burrowing in the overlying dark-gray shales (cf. the planar bedding seen in Figure 33 with the mottled silty shales in Figure 35). An interesting feature of the "B" Sandstone is that it contains near-vertical fractures that are clearly visible both on the image log (Figure 35) and in the core photos (Figure 36). These fractures form one of the four Blackhawk intervals selected for fracture stimulation and probably contributed significantly to the well's initial production of 906 MMCFGPD.

Examination of the core revealed a variety of features including a few concentrations of thin (3-mm-thick) *Inoceramus* shells. It was hoped that these bivalves, which lived on a soft, muddy sea floor, might be visible on the image log because they are up to 3 inches long. Figure 37 presents the part of the image log that should contain these shell fragments, but it takes a bit of imagination to see them, although the darker, more resistivity dolomitic silt-stone just above them shows up quite clearly. Also of interest is that the fracture clearly seen on the image log just above the *Inoceramus* shell bed could not be detected in the core.

Another comparison of the image log and a set of core photos (Figure 38) provides a striking example of an interval of distal lower shoreface bedded siltstones and shales. Individual siltstone beds less than an inch thick, which appear light gray in the core photos, are clearly imaged on the image log. Even the discontinuous siltstone lenses such as occur at 10,361.4 ft in the core photo can be identified on the image log at 10,369 ft. Unfortunately, this interval is quite shaly and lacks fractures so it offers little or no reservoir potential, but it does show nicely the resolution and quality of the image log for defining silty beds interbedded with shales.

IMAGES OF THE MANCOS "B" AND BLACKHAWK RESERVOIRS, EL PASO 3-181 PAWWINNEE WELL

As one last example of the variety of features that can be identified on image logs, let's take a tour of the Mancos "B" Sandstones, Mancos Shale, and Blackhawk sandstones in the El Paso Production Company's (now Kerr McGee) #3-181 Pawwinnee well. This well, located in the NW NW of Section 3, T9S, R21E and drilled in March, 2002, is one of a few wells in the eastern Uinta Basin initially completed just from sandstones in the Mancos "B." Three intervals of sandstone from 12,049-12,055 ft, 12,102-12,106 ft, and 12,138-12,144 ft were perforated and fracture stimulated with 600,700 pounds of sand. Initial potential was 2,079 MCFGPD and 200 BWPD (probably frac fluid), These sandstones produced 343 MMCFG in 26 month, and the well was then recompleted uphole with perforations in two sandstones in the Blackhawk from 11,260 to 11,338 ft, 14 sandstones in the Mesaverde from 8762 ft in the Upper Fluvial Interval of the Middle Mesaverde to 10,622 ft in the Lower Neslen, and 3 sandstones in the Wasatch from 7766 to 8230 ft. As in most wells in the area, no attempt was made to complete the Castlegate, Sego, or Middle Mesaverde sandstones.

The image log was run when the mud weight was 11.6 pounds per gallon, but the well is in an area of significant overpressuring so gas entry on the log is common. In almost all cases, completed intervals are those that had good gas entry on the image log. Natural fracturing appears to have played no role in selecting the completion intervals.

Figure 39 shows a portion of the image log across the deepest productive sandstone in the Mancos "B." Interesting features include the common gas entry from the sandstone and locally from the overlying shale, the very planar beds of the shales above and below the reservoir zone, an absence of any fractures, and the variety of dip directions in the sandstones (note the vector plot at lower right in Figure 39). The general dip direction is to the northwest, which is contrary to expectations for thin-bedded, "deep-water" sandstones deposited along the western margin of the Western Interior Seaway and remains enigmatic.

A closer view of the productive sandstones (Figure 40) clearly reveals their thin-bedded nature (all are less than 1 ft thick), and the planar nature of the interbedded shales, some of which are less than a quarter inch thick (e.g., at 12,143.25 and 12,143.75 ft). Graded bedding is not obvious in the image log, but was noted in a core from the Mancos "B" cut in the El Paso #6-154 Weeks well located 3 miles to the west in Section 6, T9S, R21E. From the nature of the bedding, the thin, planar shale beds, and the analog seen in the Weeks core, it is concluded that the sandstones of the Mancos "B" were deposited as turbidites. Pattison (2005) describes similar turbidites in the Kenilworth Member in the Book Cliffs.

Figure 41 is a portion of the image log across the middle of the three productive sandstone intervals in the Mancos "B." Like Figure 39, it reveals a reservoir zone composed of thin (<1 ft) sandstones dipping westward at 5 to 10 degrees (after structural dip has been removed) with interbedded thin shales. Gas entry is less obvious from this sandstone, and some beds show minor disruption (e.g., at 12,106 ft), but the most distinctive feature in this interval is the planar nature of the interbedded sandstones and shales (something not seen in any of the fluvial sandstones higher in the Mesaverde). As in the other sandstones in the Mancos "B," no natural fractures are visible on the image log. The nature of this bedding is consistent with deposition as turbidites in a relatively deep marine environment.

Possibly surprising to some is the occurrence of significant gas entry on the image log from the Mancos Shale (Figures 42, 43, and 44). In some cases (e.g., Figures 43 and 44), this gas entry may be coming from fractures and sand-rich intervals, but in other cases it is clearly coming from unfractured shale as at 12,004 ft in Figure 42. None of these sites of gas entry in the Mancos "B" has been completed in the Pawwinnee well, but with marine black shales becoming an increasingly recognized gas reservoir (e.g., Mavor et al., 2003; Gustason and Sageman, 2004, Montgomery et al., 2005), it is likely that intervals in the Mancos Shale in the Uinta Basin yielding gas shows will be completion targets some day.

Portions of the image log across Blackhawk "D" sandstone are shown in Figures 45 and 46. Although this sandstone was not completed, the image log shows good gas entry suggesting a potential pay zone. Also of interest is the vector plot, which appears to show shoreline progradation and backstepping that suggest a paleoshoreline trending nearly east-west. Although irregularities in the western shoreline of the Western Interior Seaway are becoming increasingly recognized, an east-west shoreline in the Blackhawk "D" would be unexpected. Alternatively, the vector plot could represent migrating, cross-stratified tidal channels with accretion beds paralleling the shoreline, but such a thick package of these beds is also unusual.

A closer view of the Blackhawk "D" Sandstone (Figure 46) shows some burrowing and planar beds dipping mostly southward at up to 10 degrees. These features are consistent with deposition in a middle shoreface environment. Common cementation of some beds, mainly with dolomite, gives them a much brighter image color due to their higher resistivity (e.g., from 11,452-11,453 ft).

The shallowest water shoreline sandstones in the Blackhawk occur in the "B" Interval (Figures 47 and 48). These sandstones contain crossbeds dipping in a variety of directions at up to 15 degrees, and represent a regressive shoreline capped by upper shoreface deposits from 11,326 to 11,336 ft. A vector plot across this interval shows the mish-mash of dip directions, which probably reflects a shoreline trending in a northeasterly direction. As shown in the schematic cross-section in Figure 49, tidal channels cutting through a barrier bar system may have produced this complex pattern of tadpoles.

The Blackhawk "B" Sandstone is about 10 ft thick with 5 to 10% porosity, >50 ohm-m deep resistivity, good cross-over of the neutron and density logs, and at least one high-quality natural fracture along with some gas entry revealed by the image log (Figure 47; note that much of the gas seen on the log comes from below the "B" Sandstone). It was perforated and fracture stimulated along with the Blackhawk "A" Sandstone in late June, 2004. The frac job used 974,000 pounds of sand. These shoreface sandstones probably contributed a significant amount of the 1+ MMCFGPD produced after the recompletion.

Images of the Blackhawk "A" Sandstone are shown in Figures 50 and 51. These figures reveal a sandstone with planar beds dipping generally westward at dips of <5 degrees in the lower part of the interval. The pattern of tadpoles and the angle of dip become increasingly higher and more complex toward the top of the sandstone interval. This pattern suggests gentle westward progradation of the "A" Sand followed by upper shoreface deposition. It is interesting to note that the Pawwinnee 3-181 well is about 6 miles updip from the Chapita Wells Unit 807-10 well where both the Blackhawk "A" and "B" sandstones were highly burrowed with only minor crossbedding. Intervening logs show that these sandstones are

correlative, and that the change in facies is probably simply the result of slight deepening of the sea floor, perhaps from 10 to 20 ft to 30 or 40 ft across the intervening 6 miles between the two wells. This facies change also explains why production from the Blackhawk sandstones ceases eastward across the study area (more shaly downdip distal shoreface facies to the east of the CWU 807-10 well offer little or no reservoir potential).

DEPOSITIONAL SEQUENCE AND RESERVOIR POTENTIAL OF THE VARIOUS SAND BODIES IN THE MESAVERDE GROUP

It is clear from the changes in sand-body geometries and the distribution of coals and carbonaceous shales in the Mesaverde Group that deposition occurred during a time of major changes in sea level, accommodation space (subsidence), and climate. Figure 52 is an attempt to summarize the characteristics of the major stratigraphic intervals in the Mesaverde Group above the Castlegate Sandstone. It shows schematically the different sand-body geometries through this part of the section, and the occurrence of coals and carbonaceous shales in the Lower Mesaverde Interval.

The following section describes the main characteristics of each interval in the Mesaverde in ascending stratigraphic sequence starting with the Sego Sandstone. The focus of the discussion is on sand-body geometry and reservoir potential. Figure 53 shows schematically the distribution of gas reservoirs in the various intervals of the Mesaverde above the Buck Tongue Shale based on the 10 wells used in this study. Because lists of the specific sandstones producing in each well were provided along with the image logs, it was possible to quantify the percentage of wells producing from a particular interval. These percentages ranged from zero in the wet Sego Sandstone to 100% (all 10 study wells) in the Upper Coal-Bearing Interval. Unfortunately, it is not possible to quantify how much gas is produced from each interval, and some intervals (e.g., the Lower Nelsen) contain only minor amounts of sandstone, but we believe Figure 53 nicely summarizes production trends in the Mesaverde Group above the Buck Tongue Shale.

Just above the marine Buck Tongue Shale is the coarsening-upward Sego Sandstone interval, which has long been recognized as having been deposited in a series of progradational marine shorelines (Fischer, 1936; Franczyk, 1989, Kirschbaum and Hettinger, 2004). This widespread, cleaning-upward, blocky shoreline sandstone lacks lateral seals in the area of Natural Buttes Field and is generally wet although it does produce gas in a few wells. It was tested in the #16-1 Kennedy Wash Federal Unit well (SE NE Sec. 16, T8S, R23E) and found to produce water.

The Sego Sandstone is overlain by the Upper Sego Transitional Interval, which consists of about 70 ft of interbedded thin lagoonal sandstones, washover fan deposits, shales, and carbonaceous shales with little or no true coal. This interval, which was probably deposited mainly in a lagoonal setting behind the clean, upper shoreface sandstones of the Upper Sego, is named because it is transitional between the Sego Sandstone and the overlying Neslen coal-bearing interval, which represents coastal-plain swamps. Although many of the sandstones in the Upper Sego appear to contain gas, they are commonly shaly and burrowed, which gives them poor reservoir quality. Even worse, when these sandstones are fracture stimulated, there is the possibility that the fractures will extend down into the underlying wet Sego Sandstone and connect with a water-bearing zone. Nevertheless, thin sand-

stones in the Upper Sego Transitional Interval were completed in the 3ML-17-9-23, 7ML-17-9-23, 9ML-23-8-22, and CWU 807-10 wells, and probably yield minor amounts of gas.

The Lower Neslen Coaly Interval is defined as having coals and carbonaceous shales at its base and top and is generally about 100 ft thick. It typically consists of gray-green to brown shales that offer no reservoir potential. Coals are increasingly common to the west, and are interpreted as having been deposited in coastal plain swamps. Little reservoir-quality sandstone was deposited in this system of swamps, although locally small river channels cut through this interval and provide fair to good reservoir potential. Such sandstones were completed in all of the study wells except the 11ML-26-9-23 and KWFU #16-1 wells where no sandstones were present, and in the Stagecoach 71-8FX, where they were perforated but later cemented off. Based on the thinness of these channel sandstones, it is likely that they do not contribute a significant amount of the gas produced in any given well.

The stratigraphic change from the Lower Neslen to the Middle Neslen reflects a change in environment from coastal plain swamp to fluvial floodplain. Five to 8 fluvial channel sandstones averaging about 15 ft thick with typical net pay (6 to 11% porosity) of 8 to 12 ft are present in the Middle Neslen. These sandstones are associated with reddish-brown and gray-green floodplain shales. The disappearance of coals in the Middle Neslen probably reflects the change in depositional environment in combination with a change to a somewhat drier climate that prevented coals swamps from forming. A return to a wetter, more humid climate appears to have marked the end of Middle Neslen deposition, and the start of deposition of the Upper Coal-Bearing Interval (Figure 52).

Not surprising considering the proximity of the fluvial sandstones in the Middle Neslen to the coal gas source beds in the Lower Neslen, more than half the sandstones contain gas in the 10 study wells. Only two of the study wells, the NBU 222 and KWFU #16-1, have no producing sandstones in the Middle Neslen, and the #4-6 Bonanza has just one thin producing channel sandstone. In most of the study wells, some of the Middle Neslen sandstones have been completed and probably contribute significantly to production.

The Upper Coaly Interval is much richer in coals and carbonaceous shales than the Lower Neslen Interval, although the relative abundance of coals changes across the study area. The abundance of coal in this interval is generally obvious on good-quality mudlogs, which can be used in combination with the neutron-density and resistivity logs to help define the top and base of this interval. It is generally about 350 ft thick. Sandstones in the Upper Coal-Bearing Interval are mainly fluvial channel deposits less than 15 ft thick, and splay sandstones less than 6 ft thick. About 80% of the sandstones in this interval with >8% porosity have been completed. Every study well produces some gas from these sandstones with as many as 8 different sandstones being completed in some wells. The abundance of gas sandstone reservoirs in the Upper Coal-Bearing Interval is undoubtedly due to the close proximity of the sandstones with the coal gas source beds.

A return to more arid conditions such as were present during deposition of the Middle Neslen led to the end of coal deposition at the end of Lower Mesaverde time, and the onset of deposition of more fluvial channel sandstones in the lower part of the Middle Mesaverde. The increasing aridity then led to deposition of the sand-rich braided stream complex of the Middle Mesaverde.

The Lower Fluvial Interval at the base of the Middle Mesaverde is typically 140 ft thick, and the amount of sandstone is highly variable from well to well. Some wells penetrated only a few thin channel sandstones (e.g., the 3ML-17-9-23 and #3-181 Pawwinnee) whereas others encountered thick channels forming more than half the interval. Nine of the 10 study wells have been completed in sandstones in the Lower Fluvial Interval (only the 9ML-23-8-22 was not, and it has probable pay behind pipe), but some of these produce from just a single thin sandstone that is probably contributing only minor production. Most of the channels in this Lower Fluvial Interval contain gas because they immediately overlie the gas source beds in the Upper Coal-Bearing Interval.

One of the most distinctive and most sand-rich depositional units in the Mesaverde Group is the package of thick, blocky sandstones that forms the Braided Stream Complex in the middle of the Middle Mesaverde (Figure 52). This interval, which typically ranges in thickness from 350 to 400 ft, can contain >70% sandstone. It is inferred that lesser amounts of vegetation and the loss of plant-stabilized levees on the flanks of the channels, combined with episodic storms and sheetwash, prevented the “normal” fining-upward fluvial channel sandstones from forming in this interval. Instead, ephemeral braided streams were the main depositional agent. Deposition must have occurred on a very flat, relatively homogenous surface, and this package can be correlated through the study area quite easily.

With the abundance of sandstones, one might expect the Braided Stream Complex to be a major producing horizon, but this is not the case for several reasons. First, shale rip-up clasts are a common component in many of the sandstones and reduced reservoir quality. Many of the sandstones in this interval are also quite tight with <6% porosity so they offer little reservoir potential. Finally, the braided stream deposits appear to have a high level of lateral continuity, which decreases the potential for stratigraphic traps. It turns out that most of the braided stream sandstones are wet or too tight to produce. Only half of the 10 study wells have any production from this interval, and the amount of production is relatively low where production test data are available.

A return to wetter conditions and more evenly distributed rainfall probably allowed plants to recolonize and stabilize flanks of the ephemeral braided streams, and led to localized deposition of fluvial channel sands in streams and rivers that meandered across a broad, shale-dominated floodplain during deposition of the Upper Fluvial Interval in the Middle Mesaverde. It is interesting to note that the thickness of the channel sands in the upper and lower parts of the Middle Mesaverde above and below the braided stream complex is quite comparable, typically 10 to 20 ft, suggesting river systems of similar size.

Because the Upper Fluvial interval is the thickest of those defined in the Mesaverde (typically 550 to 700 ft), it contains numerous channel sandstones. Each study well encountered 7 to 10 such sandstones with >8% porosity along with some thin splay sandstones and rare blocky braided stream sandstones. Perhaps partly because these numerous channel sandstones create good potential for localized stratigraphic traps, 8 of the 10 study wells were completed in at least one or two sandstones in the Upper Fluvial Interval. The two non-producing wells are the CWU 807-10 and the #4-6 Bonanza and each has some sandstone intervals that may contain gas. However, it is clear from the logs that many (perhaps 60%) of the sandstones in this interval are wet. Distance from the gas source rocks and limited migration into the isolated channel sands probably explains this high percentage of wet, porous sandstones.

The Upper Mesaverde interval with its blocky sandstones that average about 40 ft thick is a bit enigmatic. We interpret the blocky sandstones to represent another set of braided stream deposits, but the interval is much more shaly than the Middle Mesaverde Braided Stream Complex with <40% average gross sandstone thickness. The shales in the Upper Mesaverde are generally described on mudlogs as being medium to dark gray, which is somewhat surprising for a subaerially exposed braided stream complex. In any case, these blocky sandstones are locally productive, particularly in the western part of the study area. Four of the 10 study wells (the 3ML-17-9-23, 9ML-23-8-22, NBU 222, and KWFU #16-1) were completed in sandstones of the Upper Mesaverde, but the interval appears to yield relatively minor amounts of gas.

DEPOSITIONAL TRENDS IN THE MESAVERDE GROUP INFERRED FROM VECTOR PLOTS

A useful way to define depositional trends for a specific interval of sandstones is to generate vector plots for that interval for each available well and plot them on a map. Where the sandstones represent a fairly consistent environment, such as the braided stream package in the Middle Mesaverde shown in Figure 54, a general flow direction can be defined, in this case to the east-southeast. The irregularities to the north and south in the vector plot represent the lateral accretion on the flanks of the braided channels whereas the overall easterly migration of the vector tadpoles represents migrating sand waves prograding to the east through the 280-ft thick package of braided stream deposits in the 71-8FX well.

Of course, not all vector plots are as easy to interpret, particularly if they represent several different depositional environments like the one for the Lower Neslen Interval in the 71-8FX well (Figure 55). Here, the collection of vector tadpoles covers about 7 mostly thin sandstones in a 200-ft interval. One interpretation for this mix of dip directions is that the basal Neslen represents a river system flowing south-southwest, and that a marine transgression then flooded the area. As shown in Figure 55, this transgression may have resulted in initial shoreline progradation, followed by back-stepping and another progradation. Even if this interpretation is true, it is difficult to build a logical story for the uppermost sand from 9798 to 9823 ft (red on the vector plot), which has dips in many different directions.

Vector plots of sandstone packages can prove particularly useful when working with shoreline and shallow marine sandstones. In such settings, they commonly reveal the trend of the shoreline perpendicular to progradational and back-stepping deposits, and tidal channels, which may have lateral accretion beds. Defining the farthest updip or downdip shoreline along a regionally tilted basin margin can aid in defining potential stratigraphic traps. Shoreline trends can also be used to define embayments or capes that could influence hydrocarbon entrapment. In addition, working with multiple image logs across a particular shoreline trend can reveal the uniformity or irregularity of the shoreline.

A map of vector plots showing flow patterns in the numerous fluvial sandstones in the Upper Fluvial Interval of the Middle Mesaverde, plotted on an isopach map of the interval in Figure 56, reveals a fairly consistent flow direction to the east and east-northeast. Such a flow direction is easily explained when one envisions the source for the sediments far to the west in the Sevier orogenic belt of west-central Utah, and easterly flowing drainages dump-

ing into the remnants of the Western Interior Seaway far to the east of the study area (Figure 57). The most anomalous of the study wells is the Kennedy Wash Federal Unit (KWFU) #16-1, which seems to have a general flow direction to the west-northwest, although with considerable "noise." A possible explanation for this anomalous flow is that a paleohigh developed east of the KWFU #16-1 well, causing rivers to flow counter-regionally on a local scale.

Another odd well is the 7ML-17-9-23, which has a vector plot with many different dip directions in a complex pattern. This probably represents a mix of lateral accretion beds dipping perpendicular to flow, and sand waves in the thalweg dipping parallel to flow. Smoothing out all the complexities, the general flow direction seems to be from west to east, but it would be hard to attribute much reliability to such a complex vector plot.

Plotting the vector diagrams for the study wells with an image log across the Braided Stream Interval of the Middle Mesaverde (Figure 58), again on an isopach base map, reveals flow patterns that are quite comparable to those seen in Figure 56. Almost all wells have an easterly flow direction, although two wells (the 9ML-23-8-22 and 11ML-26-9-23) show significant bends in the direction of flow. Considering the stratigraphic proximity of the Upper Fluvial and Braided Stream intervals, and the regional depositional picture (Figure 57), it is no surprise that both intervals have predominantly eastward flow.

Vector plots for the thin fluvial channel sandstones in the Upper Coaly Interval of the Lower Mesaverde, which is about 350 ft thick, also have a generally easterly flow (Figure 59), although there is considerable "noise" in the data due to the nature of the meandering channels. The Chapita Wells 807-10 well has the most complex vector plot and it is difficult to identify a flow direction. Probably the most anomalous well is the 11ML-26-9-23, which has a generally northeasterly flow direction, but this vector plot is also complex.

A particularly interesting map of vector plots shows the shoreline sandstones of the Blocky Sego Sandstone (Figure 60). In most of the patterns, the shoreline (parallel black lines) trends roughly north-south, with progradational and back-stepping packages indicated by the eastward- and westward-pointing arrows, respectively. The two westernmost study wells, the 3-181 Pawwinnee and Stagecoach 71-8FX, and the northeasternmost well, the KWFU #16-1, reveal shorelines that trend northeastward, whereas the shoreline in the 11ML-26 well trends northwestward. Shorelines for the other wells are nearly north-south. Taken together, these vector plots suggest a moderately complex shoreline system with embayments and capes.

Vector plots for the Castlegate Sandstone (Figure 61) reveal a set of complex dip directions in most of the wells, probably reflecting at least two depositional environments: marine shoreline and braided stream to alluvial fan. Only a few of the more obvious flow directions are indicated. Most of the vector plots reveal little useful data.

FRACTURE ANALYSIS OF THE MESAVERDE SANDSTONES

One of the major strengths of image logs is that they so nicely reveal open and healed fractures with apertures as small as a few microns. Furthermore, because the logging tool is

directionally oriented, both the strike of the fracture and its dip can be easily determined. An example of one open fracture is shown in Figure 62. As shown by the red tadpole to the right of the image, it is dipping almost due north at an angle of 70°. Its aperture, indicated by the yellow and red lines on the static black and white image, pasted into the lower right corner of Figure 62, ranges from less than 1/100th of an inch (yellow) to less than 1/1000th of an inch. Knowing these values, a true fracture porosity can be calculated for an interval by integrating data on the length of each fracture with the aperture data.

All of the wells used in this study contained dozens of open fractures in the Mesaverde Group. Most of the fractures trend in a nearly east-west direction (N 80° W) and are nearly vertical. To better display these data, rose diagrams and frequency histograms of the open fractures in each interval of the Mesaverde were prepared and posted on a Buck Tongue structure base map (Figures 63 to 70). The number of fractures in a given interval is indicated by "N," which is posted on the histograms.

For the Upper Mesaverde Interval with its blocky sandstones, each of the five wells where an image log was available reveals a dominant fracture orientation of N70°W to N90°W with most wells having fractures that strike N80°W. The number of fractures defined in the interval ranges from two in the KWFU #16-1 well, which has an Upper Mesaverde Interval just 260 ft thick with the top 35 ft not being recorded on the image log, to 32 in the Chapita Wells 807-10 well where the Upper Mesaverde is about 280 ft thick. As shown in the dip histograms, most of the fractures dip at >70° although a few fractures in the 3ML-17-9-23 well dip as little as 50°. The Upper Mesaverde was perforated in the KWFU #16-1 well, but failed to yield much production. It was not perforated in the 807-10 well because all the sandstones are tight or wet. The only well plotted on Figure 63 producing much gas from the Upper Mesaverde is the 3ML-17-9-23 where four of the sandstones were perforated and fracture stimulated, but it is not known how much gas these sandstones are yielding.

Fractures in the Upper Fluvial Interval of the Middle Mesaverde, which is typically about 600 ft thick, are plotted for the five wells with image log coverage in Figure 64. The number of fractures defined in the interval ranges from one in the KWFU #16-1 and 11ML-26-9-23 wells to the east, to 13 in the Chapita Wells 807-10 well. Most of the fractures strike in the standard N80°W direction, but those in the 9ML-23-8-22 well have quite variable directions and dip as little as 60°. We interpret this heterogeneity of strike directions and dips to reflect the presence of compaction fractures in the thin fluvial sandstones rather than regional tectonic fractures such as are seen in the other wells. None of the fluvial sandstones in the Upper Fluvial Interval was perforated in the most fractured 807-10 well, and only one thin sand was perforated in the KWFU #16-1 and 9ML-23-8-22 wells, neither of which contained the natural fracture nor gave up much gas production. Three or more channel sandstones were perforated in the other 2 wells shown in Figure 64, and each produced some gas from this interval, but only a few of the natural fractures occur in the perforated sandstones. It appears that production is quite independent of the natural fractures in this interval.

Fracture orientations and dips for the Braided Stream Interval of the Middle Mesaverde are shown in Figure 65. Eight of the study wells have images across this interval, and they reveal a generalized trend of fractures increasing in abundance to the south and southeast in the 4-6 Bonanza and 11ML-26-9-23 wells. The fewest fractures occur in the KWFU #16-1 well, which was also least fractured in the shallower intervals and is the poorest producing well among the 10 study wells, and in the 71-8FX well, which is a good producing well from

deeper intervals and five sets of perforations in the Braided Stream Interval. The orientation of the fractures in most wells is about N80˚W, but the two wells to the north have fracture strikes at N110˚W which is an unusual orientation. Reservoir underpressuring is present in the KWFU #16-1 well, which may contribute to this different strike direction, but nothing known about the 9ML-23-8-22 would explain its odd strike direction.

Despite the presence of natural fractures in the Braided Stream Interval in the 9ML-23-8-22 and 807-10, no attempt was made to complete this interval. Completion was attempted in the KWFU #16-1 well, but these sandstones failed to yield any gas or water. Sandstones in the Braided Stream Interval were perforated in the other 4 wells shown in Figure 65, but probably do not contribute much gas based on available production test data. Thus, it appears that the natural fractures in this interval do not significantly enhance production.

Fractures in the Lower Fluvial Interval of the Middle Mesaverde, which is typically about 140 ft thick, are plotted for the six wells with image log coverage in Figure 66. The number of fractures defined in the interval ranges from three in the Stagecoach 71-8FX well to 14 in the 4-6 Bonanza well. Most of the fractures strike in the standard N80˚W direction, and most have dips >70˚. Considering how thin the Lower Fluvial Interval is, it contains many more fractures per foot of section than the depositionally similar Upper Fluvial Interval. At least one of the fluvial sandstones in the Lower Fluvial Interval was perforated in each well plotted in Figure 66, and the natural fractures are probably enhancing gas production to some extent. This is the shallowest interval in the Mesaverde to show such fracture enhancement of production.

Fractures in the Upper Coaly Interval of the Lower Mesaverde, which is typically about 350 ft thick, are plotted for the seven wells with image log coverage in Figure 67. The number of fractures defined in the interval ranges from three in the 71-8FX well to the west, to 24 in the 3ML-17-9-23 well. As expected, most of the fractures strike in approximately the standard N80˚W direction, but those in the 4-6 Bonanza well to the south show somewhat more variable directions. Most of the fractures have dips >70˚. All the wells have production from sandstones in the Upper Coaly Interval, and fractures seem to enhance production. This is most obvious in the 7ML-17-9-23 well where four of the 10 fractures occur in the upper part of the best producing Mesaverde sandstone in the well (Figures 17 and 18).

Fractures in the Middle Neslen Interval of the Lower Mesaverde, which is typically about 300 ft thick, are plotted for the seven wells with image log coverage in Figure 68. The number of fractures defined in the interval ranges from two in the 71-8FX well to 17 in the 7ML-17-9-23 well. The fractures in three of the wells (71-8FX, 3ML-17-9-23, and 11ML-26-9-23) strike in the standard N80˚W direction, but those in the 9ML-23-8-22 and 3-181 Pawwinnee wells have quite variable directions and dips as little as 50˚. As in the Upper Fluvial Interval, this heterogeneity of strike directions and dips may reflect the presence of compaction fractures in the thin fluvial sandstones rather than regional tectonic fractures like those seen in the other wells. Also odd is that the fracture strike in the 7ML-17-9-23 and 4-6 Bonanza wells is about N55˚W, which is more northwesterly than normal. Both of these wells contain a sufficient number of fractures to suggest that the change in strike is meaningful, but it is not known why the fracture orientation should differ in the Middle Neslen in these two wells. Middle Neslen sandstones were perforated in all the wells shown in Figure 68 and it is likely that natural fractures enhance the gas production.

Fractures in the Lower Neslen Interval of the Lower Mesaverde, which is typically about 100 ft thick, are plotted for the five wells with image log coverage in Figure 69. The number of fractures defined in the interval ranges from four in the 71-8FX and 11ML-26-9-23 wells to the east, to 18 in the 9ML-23-8-22 well. Most of the fractures strike in the standard N80˚W direction and dip at 80 to 90˚, but those in the 9ML-23-8-22 well have a predominantly east-west orientation, which is somewhat unusual. This odd well also has a number of fractures dipping at just 40 to 70˚, which may again reflect the presence of compaction fractures in thin fluvial channel sandstones. Sandstones in the Lower Neslen Interval tend to be thin channel sands, but their reservoir quality is probably significantly enhanced by the natural fractures. Considering how thin this interval is, the number of natural fractures in each well is probably quite significant.

Although the Blocky Sego Sandstone is generally wet in the study area, a plot of its fractures was generated (Figure 70). It is a relatively thin interval about 70 to 90 ft thick, so one might expect the number of natural fractures to be low, and it is. Typical wells have just 1 to 4 fractures, although the 4-6 Bonanza has 6 fractures. In this interval, the fracture strike is generally about N80˚W although there is some variability, most notably in the 11ML-26-9-23 well where the lone fracture strikes at about N105˚W. The 3-181 Pawwinnee well also has one odd fracture striking about N35˚W. Those in the Bonanza 4-6 well strike N60˚W.

Fracture plots were not generated for the deeper sandstone intervals, in part because log coverage is limited to just a few wells. However, it is clear that natural fractures play an important role in the productive Blackhawk sandstones, particularly in the more burrowed and shalier lower shoreface sandstones (e.g., in the CWU 807-10 well discussed earlier in this report). The importance of fractures in the turbiditic sandstones of the Mancos “B” is less apparent. No natural fractures were noted on the image log for the 3-181 Pawwinnee well, which proved very commercial from this interval, but it is hard to imagine that natural fractures are unimportant in these relatively deep-water deposits. They certainly play a major role in contributing to gas shows in the shales of the Mancos and may yet prove to be the key to commercial production from this interval.

CHARACTERISTICS OF GAS RESERVOIRS AS SEEN ON IMAGE LOGS

One of the nicest features of an image log is that it can reveal precisely the sites of gas entry if mud weight and other factors are right. There are five major factors that influence the amount of gas entry detected by an image log. The first, of course, is mud weight during logging in combination with the mud weight history during drilling. If the mud is overbalanced, very little gas or no gas entry will be detected. If the mud weight is strongly underbalanced, there may be so much gas entry that image quality is lost or greatly reduced by the abundant gas entering the well bore. Optimum conditions for detecting gas entry are when the mud weight is slightly (~0.5 pounds) under balance, but this can vary significantly based on other factors mentioned below.

The second factor influence gas entry is reservoir permeability. Rocks too tight to flow gas will not offer gas entry even if the mud weight is underbalanced. High permeability fractures can yield gas even where the mud weight is slightly overbalanced.

Third is reservoir pressure. Overpressured reservoirs offer much better gas entry than underpressured reservoirs, but, of course, this can be partly compensated for by reducing mud weight. Not surprisingly, there are significant differences in reservoir pressure in the Mesaverde sandstones from the base to the top of the interval. More surprising, is that there are major lateral changes in reservoir pressure locally across the 9-township study area.

Fourth is whether or not lost circulation material (LCM) was used during drilling, and the amount of LCM used. If there were significant lost circulation zones and extensive use of LCM to control fluid loss, fractures and permeable sands are likely to be plugged off, even if the well is drilled with underbalanced mud. Plugging of fractures, either with LCM or just plain drilling mud, probably explains why so few open fractures show gas entry on image logs.

Fifth, the amount of time elapsed between drilling and running the image log plays an important role in influencing the amount of gas entry. In gas-rich areas, the longer the time interval, the more the sandstones in the well are likely to have "cleaned up" and the more gas entry will be detected by the image log.

Three examples of nice gas entry from fluvial channel sandstones in the 11ML-26-9-23 well are shown in Figures 71, 72, and 73. As is typical, gas entry is much less uniform around the well bore than might be expected for moderately porous (9-12%) and permeable (0.05 to 0.1 md) sandstones). Instead, the gas typically enters only 1, 2, or 3 of the pads. Another surprise is that in all three examples, gas can be seen entering the well bore away from the clean fluvial channel sandstones. In most cases, these "stray" gas entries appear on only one pad and come from unfractured shale intervals. The significance of these points of gas entry away from the sandstones remains to be determined, but if the image logs are revealing real gas entry as they should, at least some gas production may be obtained from beds other than the best fluvial channel sandstones.

It should be pointed out here that sandstones that yield no gas shows on the image log can still serve as good reservoirs. For reasons that are not clear, some sandstones with good log porosity and resistivity don't reveal gas entry on the image log even when others above and below do so. Possible explanations for the absence of gas entry include plugging of pores by drilling mud and subtle differences in reservoir pressure between beds. In either case, these "non-show" sandstones can prove to be productive after fracture stimulation.

One final point regarding gas entry is that it is commonly independent of natural fractures, and where natural fractures are present they reveal gas entry only a small percentage (<10%) of the time. Whether the lack of gas entry from fractures in reservoir intervals is due to invasion of the fractures by drilling mud causing flushing of the gas, or some other factor is not yet clear, but most natural fractures are not associated with gas entry.

An unexpected and initially enigmatic type of gas entry showed up on the image logs for a couple study wells during the course of this study. Sandstones, mainly in the Upper Mesaverde Interval, with porosity and resistivity characteristics that suggested they were clearly wet (10 to 14% porosity with 10 ohm-m deep resistivity) had yielded good gas entry during logging (e.g., Figures 74, 75, and 76). A more careful evaluation of these enigmatic beds indicated that in most cases they were strongly invaded with barite-rich drilling mud,

which fooled the lithology log to make them appear to be limestones and dolomites (colored blue). The gas also had a diffuse, blotchy appearance on the image log (best seen on the image logs at a scale of 1 inch = 1 ft; Figure 75) suggesting little energy as it entered the well bore. These characteristics indicate that the gas is not indigenous to these particular sandstones, but is instead "regurgitated gas" that came from deeper, higher pressured reservoir zones and invaded into the wet, porous Upper Mesaverde sandstones with the drilling mud.

Recognizing "regurgitated gas" can be an important part of interpreting image logs because it prevents completion attempts in what are really "wet" sandstones. It is still unclear just how important such "regurgitated gas" is in wells throughout the Uinta Basin, but its occurrence in two of the 10 study wells indicates that it is something to consider.

NATURE OF THE CONTACT BETWEEN THE MESAVERDE AND WASATCH

The contact between the Upper Cretaceous Mesaverde Group and the Paleocene to Eocene Wasatch Formation is commonly interpreted as a major unconformity representing anywhere from 10 to 20 million years of time depending on location in the Uinta Basin (e.g., Fouch et al., 1992, their Figure 5). This gap in time represents most or all of the Laramide Orogeny, so it is somewhat surprising that the contact is difficult to recognize on wireline and image logs. As suggested by Osmond (1992), the top of the Mesaverde is commonly picked at the top of a "blocky" clean sandstone (gamma-ray <75 API units) below the red and green shales of the Wasatch Formation. Careful examination of the lithodensity log commonly reveals a relatively dense dolomitic cap on the top of this shallowest blocky sandstone that may represent a caliche cap just below the unconformity.

This shallowest "blocky" sandstone and its dolomitic cap generally occur just below a washed out shale interval that marks the base of the Wasatch Formation. This contact is present at a depth of about 6015.5 in the 11ML-26 well (Figure 77) and was also imaged in the Westport Tribal 36-148 well (SW SE Sec. 36, T8S, R21E; Figure 78). In both cases, unusual bright mottling, possibly representing calcified root traces is present below the contact, and washed out shales are present above it. The contact also shows some relief that may be the result of erosion. However, there is absolutely no evidence of an angular disconformity at the contact. It is surprising that no deformation occurred in the study area during the Laramide Orogeny

CONCLUSIONS

Study of image logs provides a useful new tool for identifying, interpreting, and evaluating Upper Cretaceous Mancos and Mesaverde low-permeability gas reservoirs in the northeastern Uinta Basin and elsewhere. This study focuses on image logs run during the past 5 years across large intervals of the Mesaverde Group in 10 wells located in and around Natural Buttes Field. These image logs were created by measuring the rock's resistivity in each of 192 electrodes every tenth of an inch to create a "picture" of the walls of the well bore. Image logs clearly reveal bedding, sedimentary structures, burrowing, and fractures. Based on this study, it is concluded that image logs offer valuable data for evaluating reservoir quality in the Mesaverde in a variety of ways. These include:

1. The ability to quantify sedimentary dip directions and dip angles to aid in interpreting sandstone depositional environments and defining paleocurrent flow directions. The major environments recognized in this study include fluvial channels ranging in thickness from a few feet to more than 25 ft, splays generally <10 ft thick, braided stream packages up to 100 ft thick with anastomosing small channel sandstones and relatively low shale content (although shale rip-up clasts are locally common), distal, middle, and upper marine shoreface with a variety of bed and burrow types, lagoonal shoreline and washover fans, and relatively deep-water turbidites (only in the Mancos "B" interval).

2. In the case of fluvial channel sandstones, the potential reservoir facies can be further subdivided on image logs into three lithologies, each with distinct reservoir properties. These are: 1) the high-energy, trough crossbedded current deposits from the channel thalweg, commonly with dips >10° and sand waves that can reveal the direction of flow; 2) lateral accretion beds deposited in point bars, generally with thin interbedded shaly or silty laminae and dips <10° perpendicular to channel flow; and 3) contorted beds that may form as much as 20 to 40% of a given channel sand interval. In terms of reservoir quality, the high-energy trough crossbeds at the base of the channel offer the best properties, and the lateral accretion beds with their relatively high shale content offer the poorest. Contorted beds appear to offer intermediate reservoir quality, but form a significantly poorer reservoir than the high-energy trough crossbeds.

3. All of the various sandstone facies in the Mesaverde and Mancos produce gas in at least some of the study wells. Overall, the fluvial channel sandstones in the Mesaverde above the Sego Sandstone appear to offer the majority of Cretaceous gas production in the study area, probably due in part to their proximity with and position above the coal source beds in the Lower Mesaverde and their abundance of stratigraphic traps. However, the turbiditic sandstones in the Mancos "B" form good gas reservoirs in the 3-181 Pawwinnee well, and both middle and upper shoreface sandstones in the Blackhawk form good reservoirs locally. It should be noted, though, that the Blackhawk sandstones grade eastward across the study area into increasingly shaly, deeper water facies that offer little or no reservoir potential.

4. The poorest reservoir sandstones in the Mesaverde are the relatively laterally continuous shoreline sandstones of the upper Castlegate and upper Sego, and the Braided Stream Interval in the Middle Mesaverde. These sandstones are generally water bearing, apparently because they lack adequate lateral seals to trap gas. However, some of the braided stream sandstones do produce gas locally, particularly in the Upper Mesaverde Interval.

5. Based on interpretation of vector plots, the image logs support previous interpretations that the shoreline during deposition of the regressive Sego Sandstone was oriented generally north-south, but they reveal that there were embayments and lagoons that created a locally complex depositional package. They also show that the major flow direction for the rivers and braided streams in the Middle and Upper Mesaverde was generally eastward, although again with common exceptions.

6. Image logs are excellent at revealing open and healed natural fractures. Because image logs are directionally oriented, the strike of these fractures is easily determined along

with the dip direction and amount. Image logs also reveal well-bore breakout, which is generally oriented perpendicular to the natural fractures and can be used to indicate the directions that artificially induced fractures will follow. Most of the natural fractures in the Mesaverde in the study wells are oriented about N80˚W and dip at >70˚, although exceptions occur locally in some intervals. Image logs can define fractures with apertures as small as a few microns, and total fracture porosity over specific intervals can be quantified by measuring the length, orientation, and apertures of the fractures. In general, natural fractures play a decreasingly important role in production upward through the Mesaverde.

7. Knowing the abundance, orientation, and apertures of known open fracture systems in the Mesaverde can aid greatly in designing artificial fracture stimulation jobs that have proven critical to commercial development of the Mesaverde reservoirs.

8. One of the most interesting aspects of image logs is that they can reveal sites of gas entry into the well bore, particularly if the well is logged underbalanced with a mud weight less than reservoir pressure. About half the image logs used in this study show sandstones with good gas entry. They reveal that gas generally does not enter the well bore uniformly from all sides, even in the most porous sandstones, but only from a few points around the well bore. They also reveal surprising amounts of gas entry from shale facies, particularly in the Mancos Shale, but also in the shales associated with coals in the Lower Mesaverde. Somewhat surprising is that less than 10% of the natural fractures seen on the image logs have associated gas entry, although this may be partly because strong gas entry can conceal the natural fractures.

9. A special type of gas entry on the image logs, herein referred to as “regurgitated gas,” is that which comes out of wet, underpressured, low-resistivity sandstones that have been invaded by drilling mud and gas derived from deeper reservoir zones. This “regurgitated gas” could fool a novice interpreter into believing there are gas reservoirs where none exist.

10. Image logs run across the unconformity at the top of the Mesaverde where it lies in contact with the Paleocene to Eocene Wasatch shales reveal no evidence of an angular unconformity. Considering that the whole Laramide Orogeny occurred during the unconformity between these two formations, the absence of any angular discordance is enigmatic. However, a slightly irregular, probably erosional surface with possible calcified roots is present locally at the top of the Mesaverde along with a dolomitic caliche cap.

REFERENCES CITED

Blakey, R.C., 1997, Paleogeographic evolution of the passive-margin to active-margin transition, early Mesozoic, western North America (abstract): GSA Abstracts with Programs, figures posted at: http://jan.usc.nau.edu/~rcb7/paleogeogwus.html (last accessed May 24, 2005).

Bridge, J.S., and R.S. Tye, 2000, Interpreting the dimensions of ancient channel bars, channels, and channel belts from wireline logs and cores: AAPG Bulletin, v. 84, no. 8, p. 1205-1228.

Cole, R., and S.M. Cumella, 2003, Field Trip Guidebook: Stratigraphic architecture and reservoir characteristics of the Mesaverde Group, southern Piceance Basin, Colorado, *in* K.M. Peterson, T.M. Olsen, and D.S. Anderson, eds., Piceance Basin 2003 Guidebook, Rocky Mountain Association of Geologists, Denver, p. 387-437.

Cole, R., and S.M. Cumella, 2005, Sand-Body Architecture in the Lower Williams Fork Formation (Upper Cretaceous), Coal Canyon, Colorado, with Comparison to the Piceance Basin Subsurface: The Mountain Geologist, v. 42, n. 3, in press.

Fisher, D.J., 1936, The Book Cliffs coal field in Emory and Grand counties, Utah: U.S. Geological Survey Bulletin 852, 104 p.

Fouch, T.D., V.F. Nuccio, J.C. Osmond, L. MacMillan, W.B. Cashion, and C.J. Wandrey, 1992, Oil and gas in uppermost Cretaceous and Tertiary rock, Uinta Basin, Utah: *in* T.D. Fouch, V.F. Nuccio, and T.C. Chidsey, Jr., eds., Hydrocarbon and Mineral Resources of the Uinta Basin, Utah and Colorado: Utah Geological Association 1992 Field Symposium, p. 9-47.

Franczyk, K.J., 1989, Depositional controls on the Late Campanian Sego Sandstone and implications for associated coal-forming environments in the Uinta and Piceance basins: U.S. Geological Survey Bulletin 1787-F, p. F1-F16.

Grace, L.M., and B.M. Newberry, 1998, Geological applications of dipmeter and borehole electrical images: Schlumberger Oilfield Services Report, 158 pages.

Gustason, E.R., and B.B. Sageman, 2004, Shale Resource Core Workshop: RMAG and RMS-SEPM Core Workshop, Lakewood, Colorado, August 12, 2004, unpaginated.

Keighin, C.W., and T.D. Fouch, 1981, Depositional environments and diagenesis of some nonmarine Upper Cretaceous reservoir rocks, Uinta Basin, Utah, *in* F.G. Ethridge and R.M. Flores, eds., Recent and ancient nonmarine depositional environments–Models for exploration: Society of Economic Paleontologists and Mineralogists Special Publication 31, p. 109-125.

Kirschbaum, M.A., and R.D. Hettinger, 2004, Facies analysis and sequence stratigraphic framework of Upper Campanian strata (Neslen and Mount Garfield formations, Bluecastle Tongue of the Castlegate Sandstone, and Mancos Shale), eastern Book Cliffs, Colorado and Utah: USGS Digital Data Series DDS-69-G.

Leeder, M.R., 1973, Fluviatile fining-upward cycles and the magnitude of paleochannels: Geological Magazine, v. 110, p. 265-276.

Lindberg, F.A., 1988, Central and southern Rockies region, Correlation of stratigraphic units of North America (COSUNA) product: AAPG, 1 panel.

Lorenz, J.C., 1983, Reservoir sedimentology in Mesaverde rocks at the Multi-Well Experiment site: Sandia National Laboratories Report SAND 83-1078, 38 p.

Lorenz, J.C., D.M. Heinze, J.A. Clark, and C.A. Searls, 1985, Determination of widths of meander-belt sandstone reservoirs from vertical downhole data, Mesaverde Group, Piceance Basin, Colorado: AAPG Bulletin, v. 69, no. 5, p. 710-721.

Luthi, S.M., 1990, Sedimentary structures of clastic rocks, identified from borehole images, *in* A. Hurst, M.A. Lovell, and A.C. Morton, eds., Geologic applications of wireline logs: Geological Society (London), Special Publication 48, p. 3-10 (see also several other papers in this volume).

Mavor, M.J., S.R. Bereskin, and J.R. Robinson, 2003, Lewis Shale gas resource and production potential: Final Report: prepared for Gas Research Institute, Contract No. 5096-260-3599, 278 p. plus Appendices (on CD-Rom available through GRI).

McCubbin, D.G., 1982, Barrier island and strand plain facies, *in* P.A. Scholle and D. Spearing, eds., Sandstone Depositional Environments: AAPG Memoir 31, p. 247-279.

Montgomery, S.L., D.M. Jarvie, K.A. Bowker, and R.M. Pollastro, 2005, Mississippian Barnett Shale, Fort Worth Basin, north-central Texas: Gas shale play with multi-trillion cubic foot potential: AAPG Bulletin, v. 89, n. 2, p. 155-175.

Osmond, J.C., 1992, Greater Natural Buttes Gas Field, Uintah County, Utah: *in* T.D. Fouch, V.F. Nuccio, and T.C. Chidsey, Jr., eds., Hydrocarbon and Mineral Resources of the Uinta Basin, Utah and Colorado: Utah Geological Association 1992 Field Symposium, p. 143-163.

Pattison, S.A.J., 2005, Storm-influenced prodelta turbidite complex in the lower Kenilworth Member, Hatch Mesa, Book Cliffs, Utah, U.S.A.: Implications for shallow marine facies models: Journal of Sedimentary Research, v. 75, n. 3, p. 420-439.

Pitman, J.K., K.J. Franczyk, and D.E. Anders, 1987, Marine and nonmarine gas-bearing rocks in the Upper Cretaceous Blackhawk and Neslen formations, Eastern Uinta Basin, Utah: Sedimentology, diagenesis, and source rock potential: AAPG Bulletin, v. 71, no. 1, p. 76-94.

Safinya, K.A., P. Le Lan, M. Villegas, and P.S. Cheung, 1991, Improved formation imaging with extended microelectrical arrays: Society of Petroleum Engineers Paper SPE 22726, 12 p.

Thompson, L.B., 2000, Atlas of Borehole imagery: AAPG/Datapages Discovery Series 4, 2 CD set.

USGS Uinta-Piceance Assessment Team, 2003, Petroleum systems and geologic assessment of Oil and Gas in the Uinta—Piceance Province, Utah and Colorado, USGS Digital Data Series DDS 69-B.

Van Wagoner, J.C., 1995, Sequence stratigraphy and marine to nonmarine facies architecture of foreland basin strata, Book Cliffs, Utah, U.S.A., in J.C. Van Wagoner and G.T. Bertram, eds., Sequence Stratigraphy of Foreland Basin Deposits: AAPG Memoir 64, p. 137-223.

The Formation MicroImager (FMI) Logging Tool

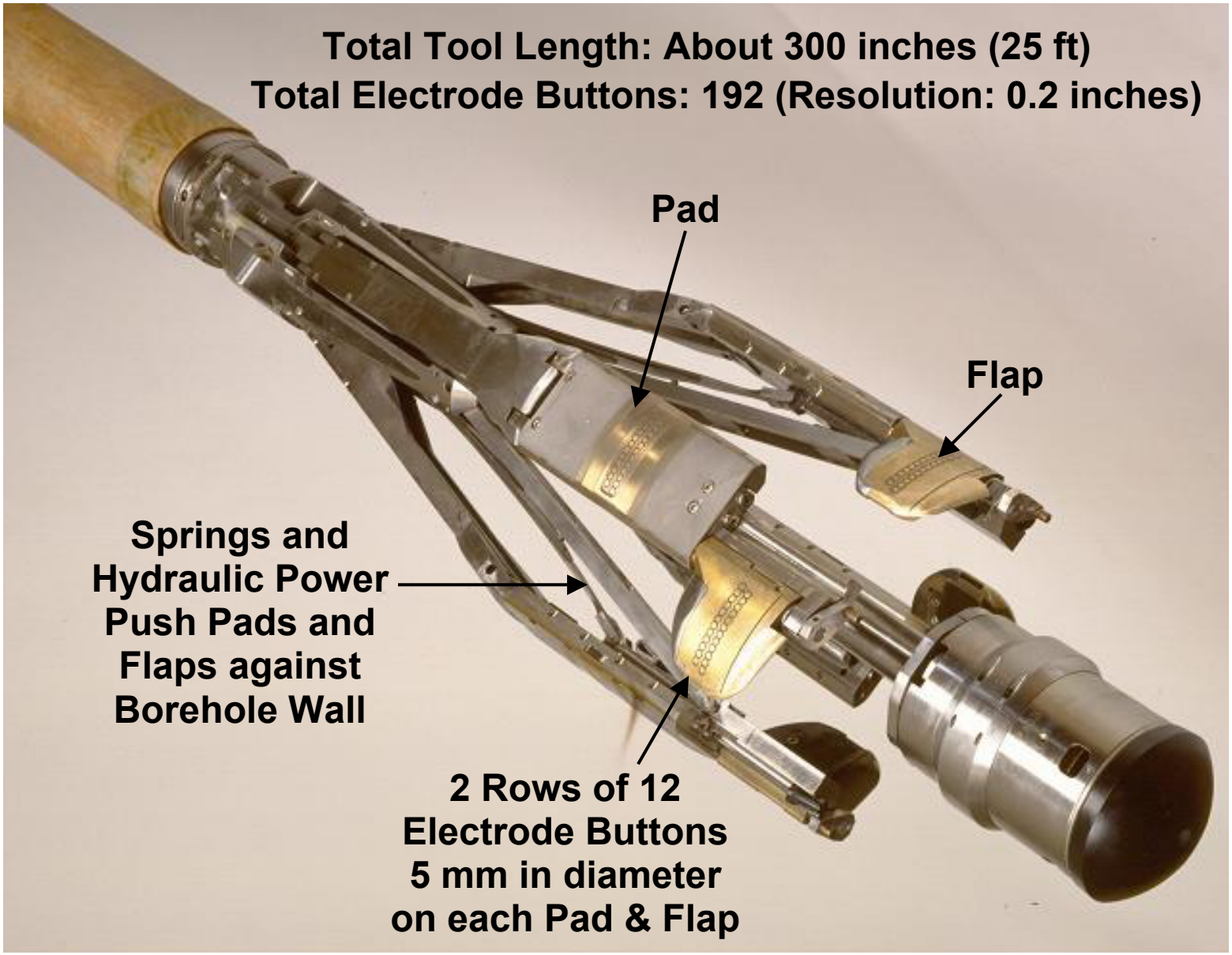

Figure 1. View of a Formation MicroImager (FMI) logging tool like the one used by Schlumberger to log the wells used in this study.

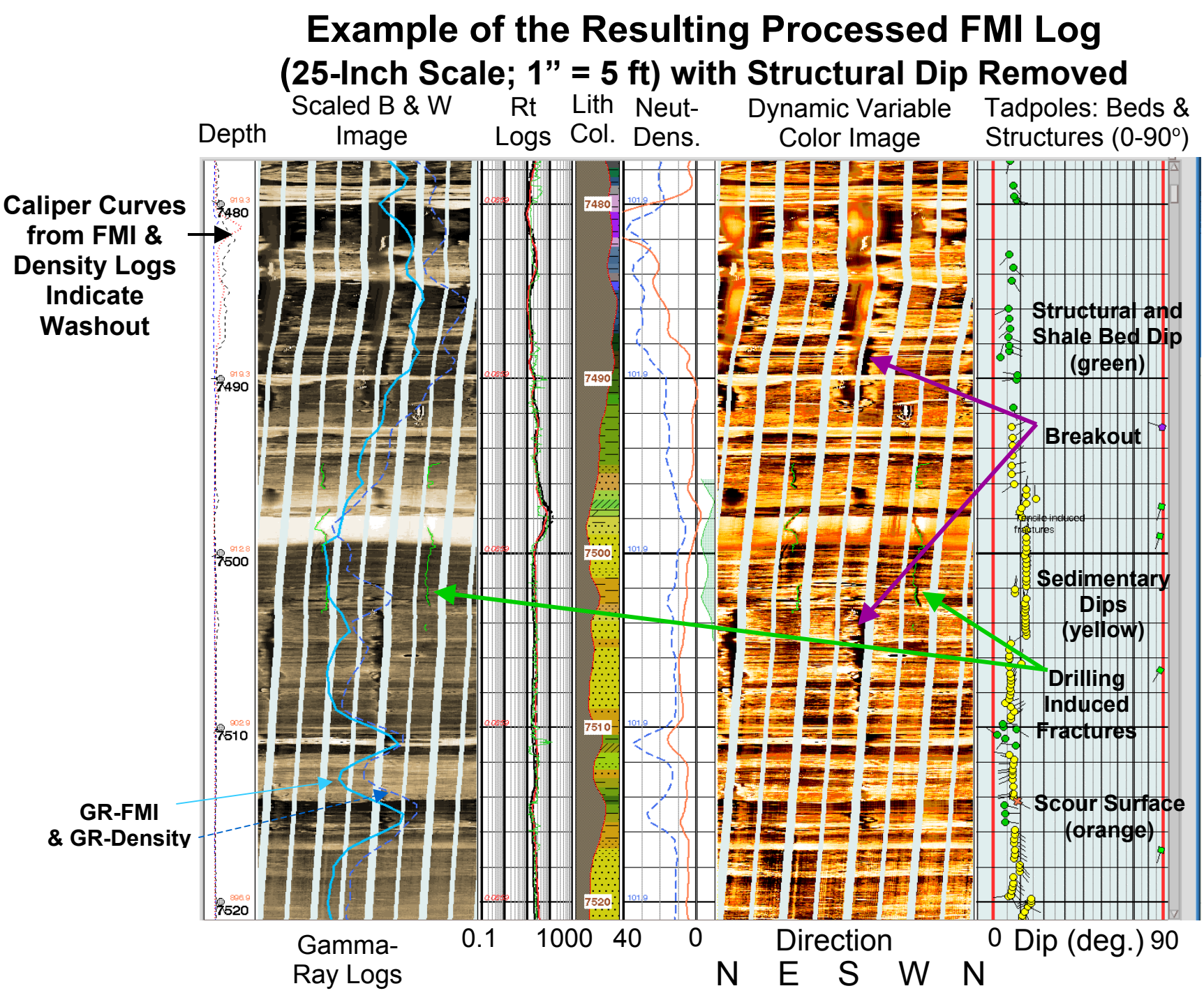

Figure 2. Example of a Formation MicroImager (FMI) log showing the various components. Structural dip has been removed at right.

Questar 7ML-17-9-23

Scale: 1” = 5’

Middle Mesaverde: Upper Fluvial Interval

Density Porosity: 6%
Avg. Gamma Ray: 50 API
Natural Fractures: None

Deep Rt: 30 ohm-m
Breakout: Some
Gas Entry: No
Perforated: No

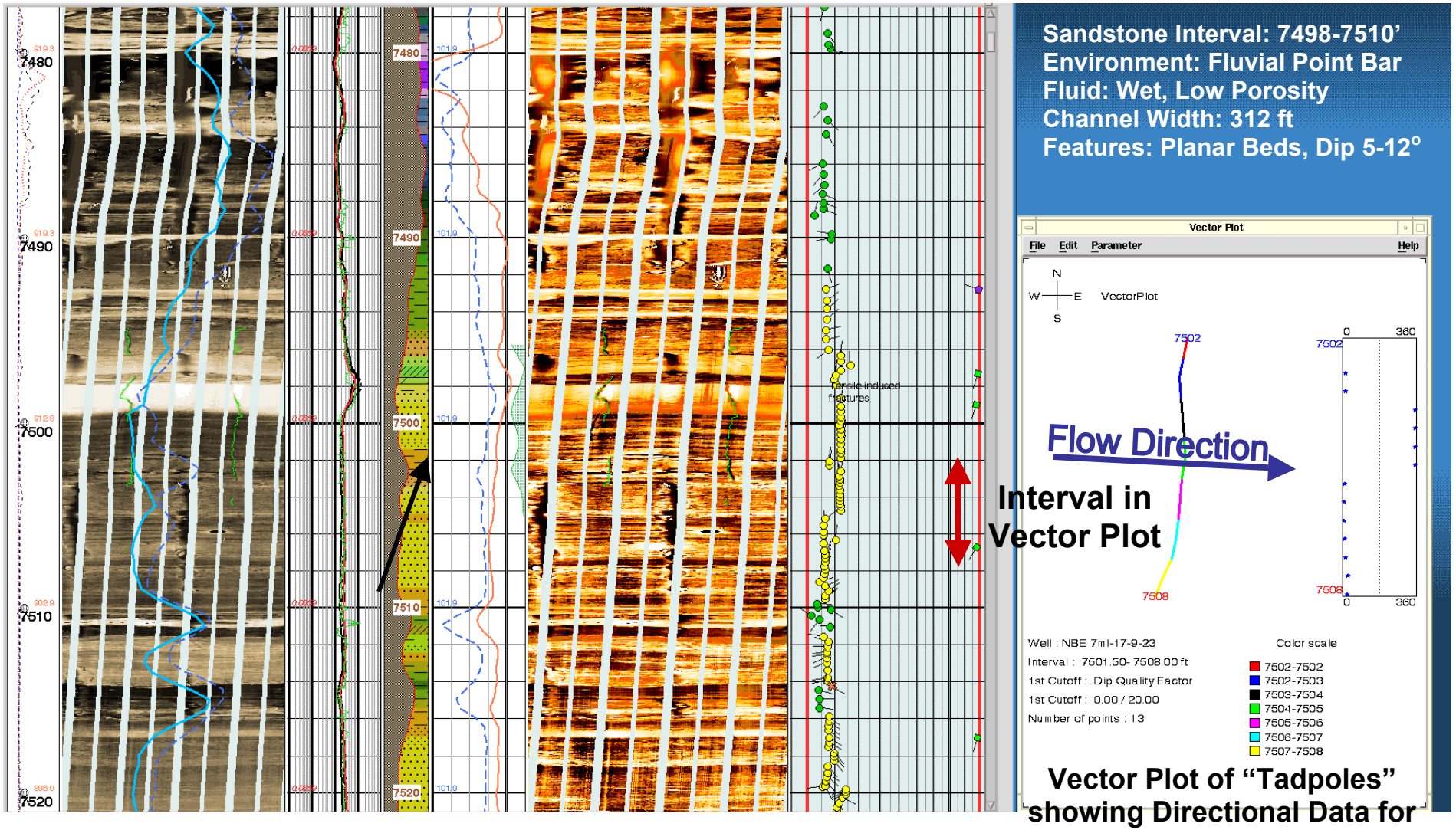

Figure 3. Portion of an FMI log showing lateral accretion beds in a fluvial point bar deposit in the Middle Mesaverde's Upper Fluvial Interval.

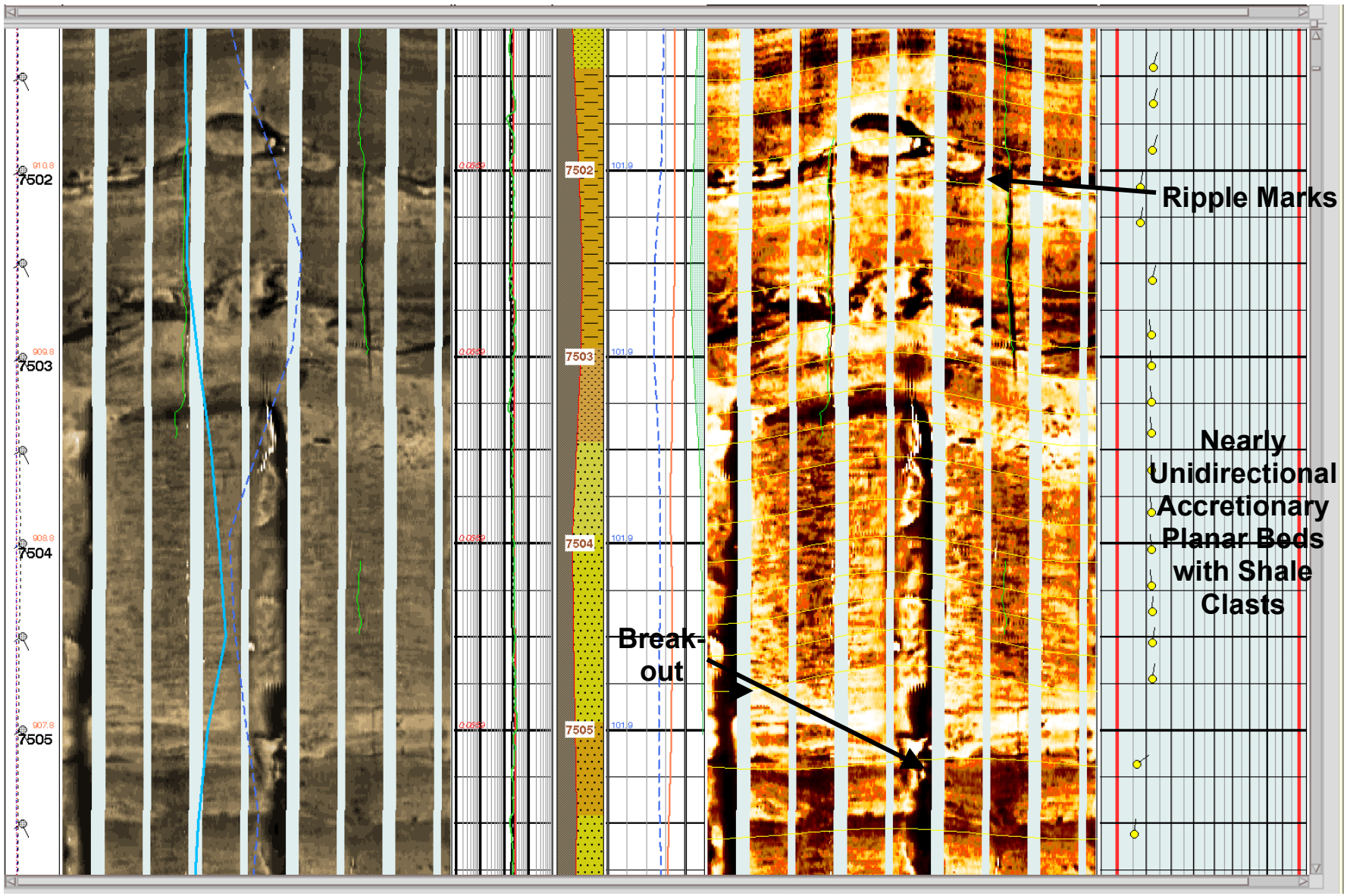

Figure 4. Part of the FMI log shown in Figure 3 at a scale of 1 inch = 1 ft showing bedding features, breakout, and ripple marks.

Questar 7ML-17-9-23

Scale: 1” = 5’

Middle Mesaverde: Upper Fluvial Interval

Density Porosity: 6%
Avg. Gamma Ray: 50 API
Natural Fractures: None

Deep Rt: 45 ohm-m
Breakout: None
Gas Entry: No
Perforated: No

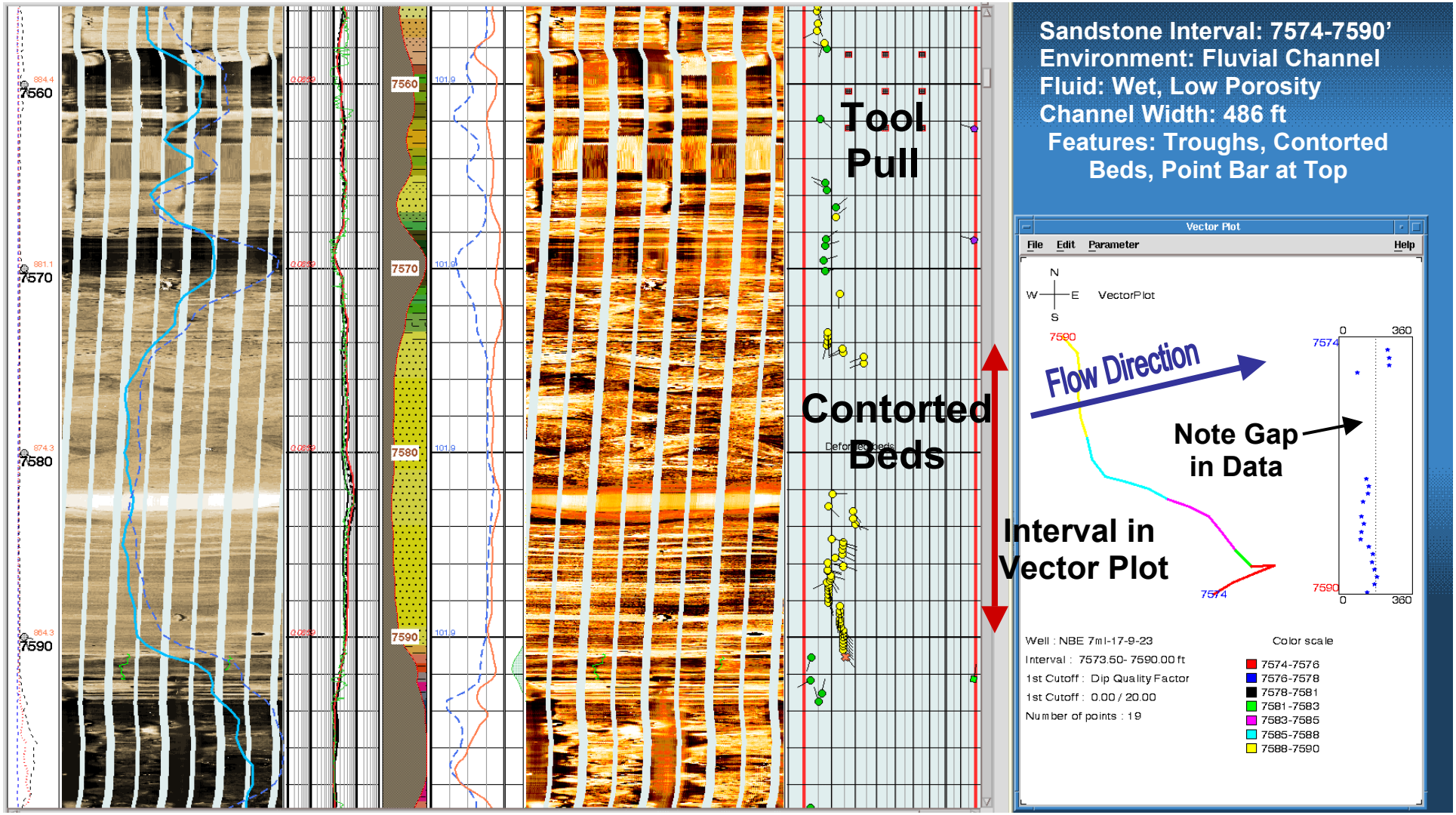

Figure 5. Portion of the FMI log across another fluvial channel sand with great contorted bedding, which is better seen in Figure 6.

Questar
7ML-17-9-23

Scale: 1” = 1’

Great Contorted Beds in Fluvial Sandstone, Probably Reducing Reservoir Quality

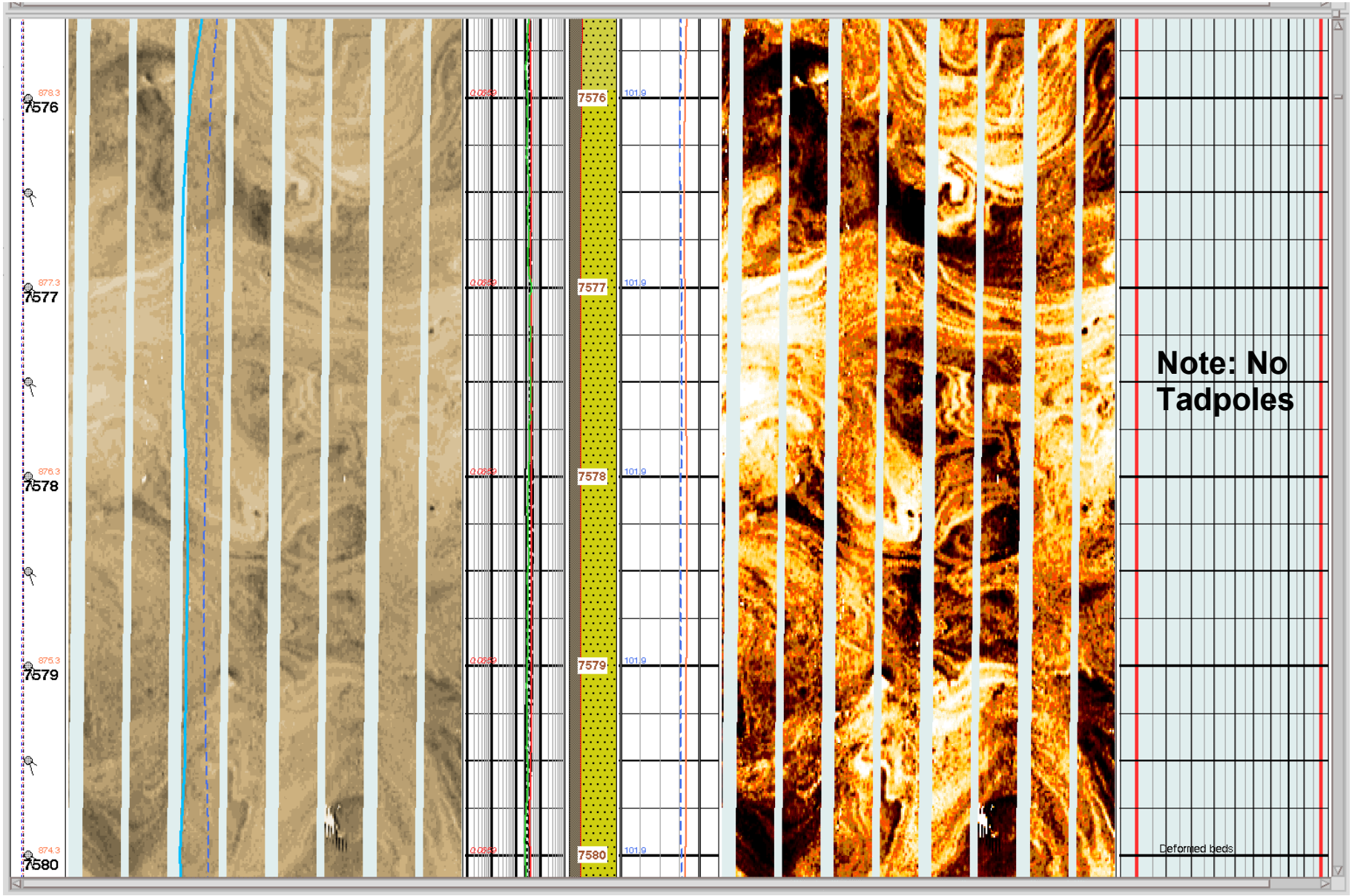

Figure 6. Part of the FMI log shown in Figure 5 at a scale of 1 inch = 1 ft showing great contorted beds in a fluvial channel sand.

Questar 7ML-17-9-23

Middle Mesaverde: Upper Fluvial Interval

Density Porosity: 10% **Deep Rt: 40 ohm-m**
Avg. Gamma Ray: 60 API **Breakout: None**
Natural Fractures: None **Gas Entry: No**
Perforated: Yes, Some Production

Scale: 1” = 5’

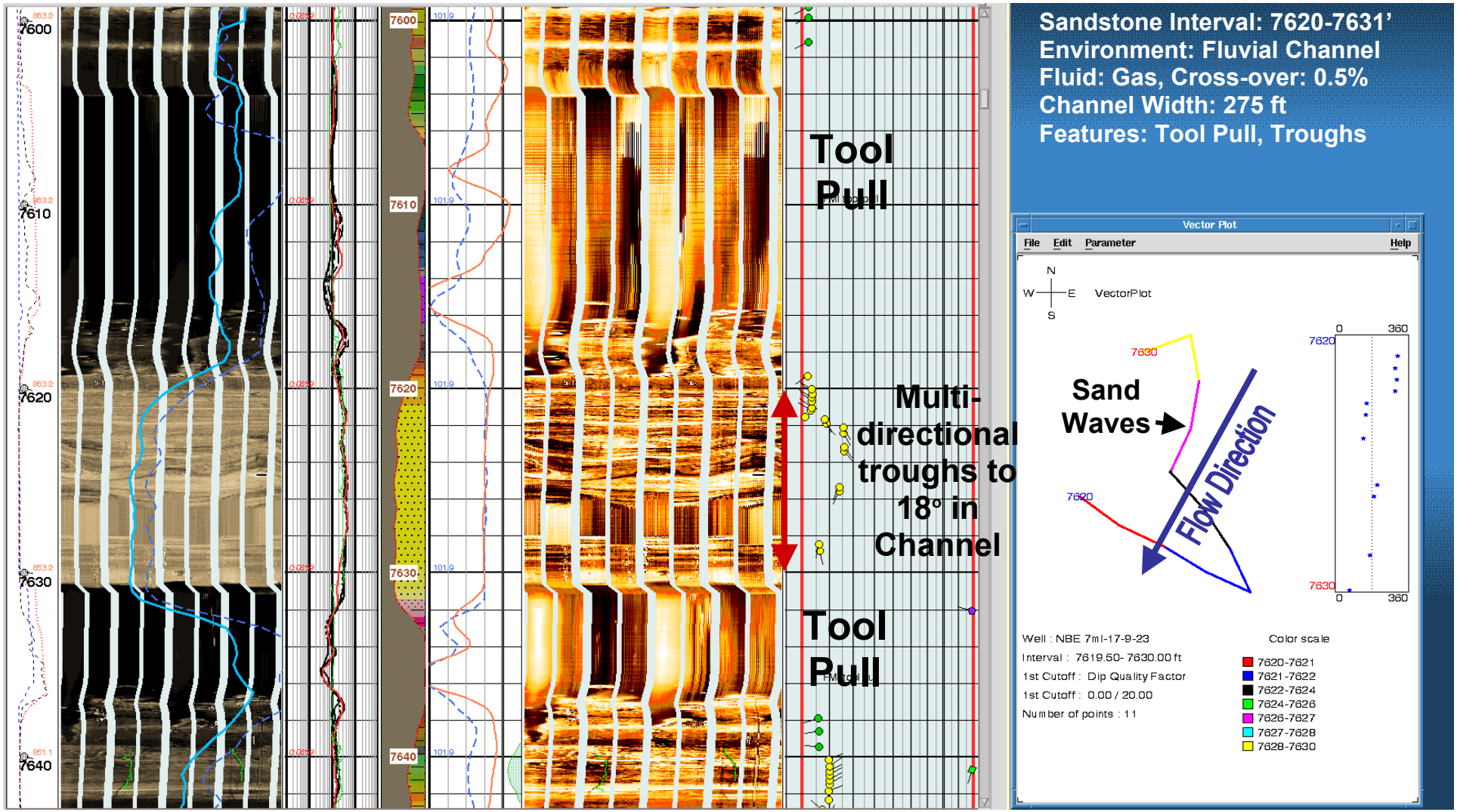

Figure 7. Portion of the FMI log across a gas-bearing fluvial channel sand with multi-directional trough crossbeds and tool pull.

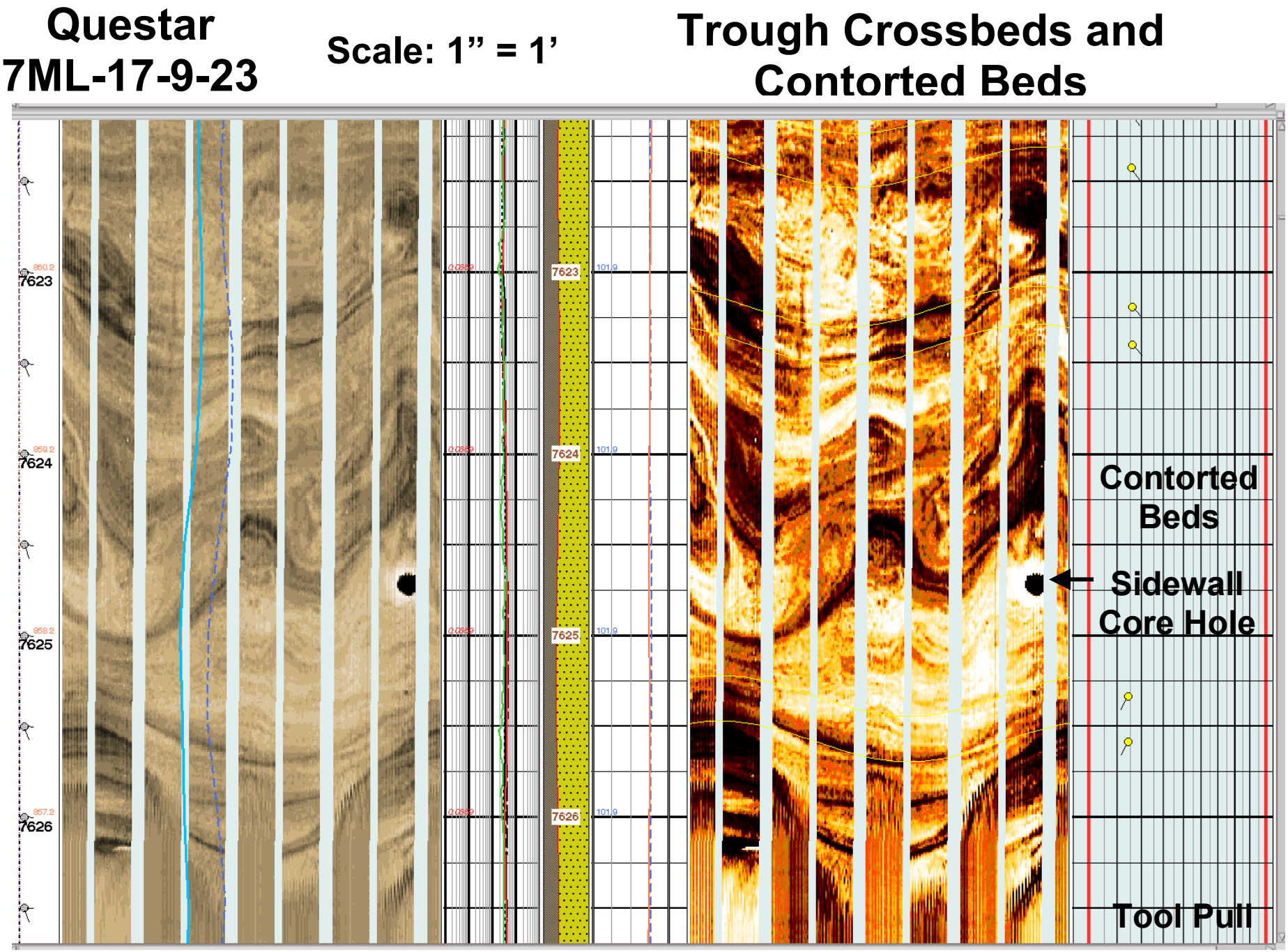

Figure 8. Part of the FMI log shown in Figure 7 at a scale of 1 inch = 1 ft showing bedding features including minor contorted bedding.

Questar 7ML-17-9-23

Scale: 1” = 5’

Middle Mesaverde: Upper Fluvial Interval

Density Porosity: 14→¨4%
Avg. Gamma Ray: 70 API
Natural Fractures: None

Deep Rt: 10 ohm-m
Breakout: None
Gas Entry: Minor
Perforated: No

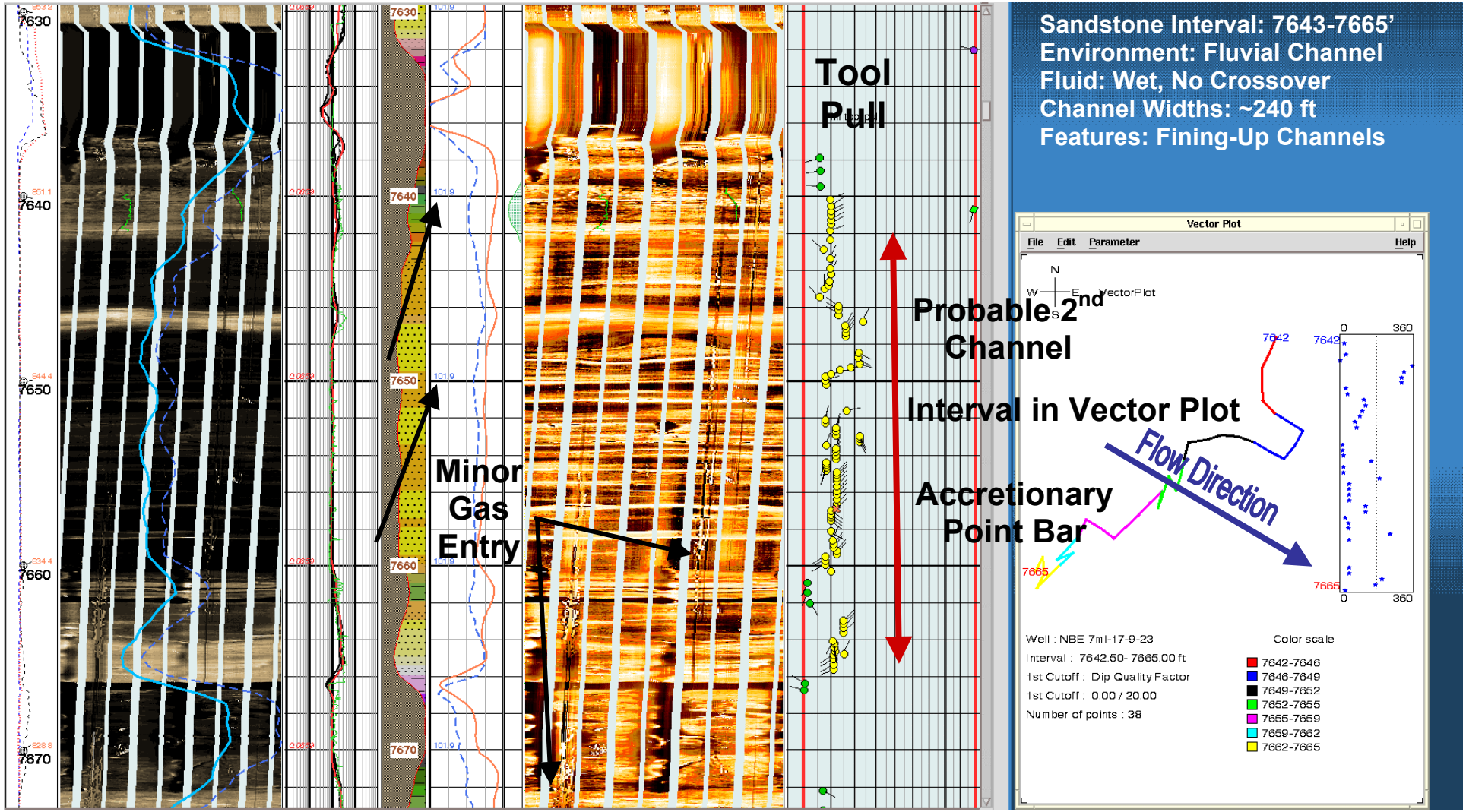

Figure 9. Portion of the FMI log across two, possibly 3, stacked fluvial channel sands with basal troughs and accretionary point bars.

Model for Deposition of Lateral Accretion Beds with Consistent Orientation and Dip in Fluvial Point Bar System

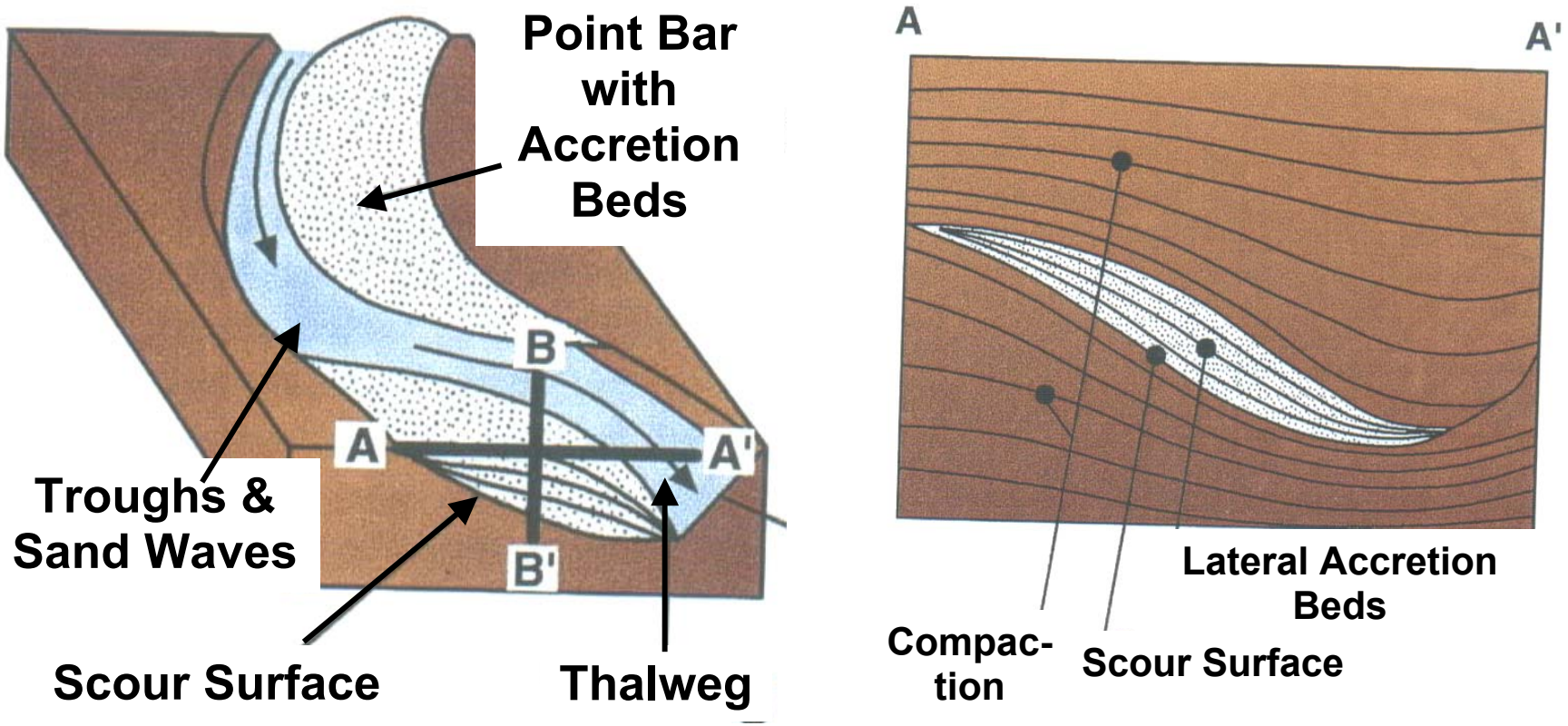

Adapted from Grace and Newberry, 1998

Figure 10. Schematic model for a meandering fluvial channel sand with lateral accretion beds being deposited in point bar environments.
Copyright Schlumberger® 1998, used with permission of Schlumberger Oilfield Services.

Questar
7ML-17-9-23

Scale: 1” = 5’

Middle Mesaverde: Braided Stream Complex

Density Porosity: 10→¨4%
Avg. Gamma Ray: 60-90 API
Natural Fractures: None

Deep Rt: 30 ohm-m
Breakout: Minor
Gas Entry: Minor
Perforated: Yes, No Gas Entry

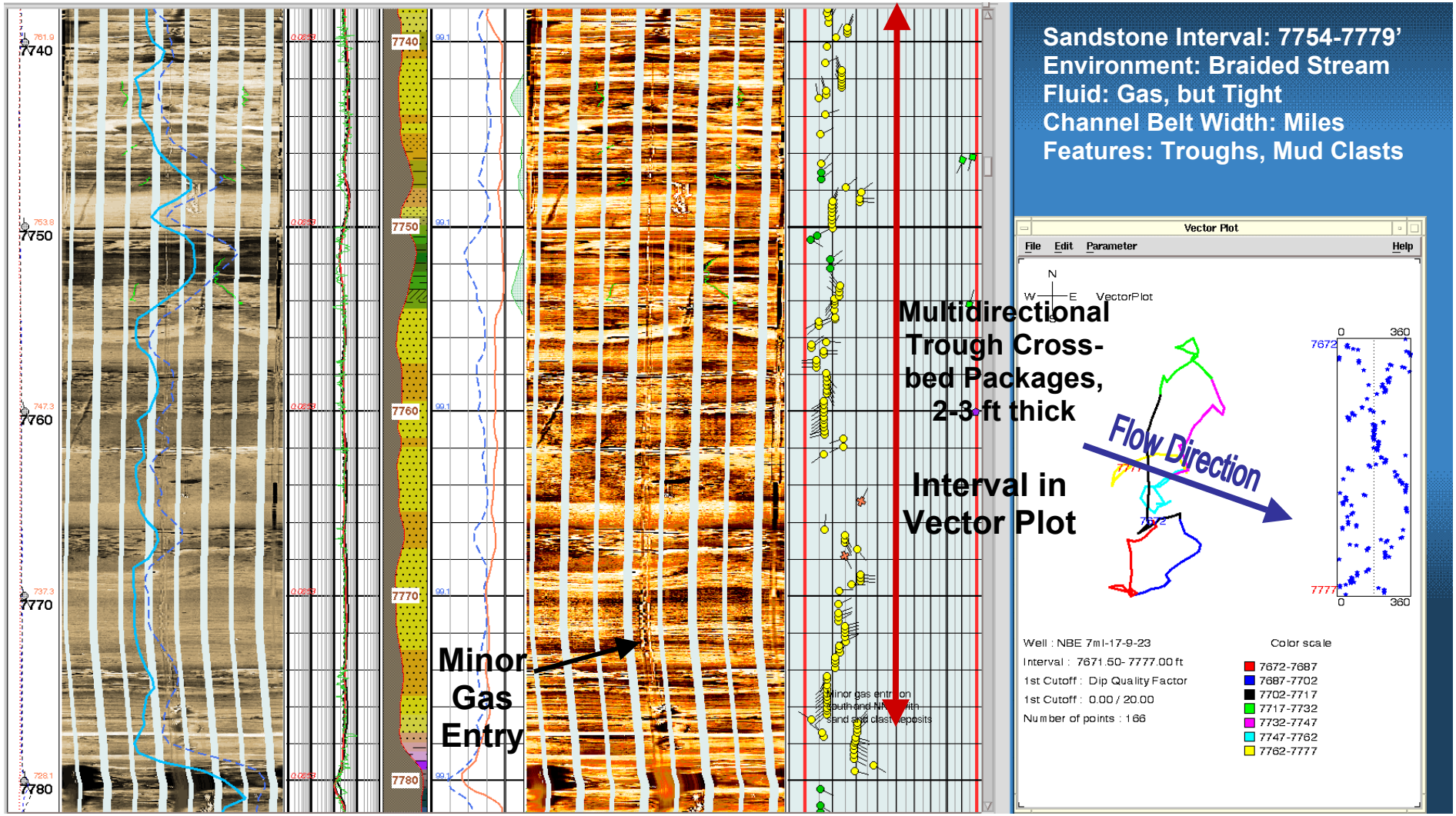

Figure 11. Portion of the FMI log across a braided stream deposit of small channels with trough crossbeds in 2- to 3-ft packages.

Questar 7ML-17-9-23

Scale: 1” = 1’

Troughs and Rip-Up Clasts, Braided Stream Deposit

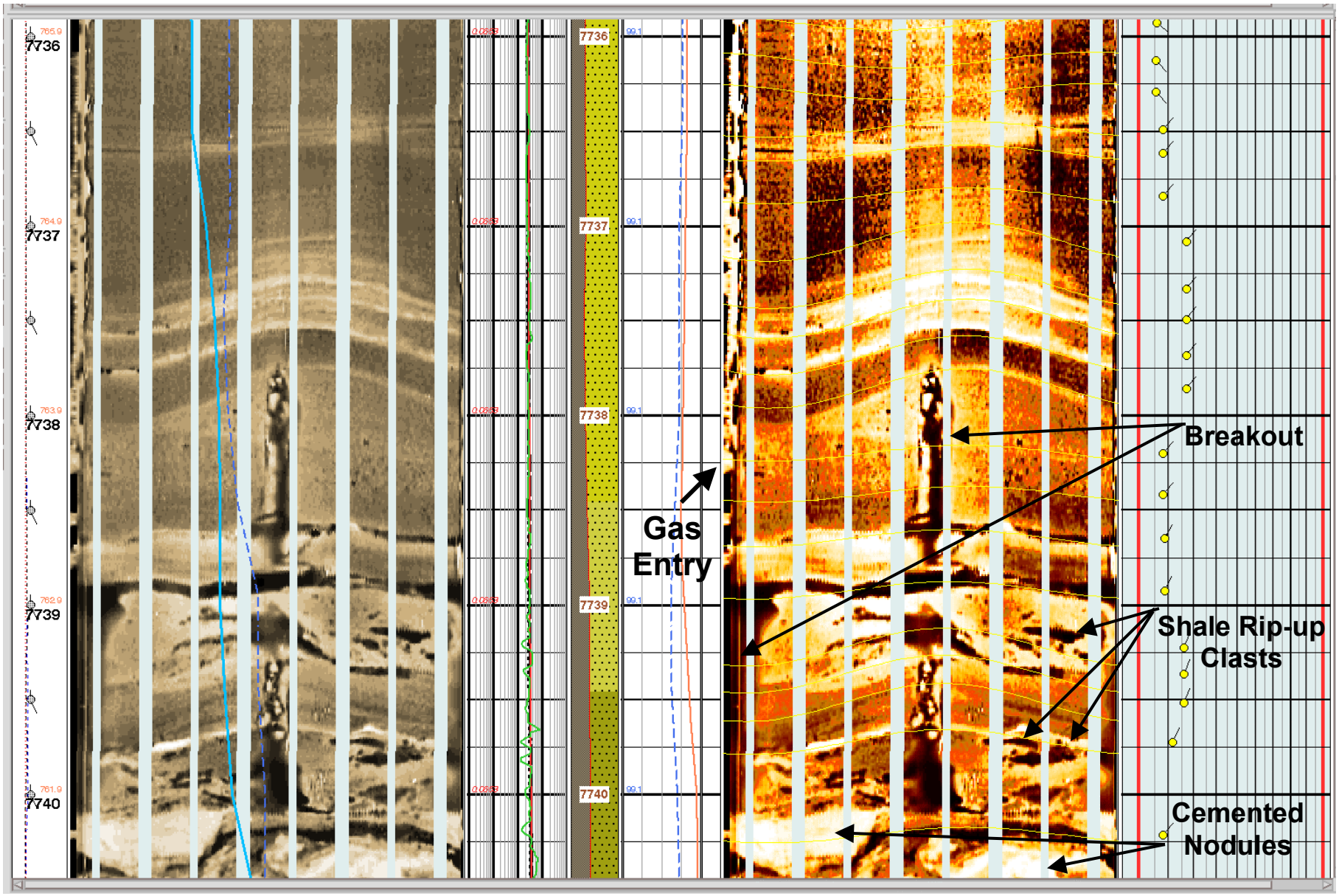

Figure 12. Part of the FMI log shown in Figure 11 at a scale of 1 inch = 1 ft showing bedding features, breakout, and shale rip-up clasts.

Questar 7ML-17-9-23

Scale: 1” = 5’

Middle Mesaverde: Braided Stream Complex

Density Porosity: 2-8%
Avg. Gamma Ray: 60-80 API
Natural Fractures: None

Deep Rt: 40 ohm-m
Breakout: Minor
Gas Entry: Some
Perforated: Yes, No Production

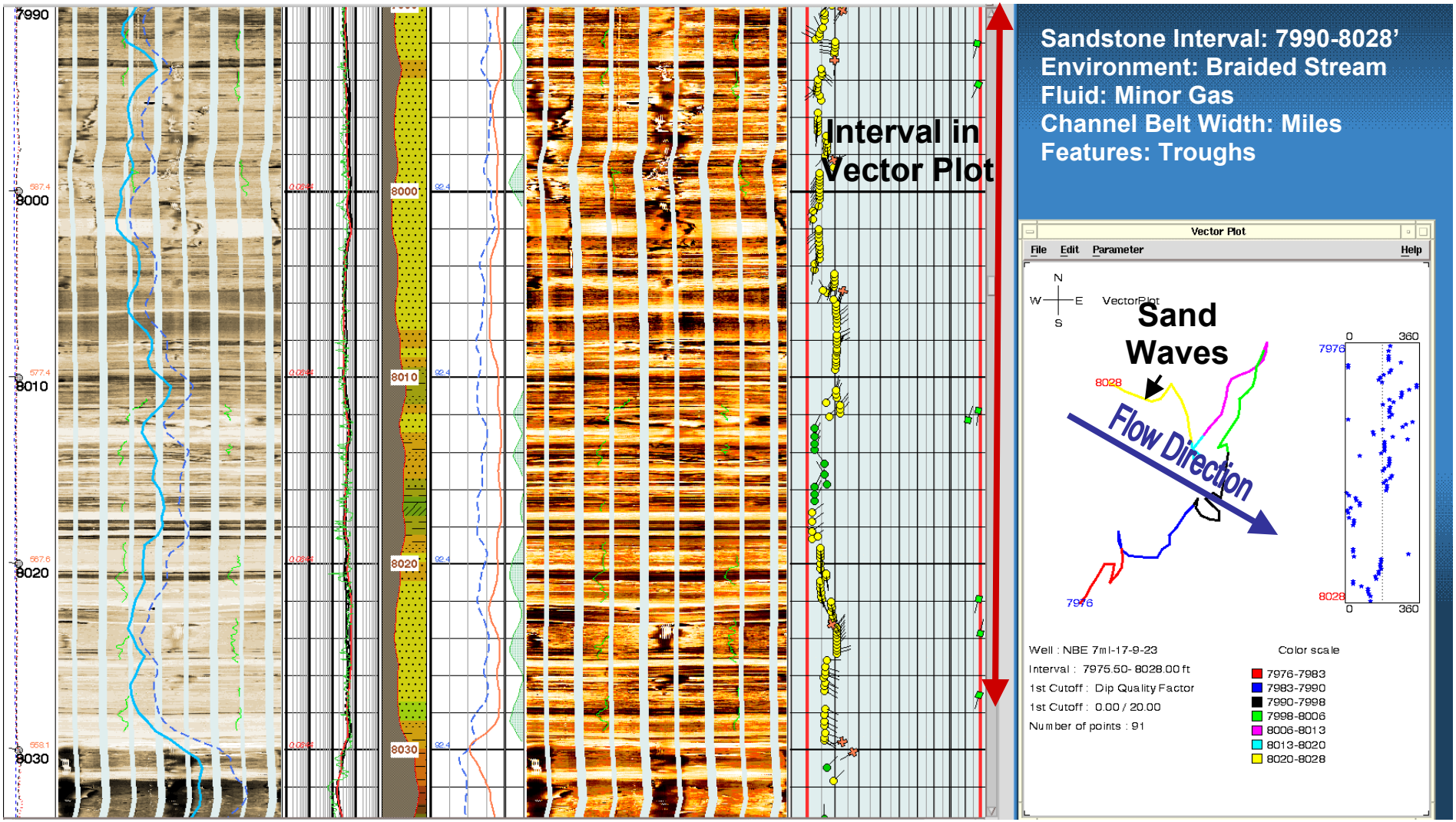

Figure 13. Portion of the FMI log across another braided stream deposit that was perforated, but yielded no gas or water production.

Modern Example of a Braided Stream Complex: Colville River Floodplain, North Slope, Alaska

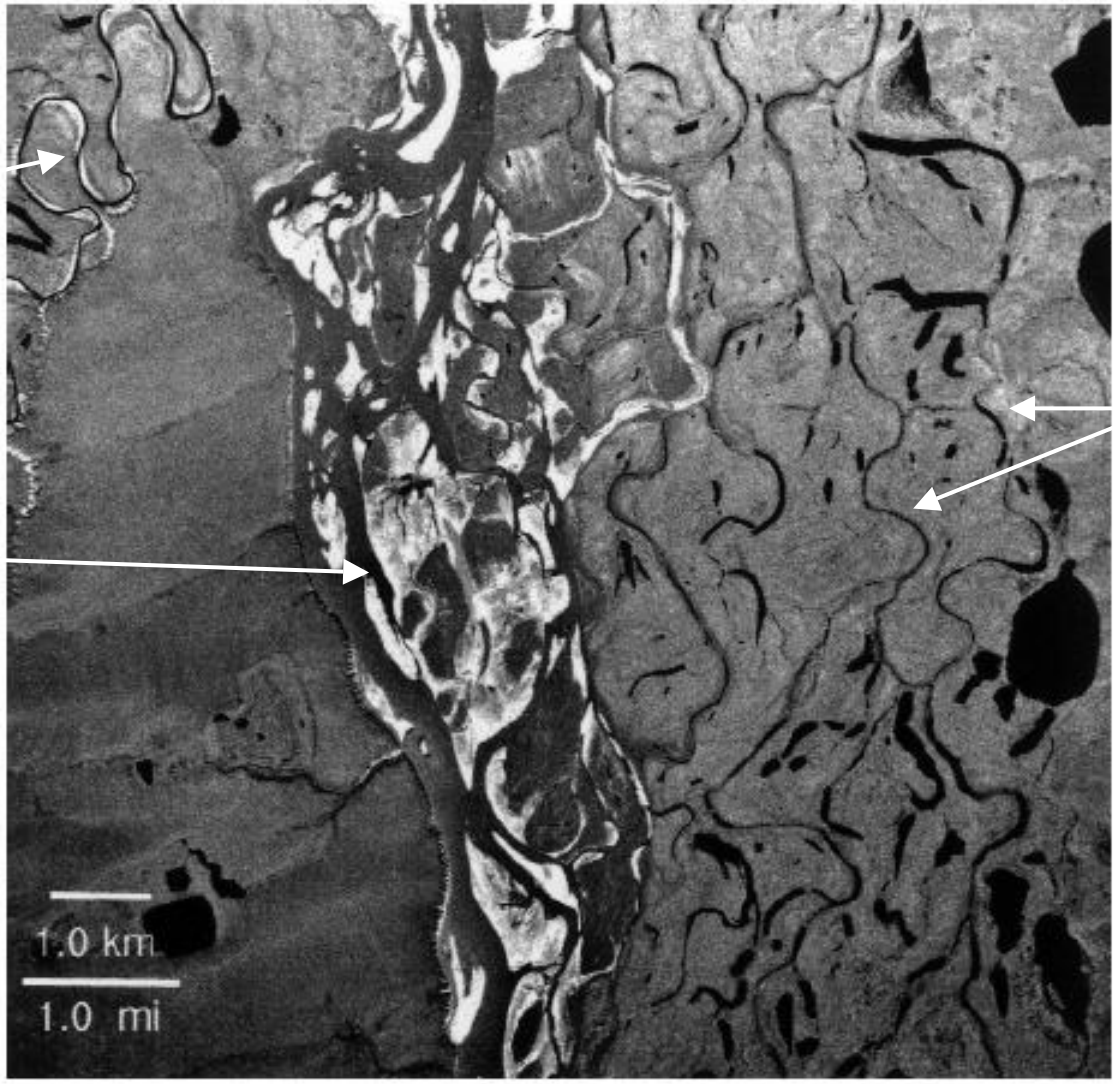

From Bridge and Tye, 2000

Figure 14. Aerial photo of fluvial channels on Alaska's North Slope where the Colville River forms a braided stream complex a mile wide.

Questar
7ML-17-9-23

Scale: 1” = 5’

Middle Mesaverde: Lower Fluvial Interval

Density Porosity: 10-12%
Avg. Gamma Ray: 52 API
Natural Fractures: None

Deep Rt: 40 ohm-m
Breakout: Yes
Gas Entry: Minor
Perforated: Yes, Minor Production

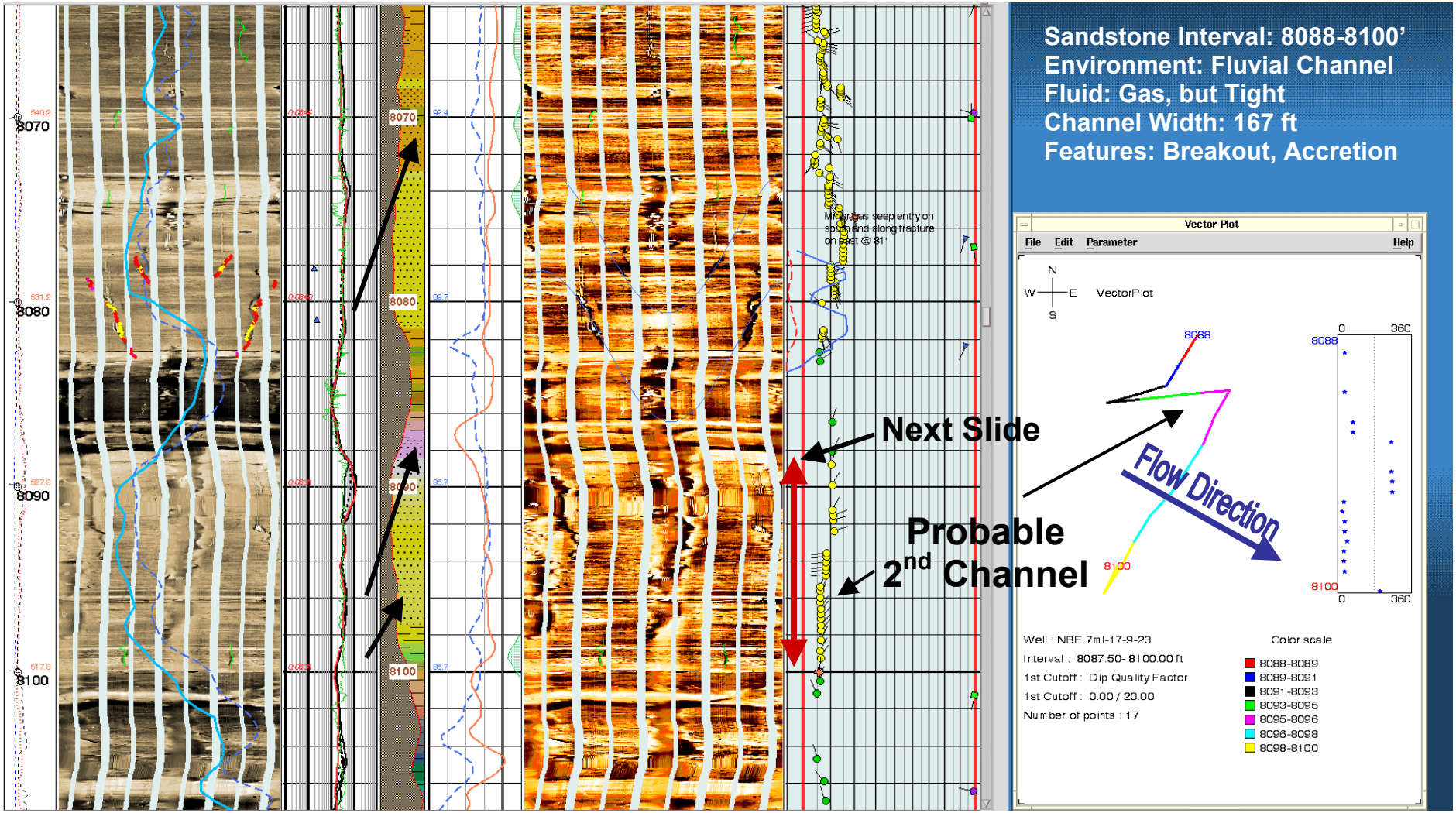

Figure 15. Part of the FMI log showing more stacked fining-upward fluvial channel sandstones: Middle Mesaverde's Lower Fluvial Interval.

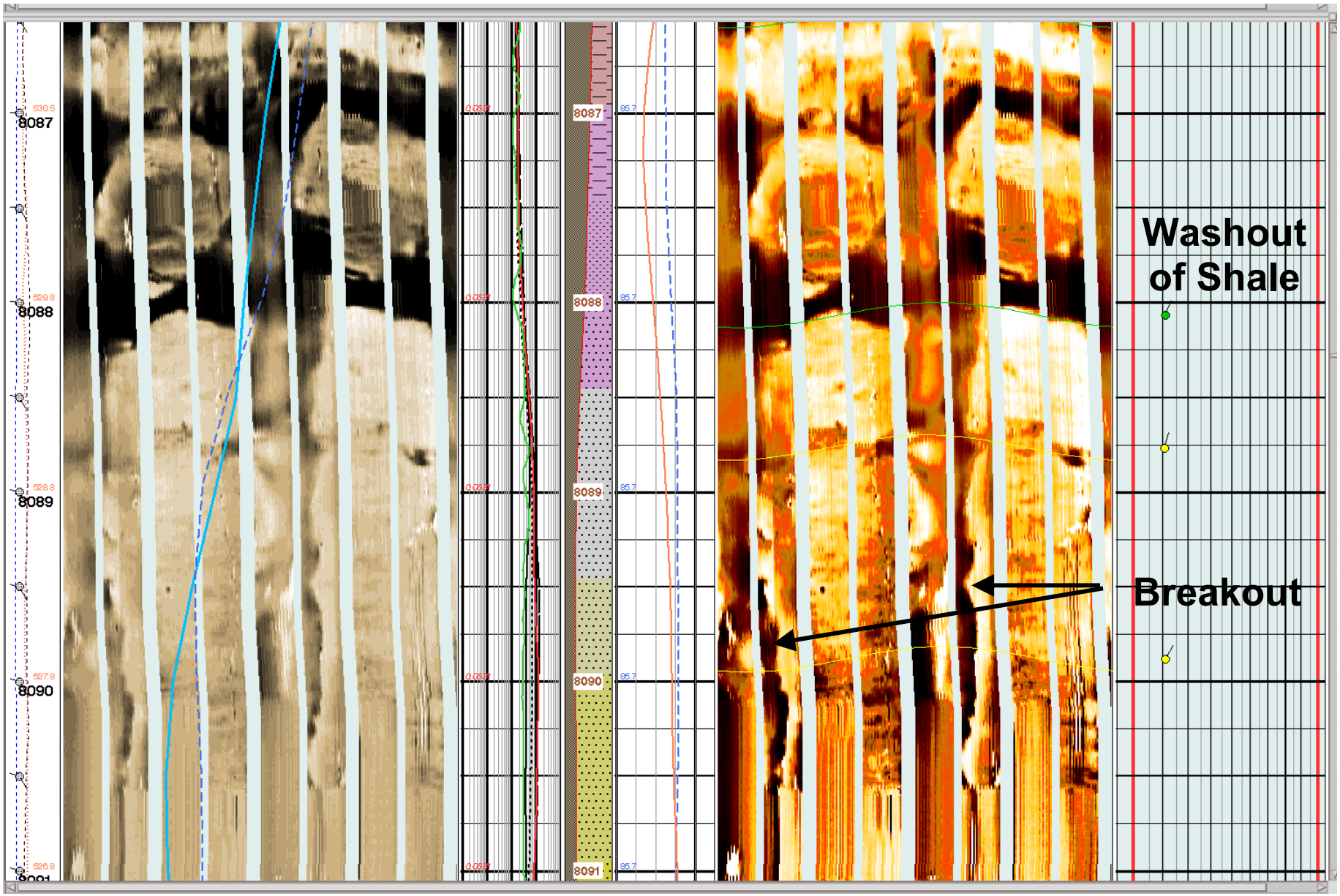

Figure 16. Part of the FMI log in Figure 15 showing the top of a fluvial channel sandstone where the overlying shale has considerable washout.

Questar 7ML-17-9-23

Scale: 1” = 5’

Lower Mesaverde: Upper Coaly Interval

Density Porosity: 14% **Deep Rt: 50 ohm-m**
Avg. Gamma Ray: 28 API **Breakout: Yes**
Natural Fractures: Common **Gas Entry: Poor Data**
Perforated: Yes, Best Mesaverde Zone in Well

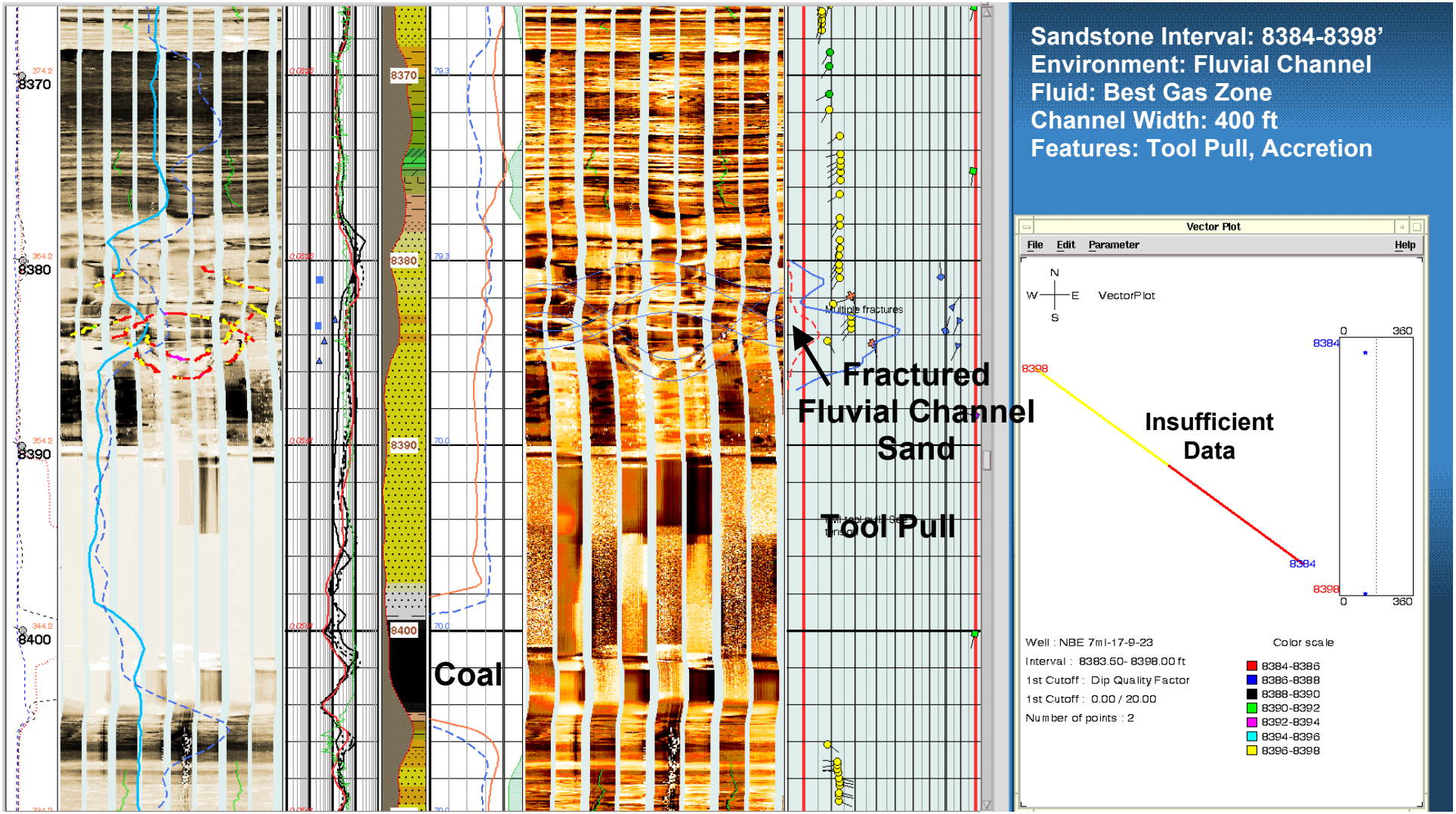

Figure 17. Part of the FMI log showing fractures in the best gas-producing fluvial channel sand in the Mesaverde Group and tool pull.

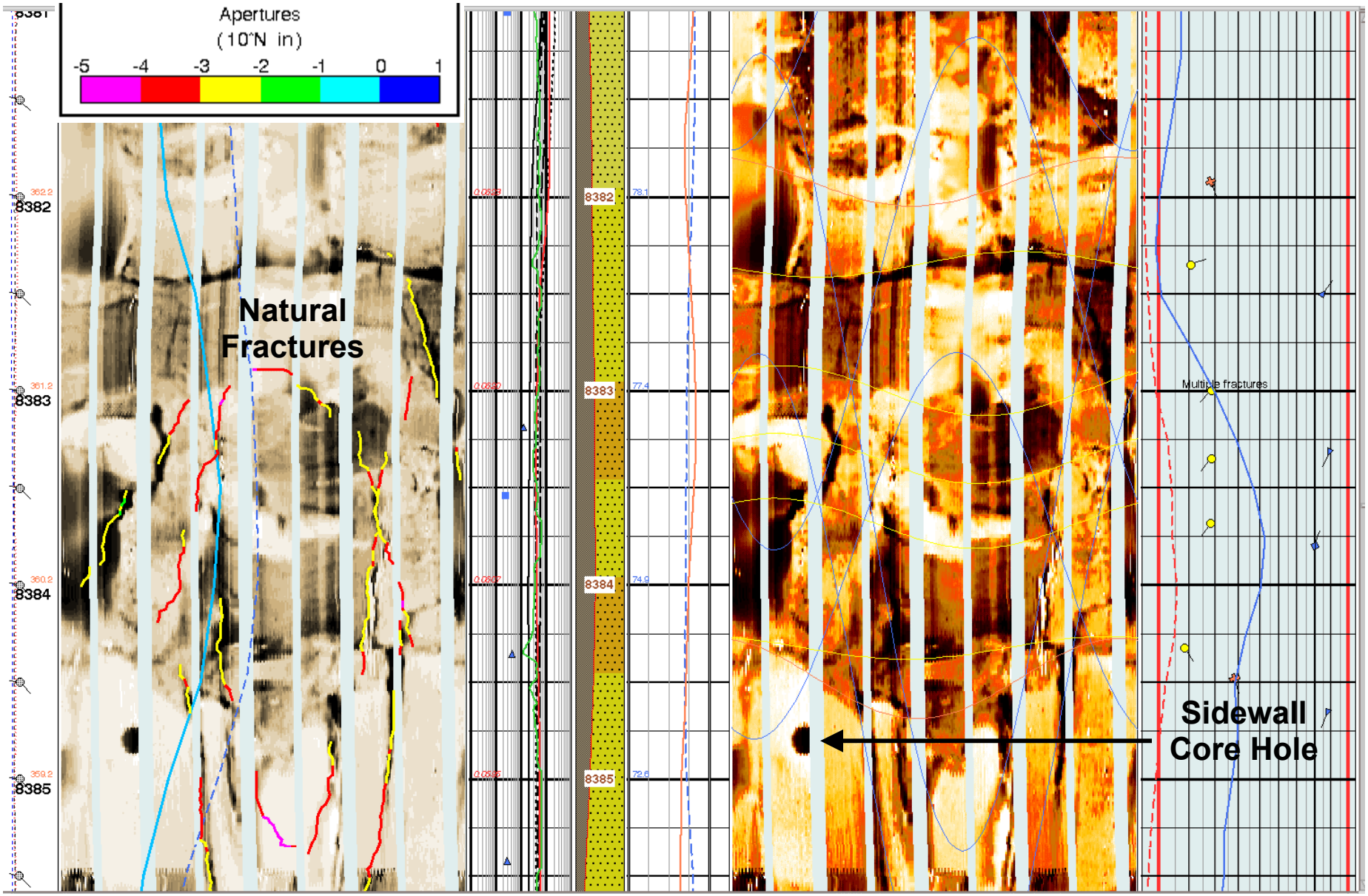

Figure 18. Closer view of the FMI log across the fractured fluvial channel that yielded significant amounts of gas in the 7ML-17 well.

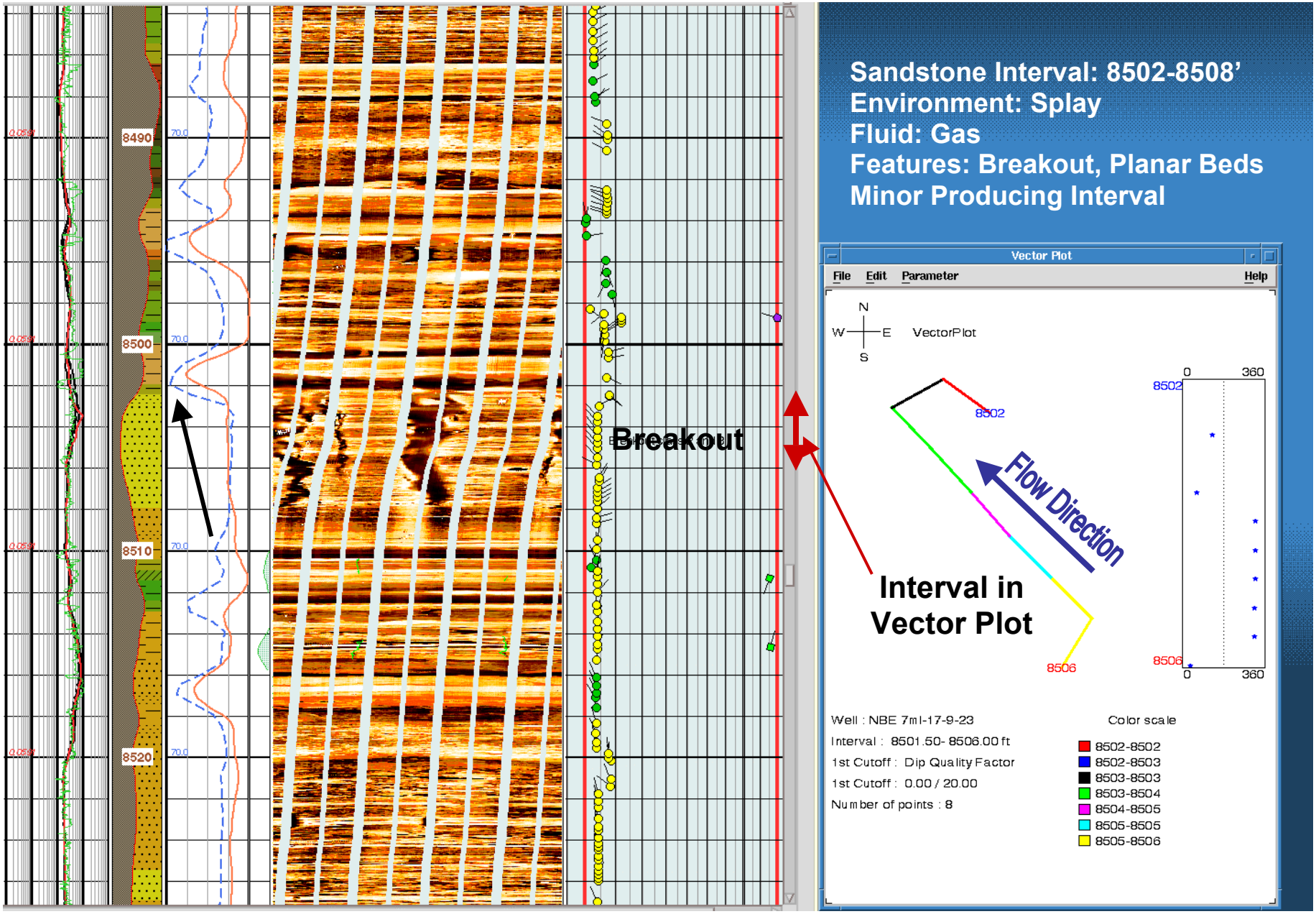

Figure 19. Part of the FMI log showing a thin (6-ft) splay sandstone with common breakout. This sandstone yielded some gas.

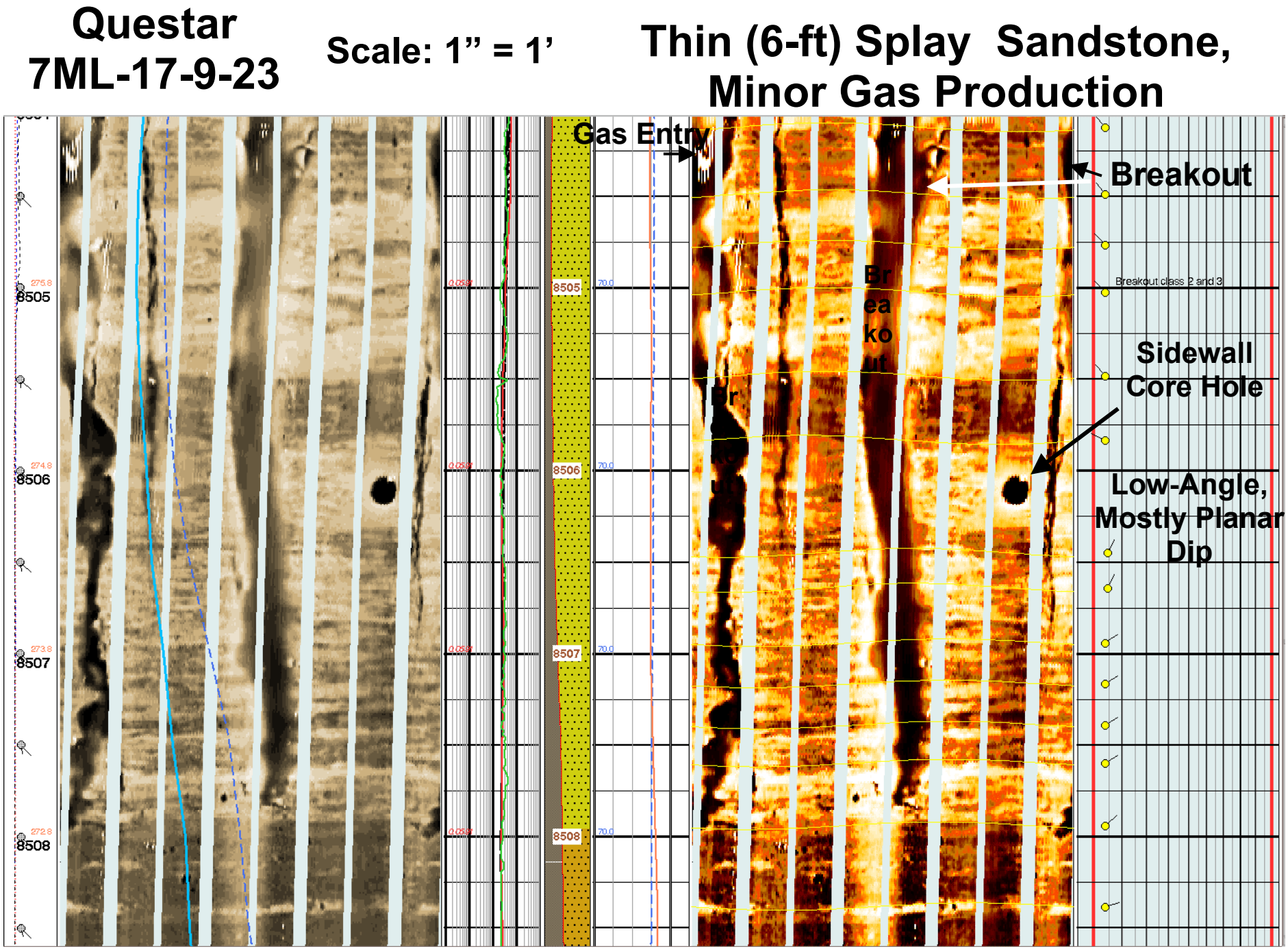

Figure 20. Closer view of the same splay sandstone shown in Figure 19 with low-angle planar bedding and common breakout.

Questar 7ML-17-9-23 Scale: 1” = 5’

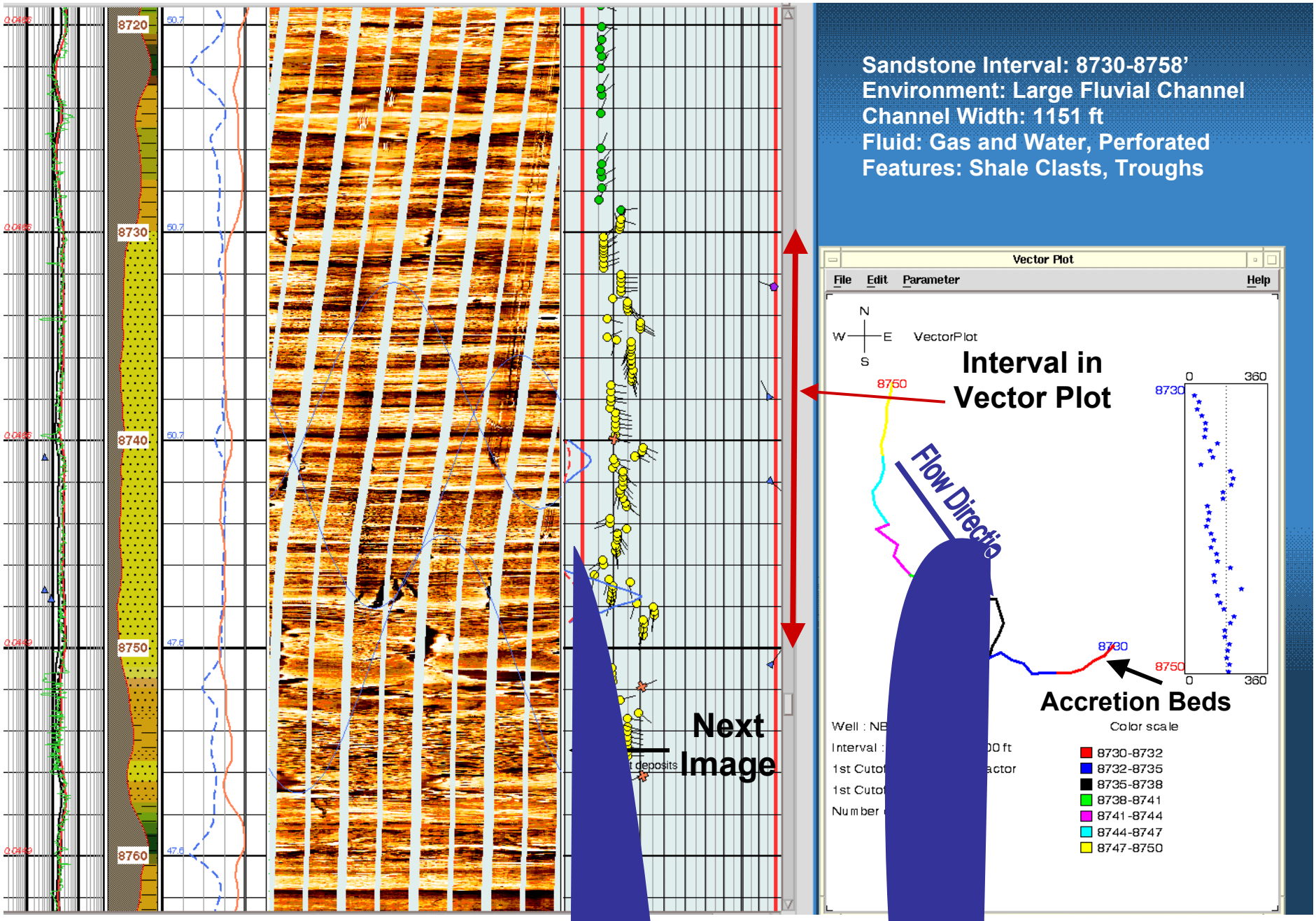

Figure 21. Part of the FMI log s ng a thick fluvial nel sand in the Lower Mesaverde wi at rip-up clasts a ase.

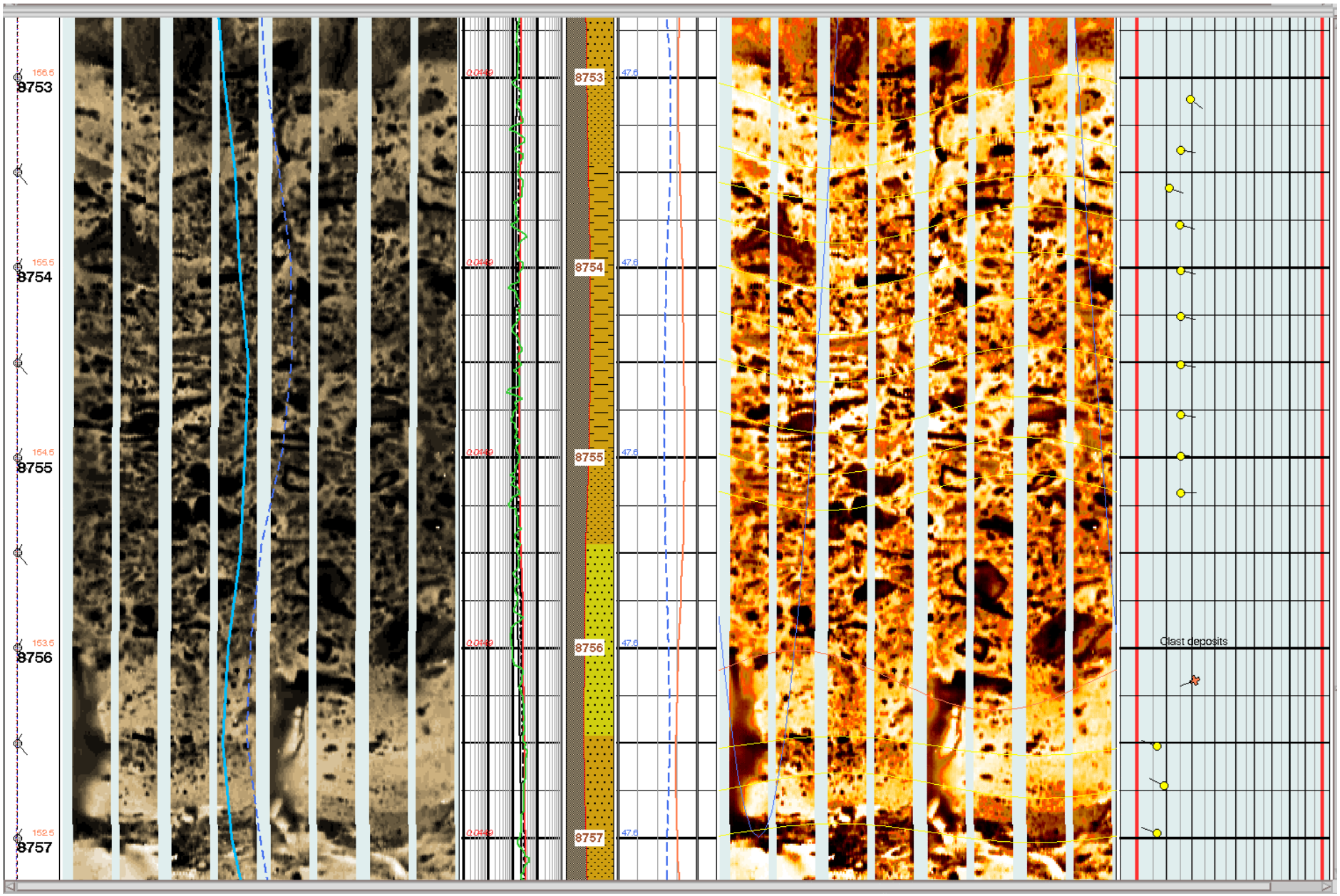

Figure 22. Closer view of the shale rip-up clasts at the base of the fluvial channel shown in Figure 21.

Questar 7ML-17-9-23

Scale: 1” = 5’

Burrows in Lagoonal Sands: Upper Sego Transitional Interval

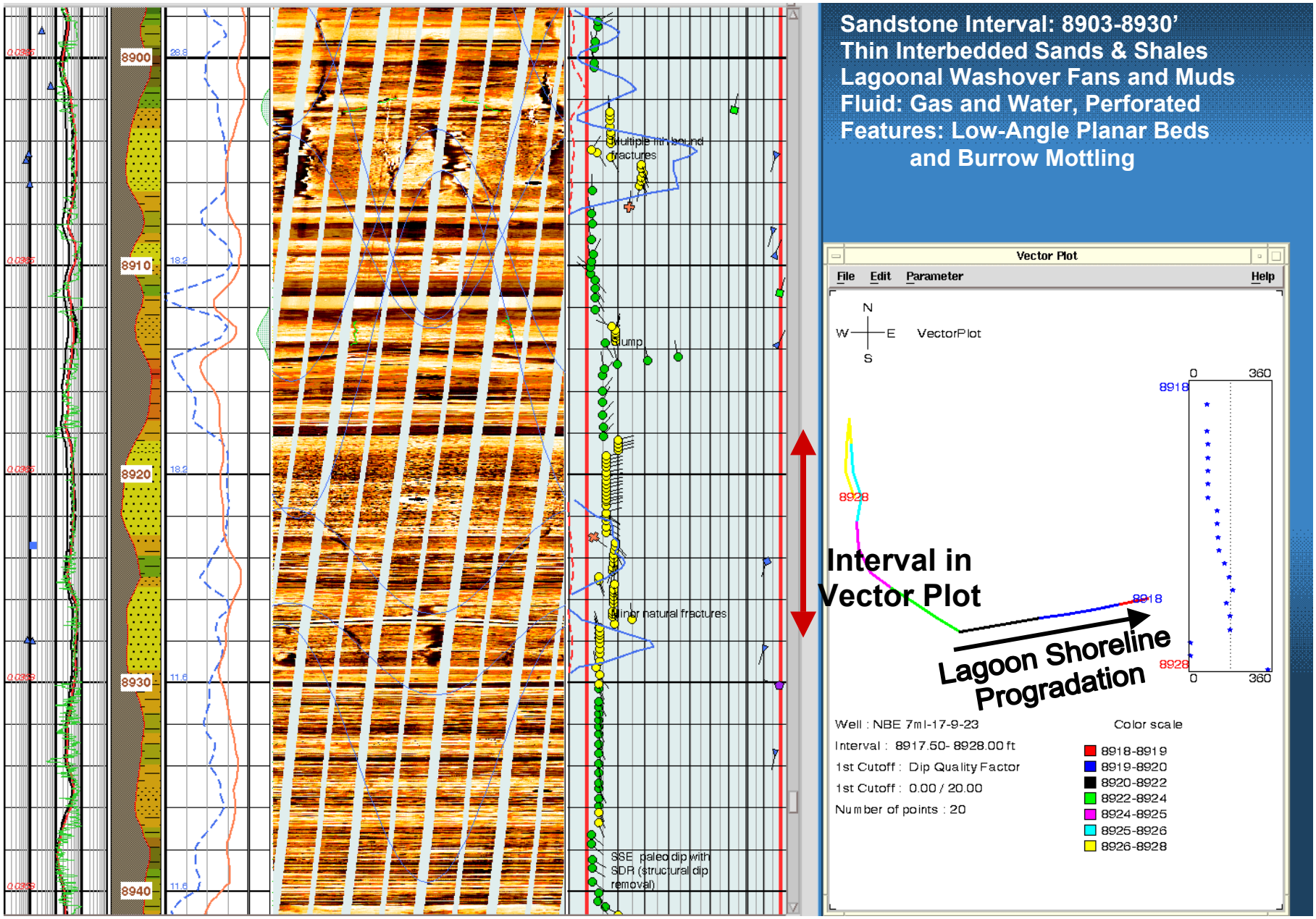

Figure 23. Part of the FMI log from lagoonal deposits in the Upper Sego Transitional Interval showing bioturbation in washover fans.

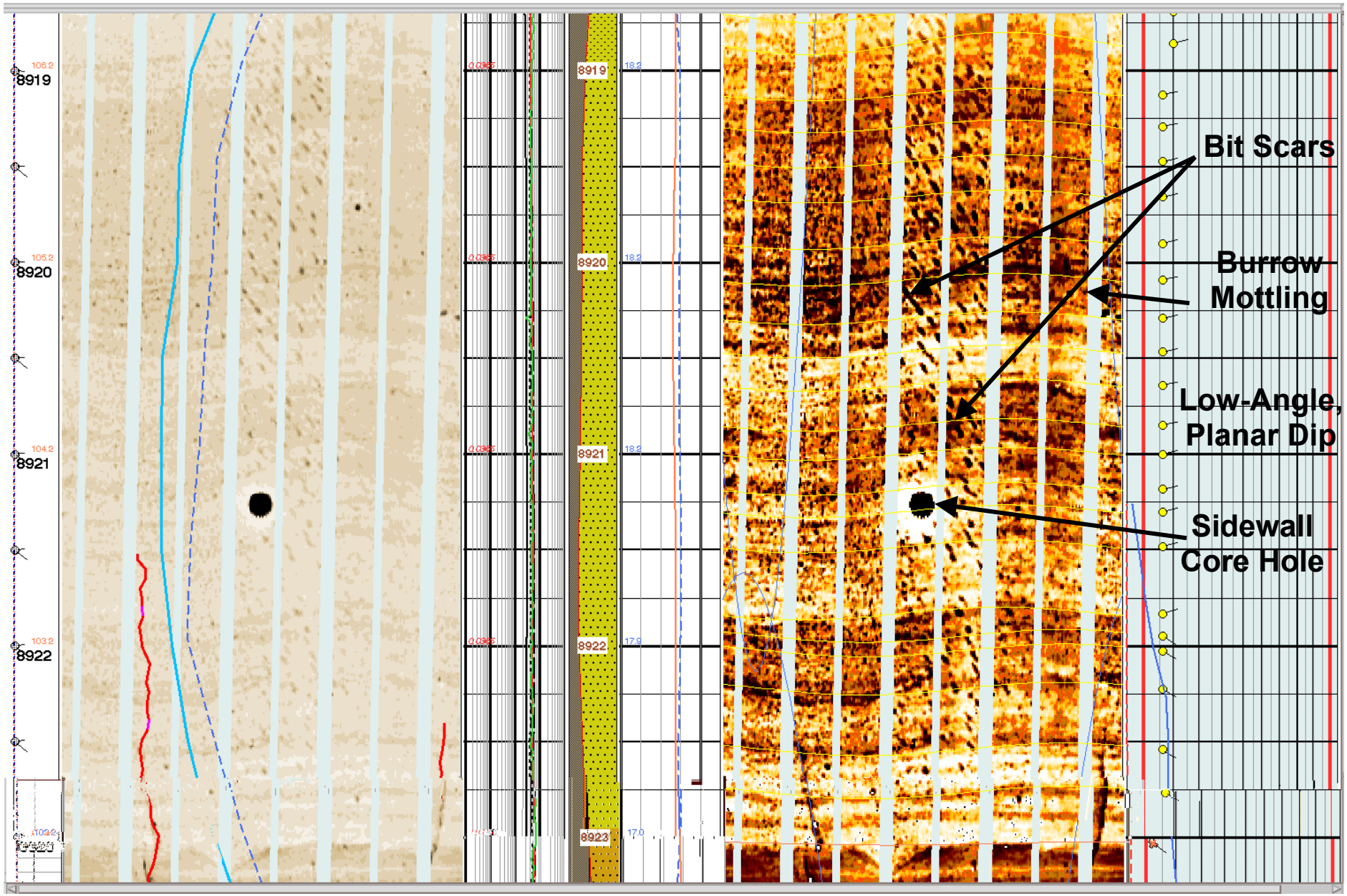

Figure 24. Closer view of the same burrowed sandstones shown in Figure 23 that also contain some oblique bit scarring.

Depositional Model for Burrowed Lagoonal Sands with Washover Fans

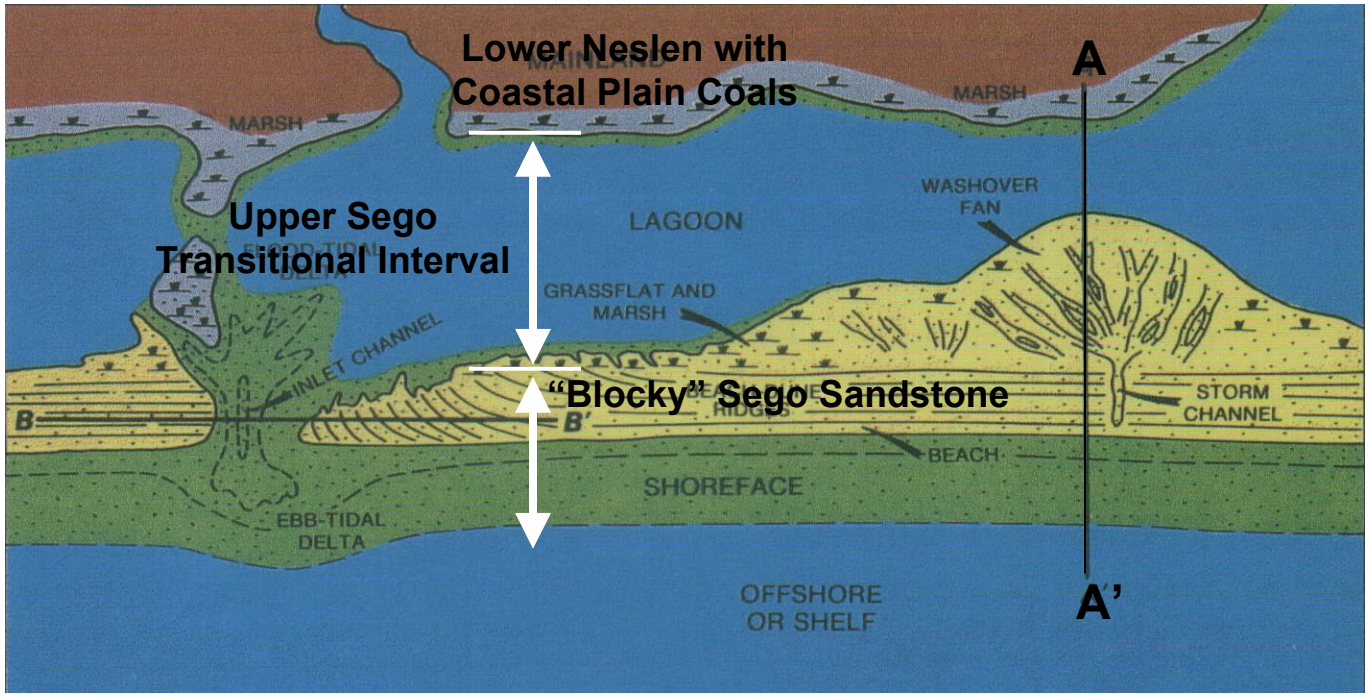

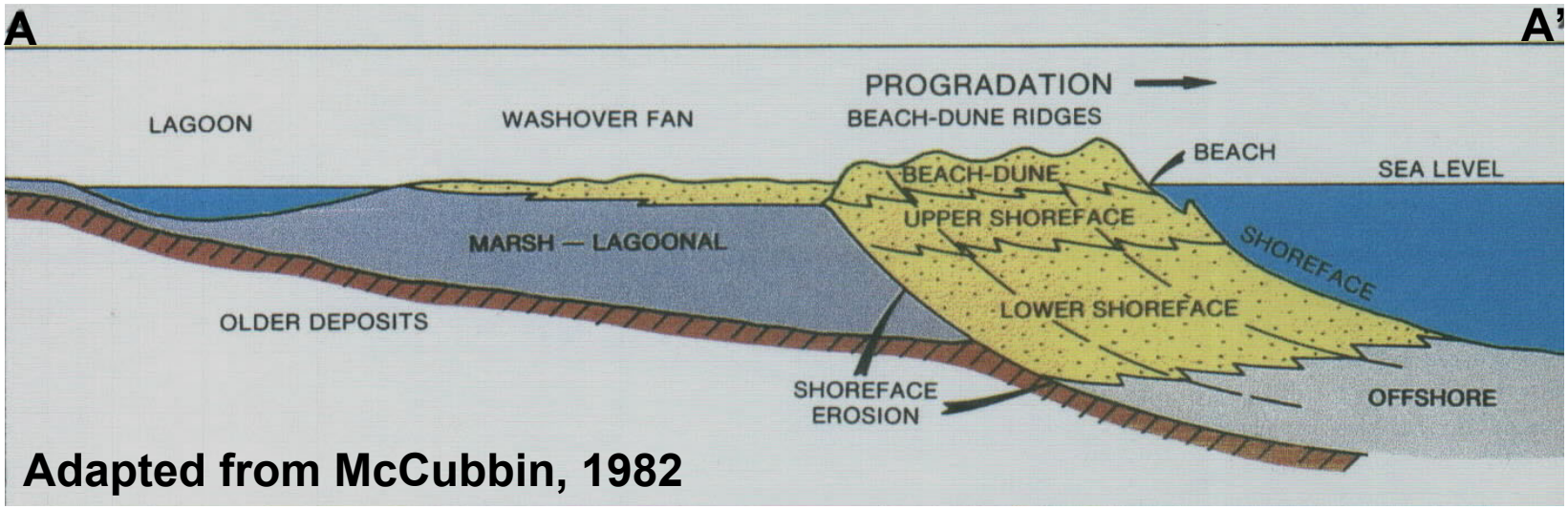

Figure 25. Schematic model for lagoonal sandstones and washover fans in the Upper Sego coastal complex. Adapted from McCubbin, 1982.

Questar 7ML-17-9-23

Scale: 1” = 5’

Burrows and Crossbedding: Upper Sego Sandstone

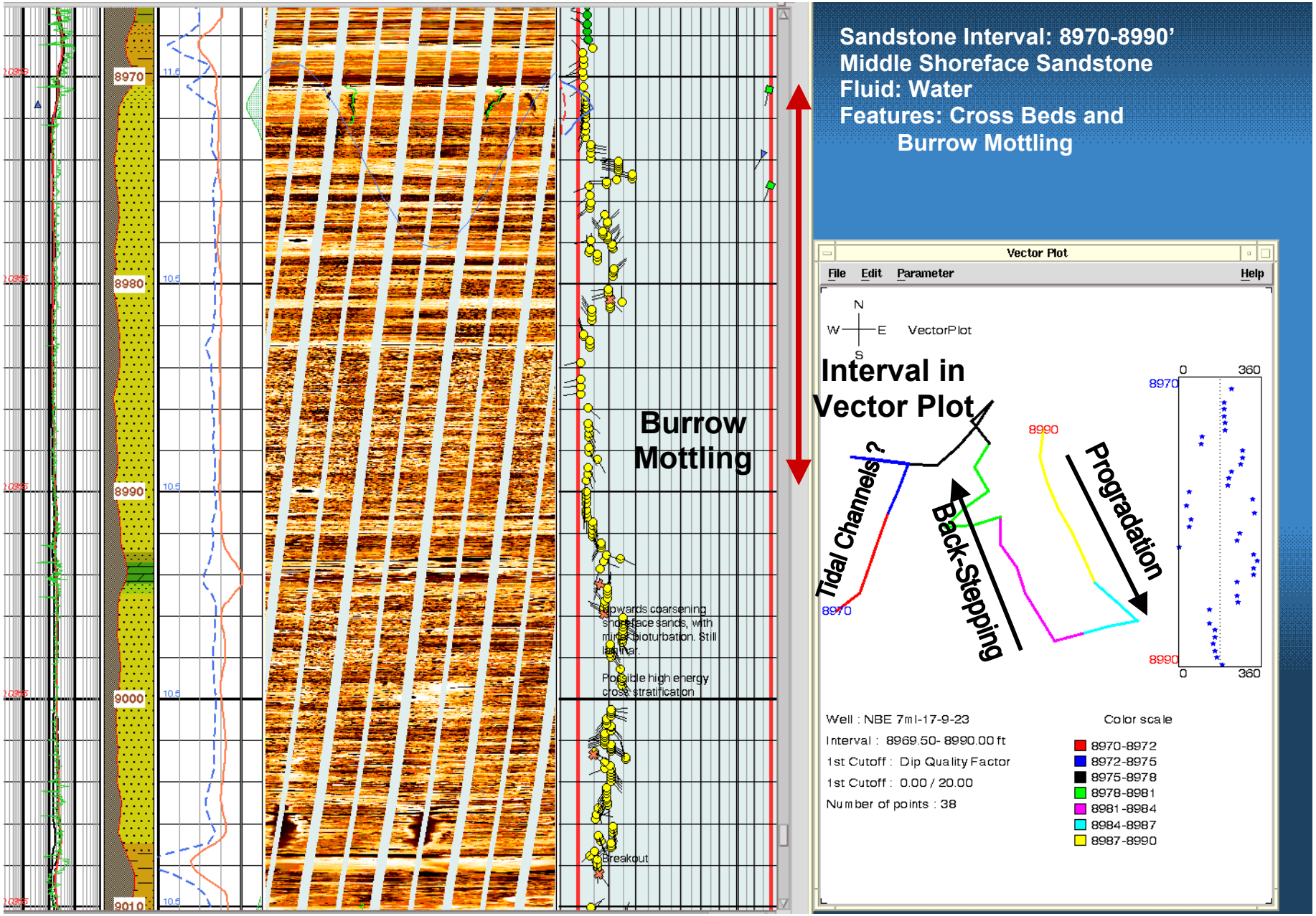

Figure 26. Part of the FMI log from the Upper Sego "Blocky" Sandstone, a lower and middle shoreface coastal environments.

Questar 7ML-17-9-23

Scale: 1” = 1’

Burrows and Crossbedding: Upper Sego Sandstone

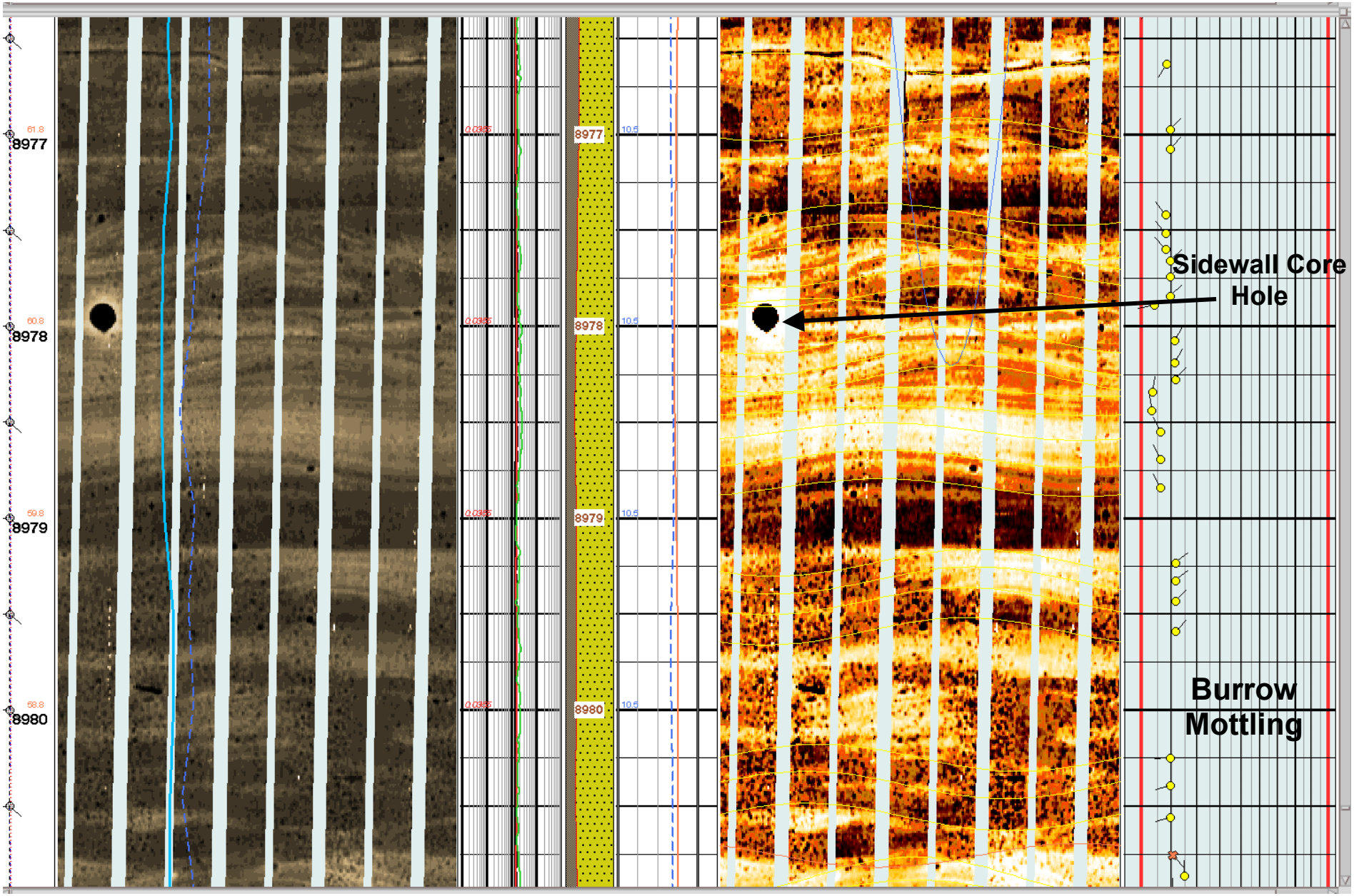

Figure 27. Closer view of the crossbedding and burrowing in the lower to middle shoreface sandstones of the "Blocky" Sego Sandstone.

Questar 7ML-17-9-23

Scale: 1” = 5’

Burrows and Planar Beds: Lower Sego Sandstone

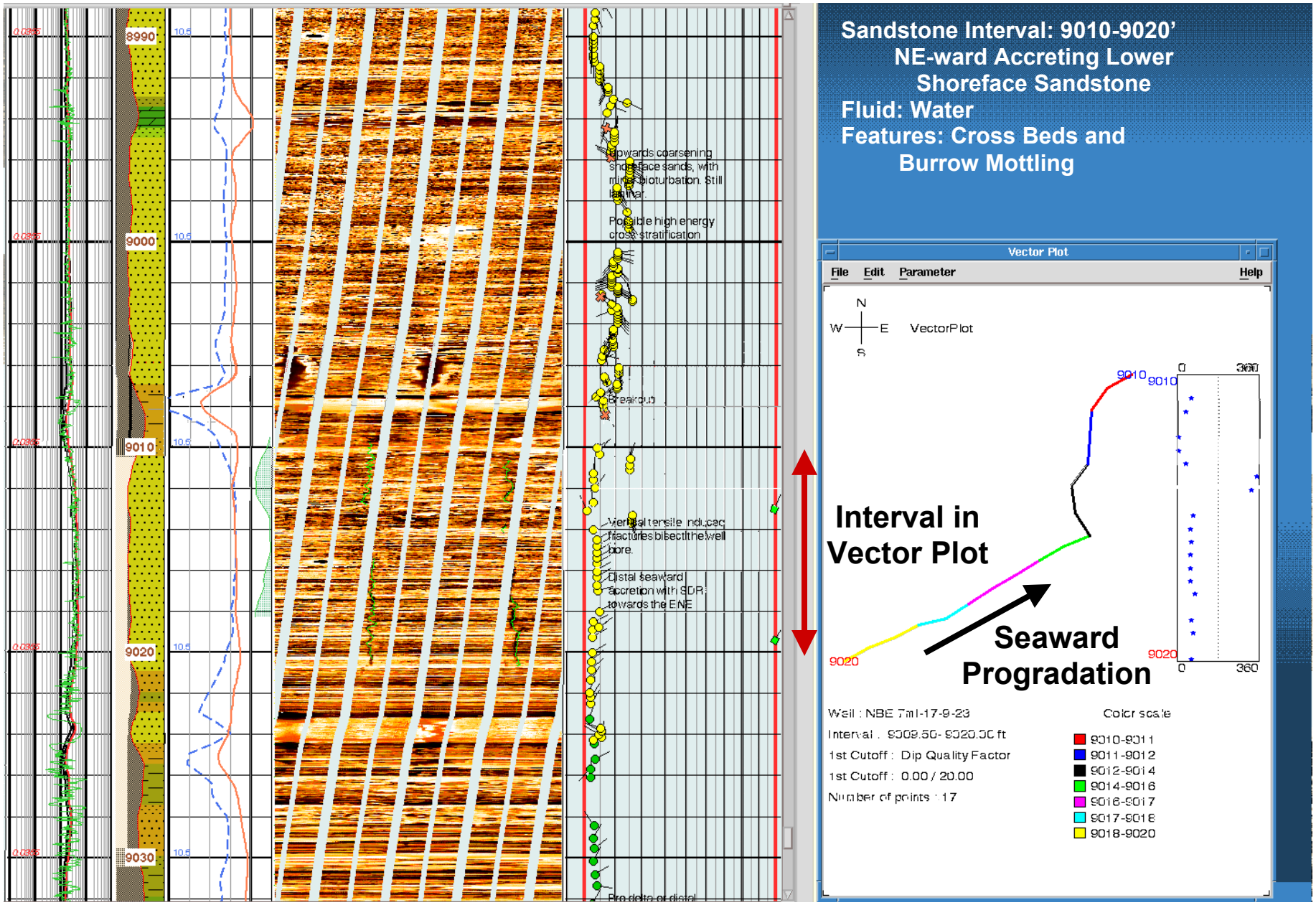

Figure 28. Part of the FMI log from lower part of the Sego Sandstone showing low-angle planar beds prograding seaward.

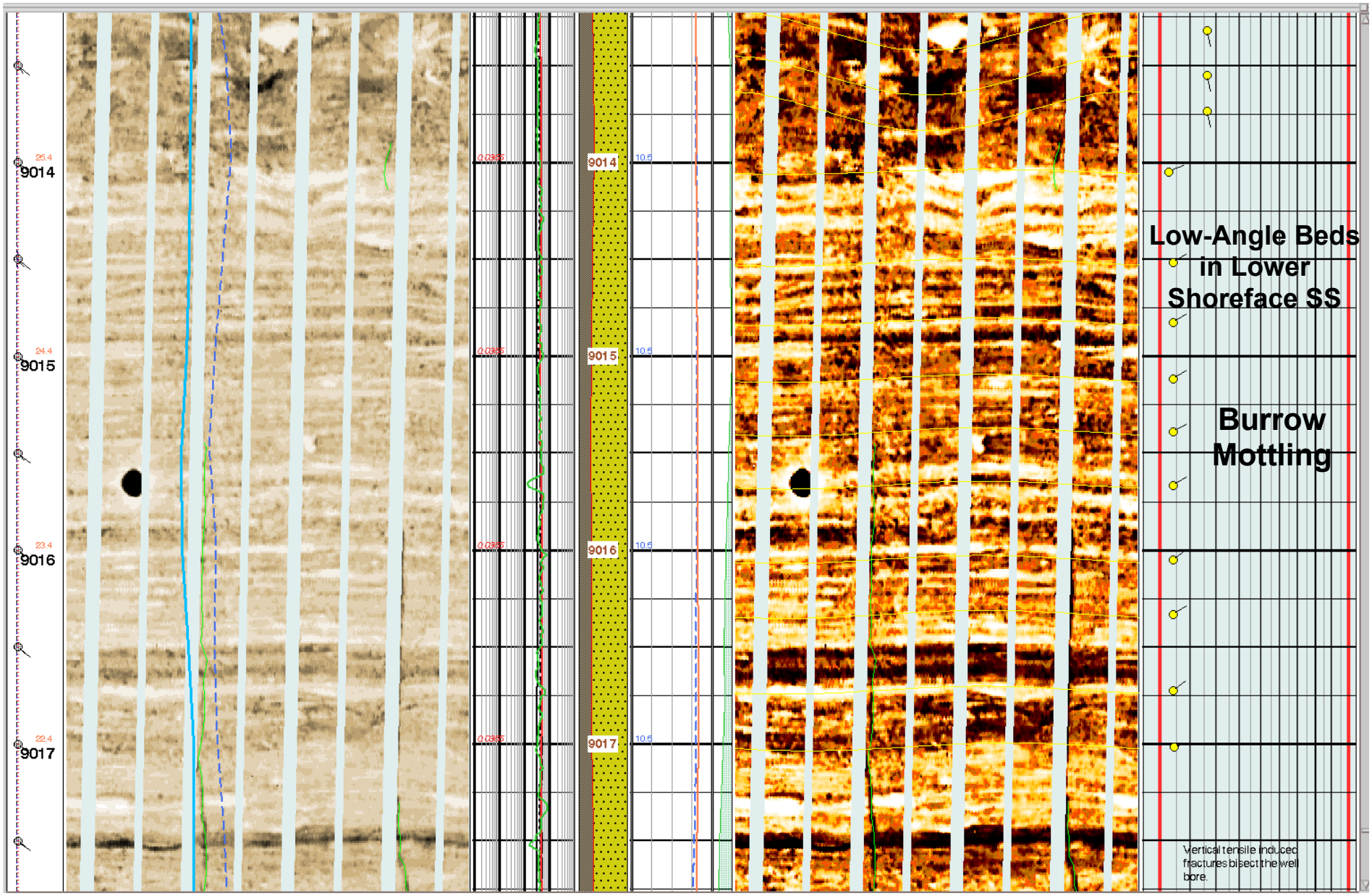

Figure 29. Closer view of the same burrowed sandstones shown in Figure 28 along with thin, resistive carbonate-cemented beds.

Questar 7ML-17-9-23

Scale: 1” = 5’

Planar Beds in Buck Tongue Shale on Wet Castlegate Sandstone

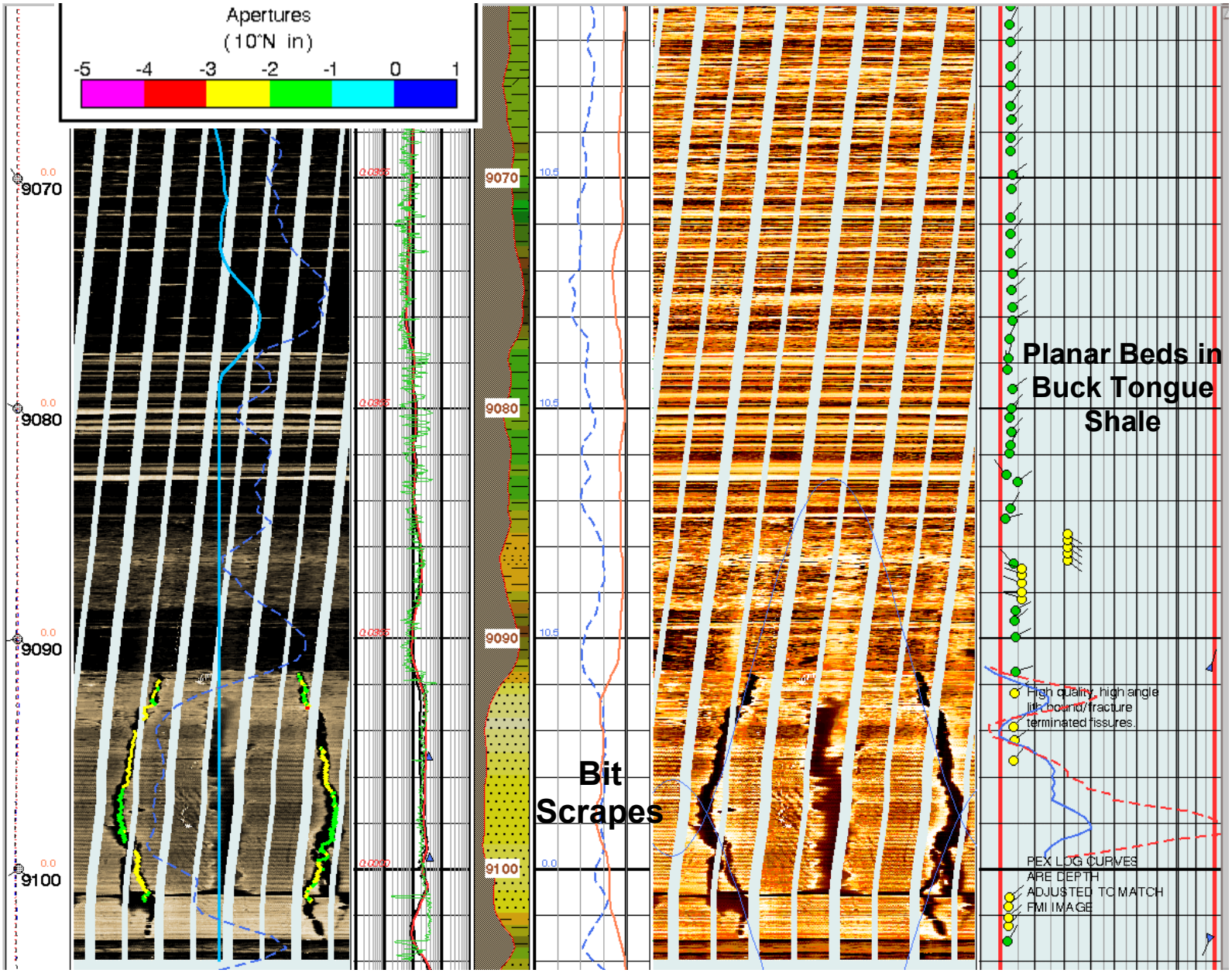

Figure 30. Part of the FMI log showing the contact between the Castlegate Sandstone and overlying Buck Tongue marine shale.

Questar 7ML-17-9-23

Scale: 1” = 1’

Lithology-Bound Fractures and Burrows in Wet Upper Castlegate Sandstone

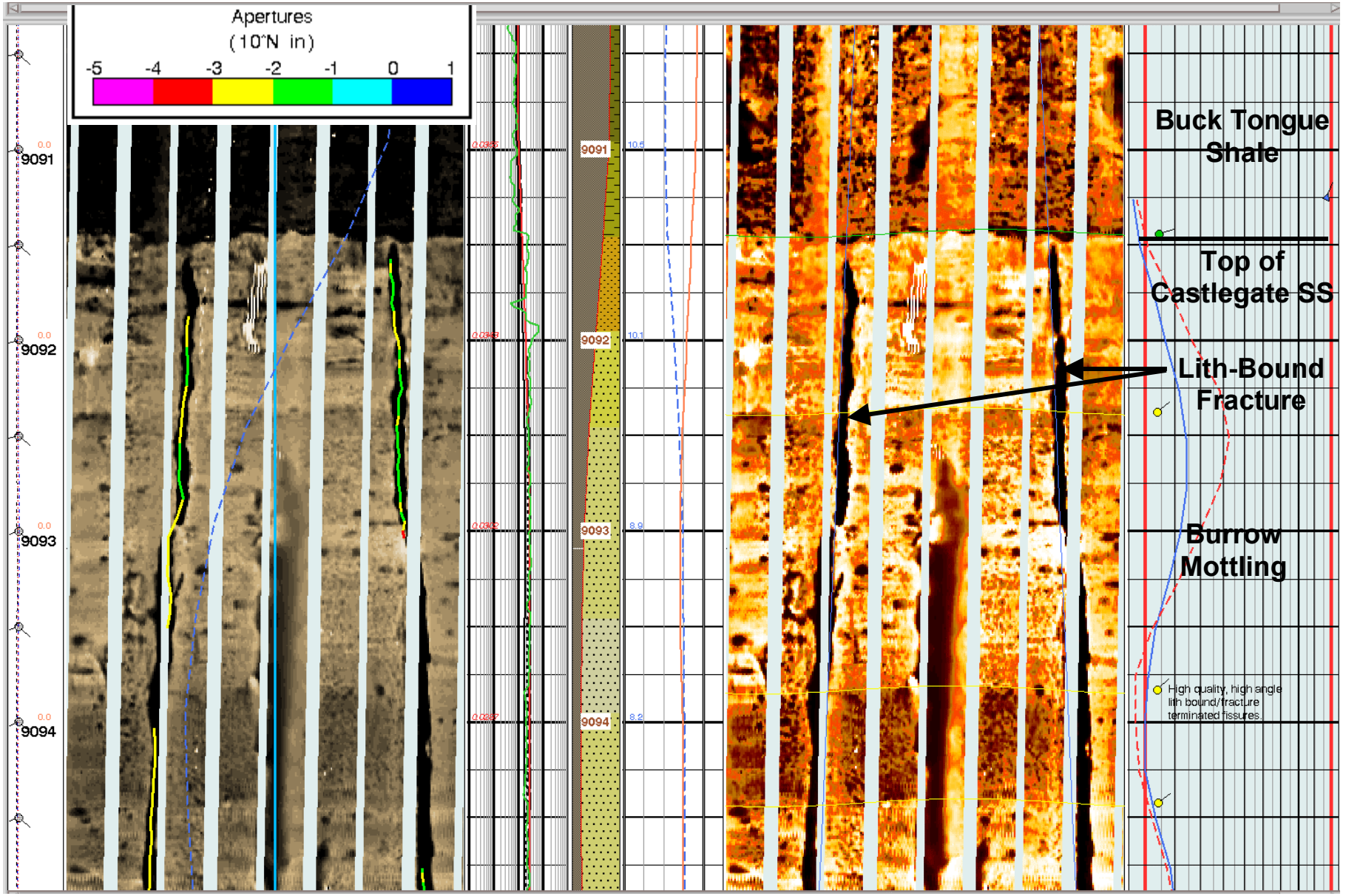

Figure 31. Closer view of lithology-bound fractures at the top of the Castlegate Sandstone, which has some burrows.

EOG CWU 807-10

Scale: 1” = 5’

Uppermost Blackhawk Sandstone Capped by Mancos Shale

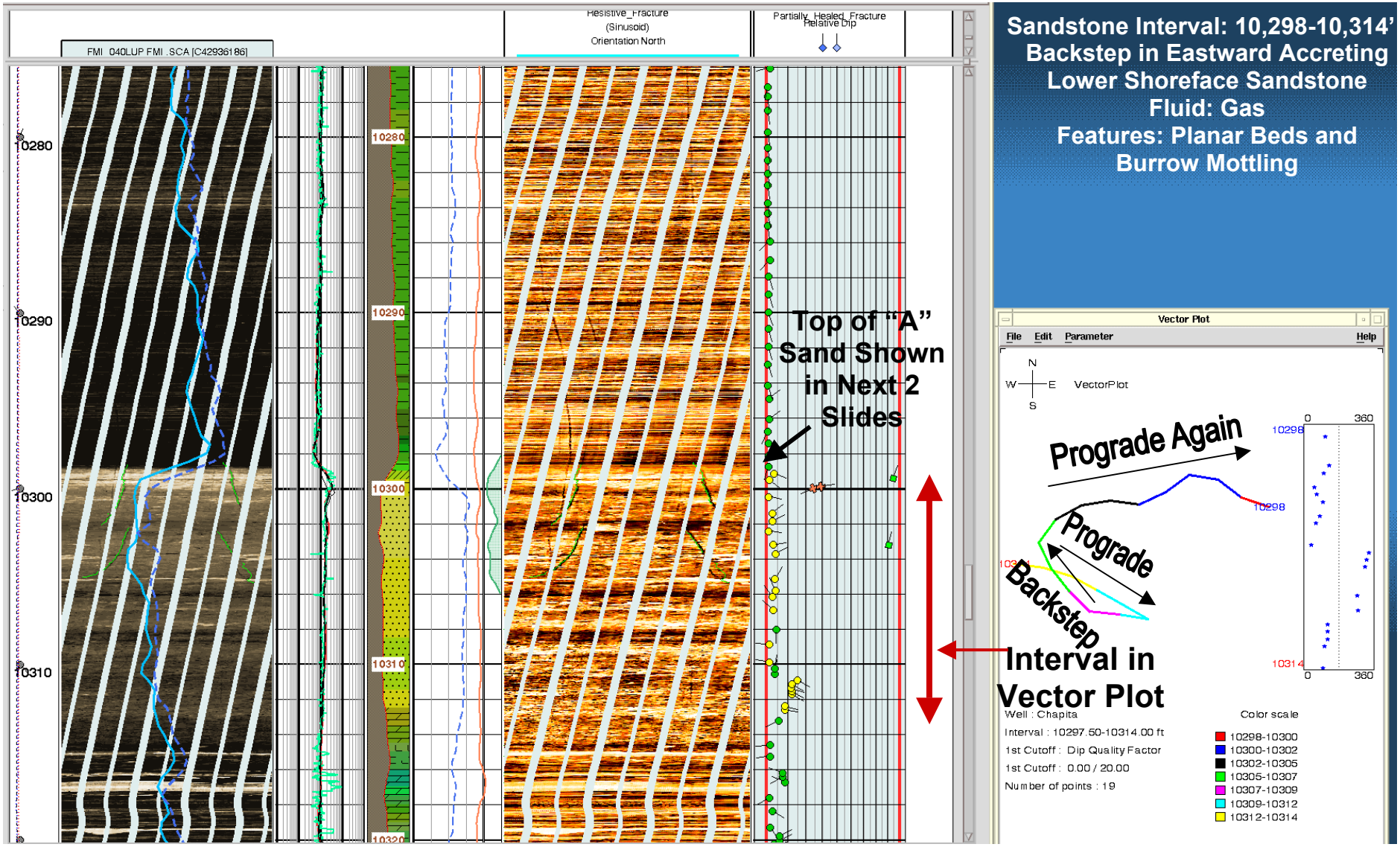

Figure 32. Part of the FMI log from the CWU 807-10 showing the top of the Blackhawk "A" Sandstone and overlying marine shales.

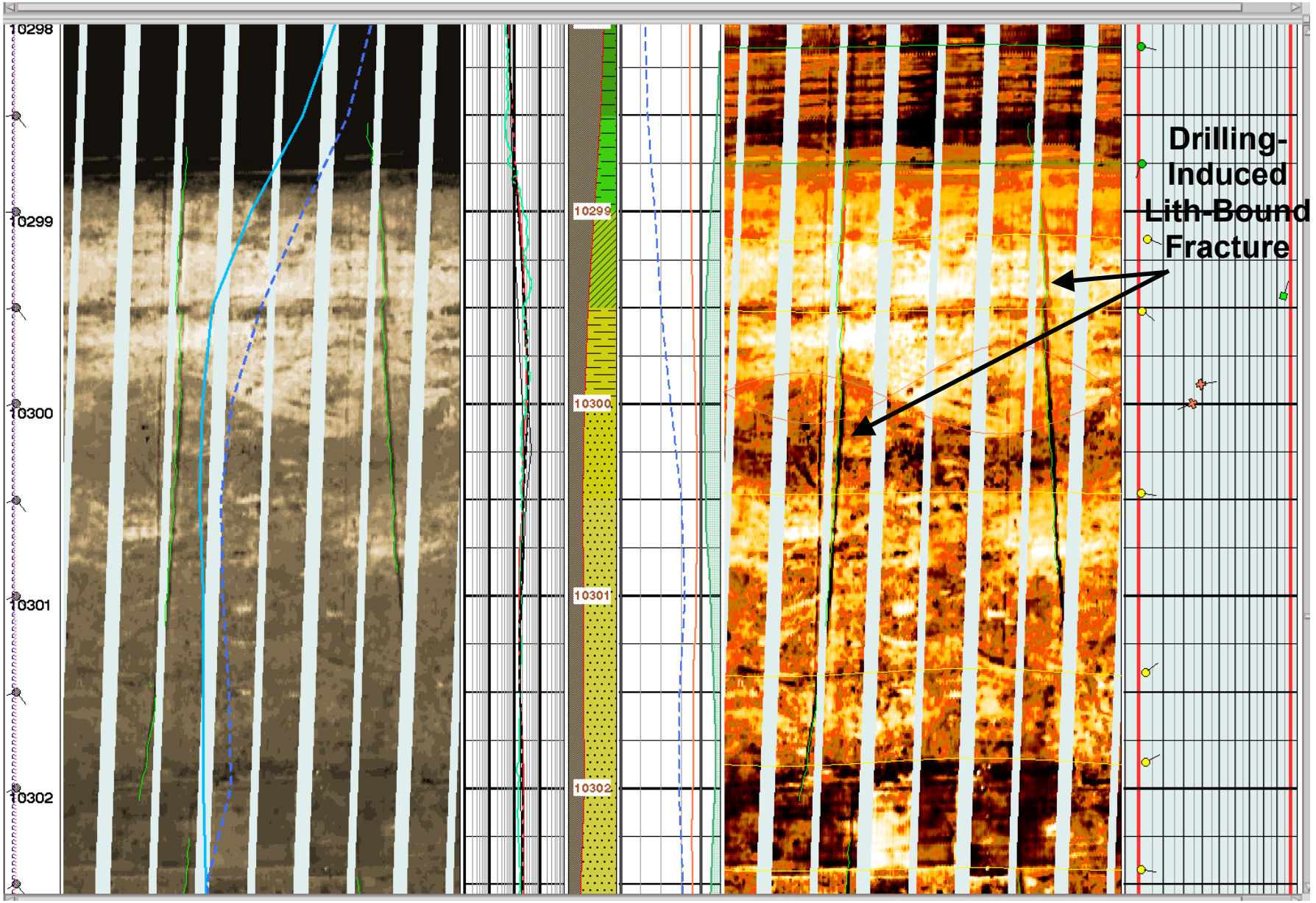

Figure 33. Closeup of the top of the highly burrowed Blackhawk "A" Sandstone. A core photo of this contact is shown in Figure 34.

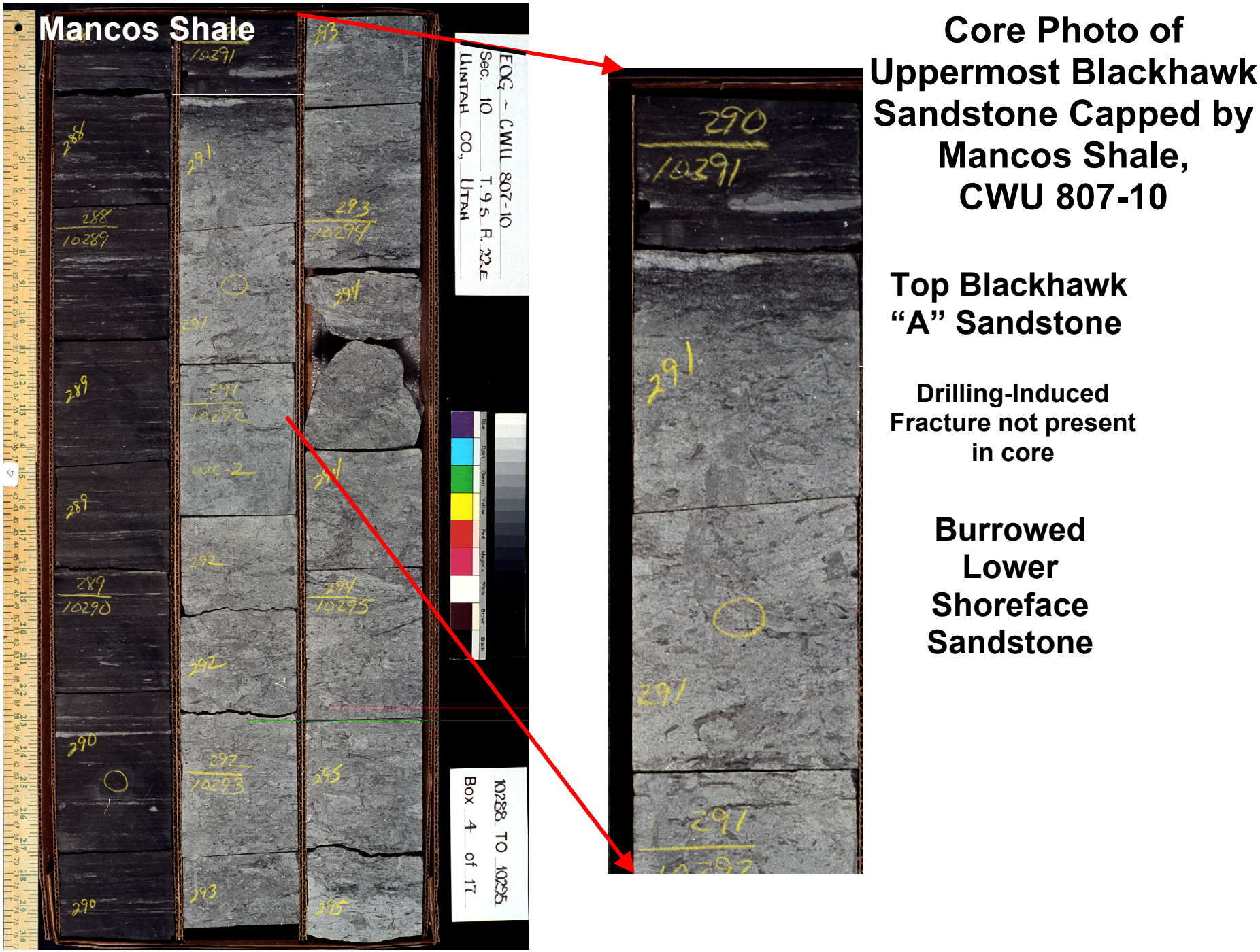

Figure 34. Core photo of 8 ft of section near the contact between the Blackhawk "A" Sandstone and overlying dark-gray marine shales.

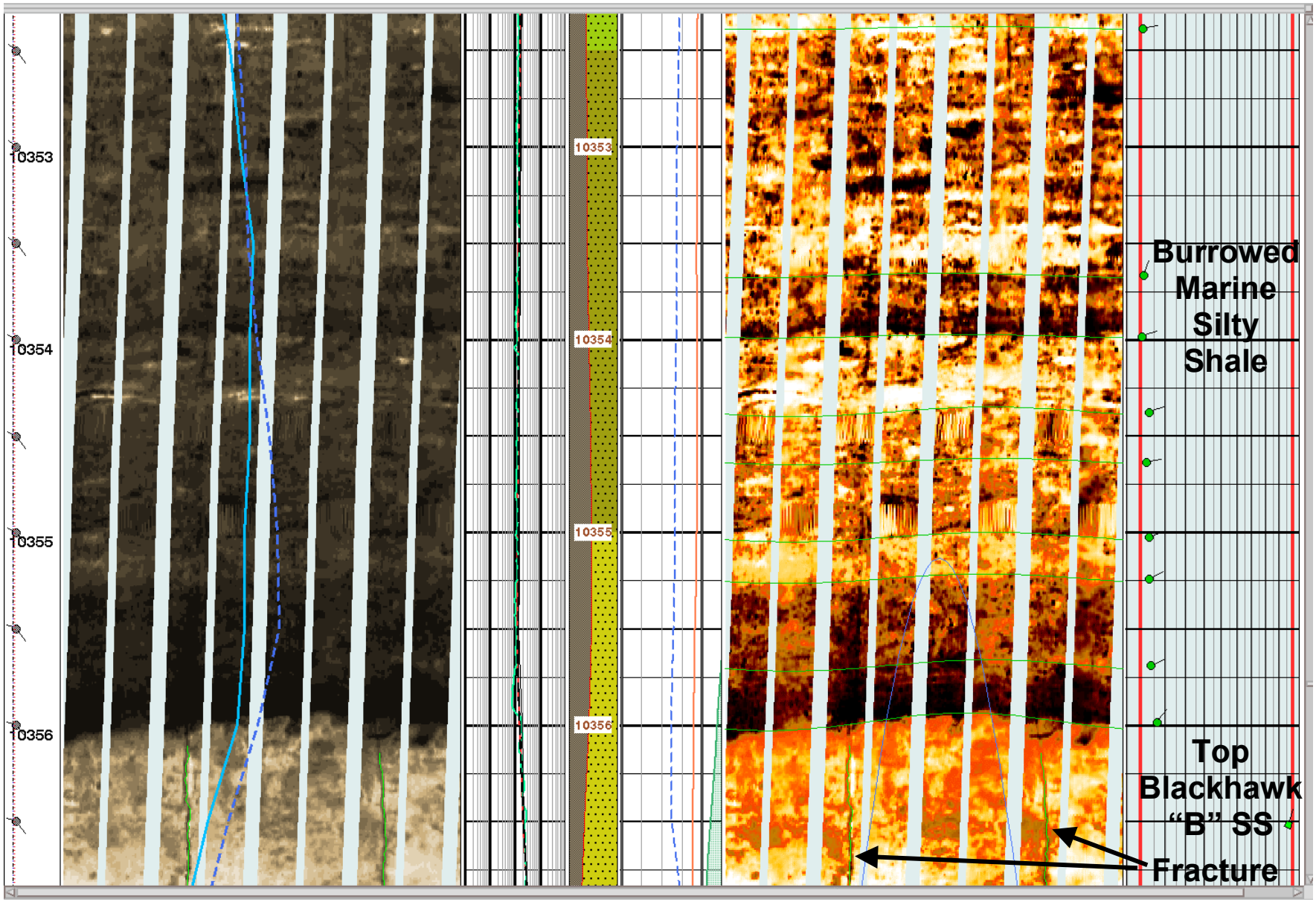

Figure 35. Part of the FMI log across the top of the Blackhawk "B" Sandstone, which is very similar to the Blackhawk "A" Sandstone.

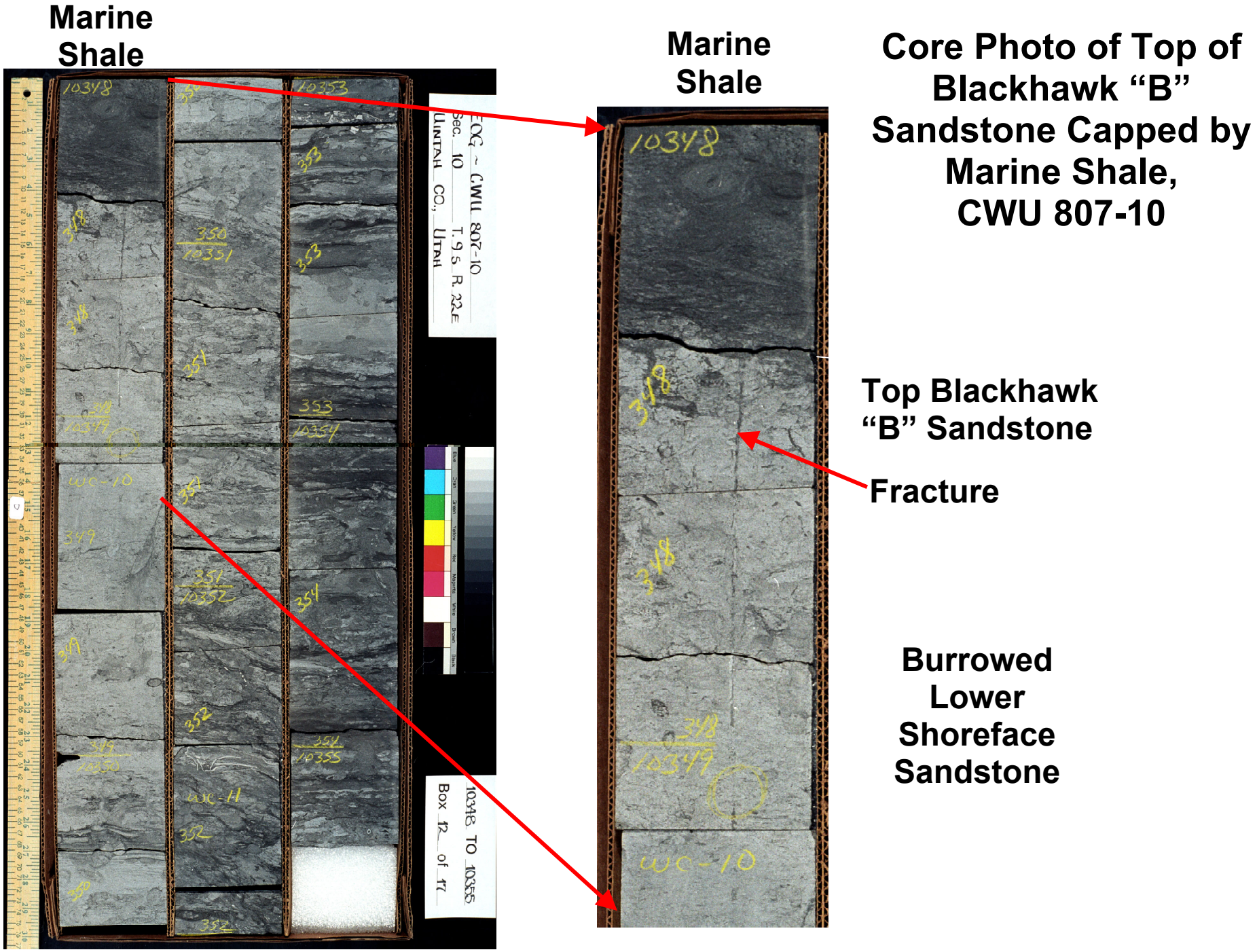

Figure 36. Core photo of the top of the Blackhawk "B" Sandstone showing a near-vertical fracture also seen on the FMI log.

EOG CWU 807-10

Scale: 1” = 1’

Inoceramus Shells in Burrowed, Fractured Lower Shoreface Shaly Sandstone

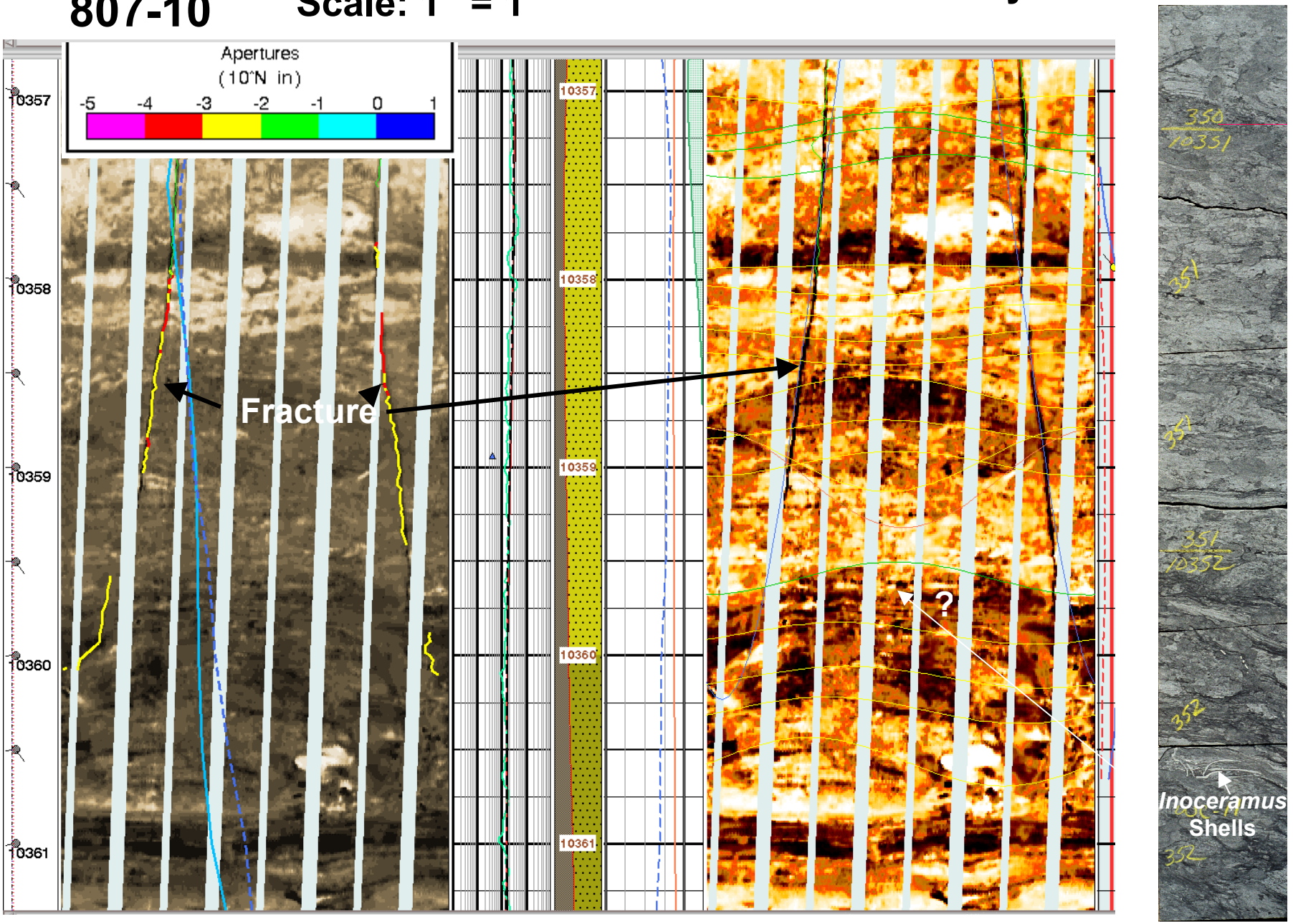

Figure 37. Part of the FMI log across part of the Blackhawk "B" Sandstone where *Inoceramus* shells occur in the core.

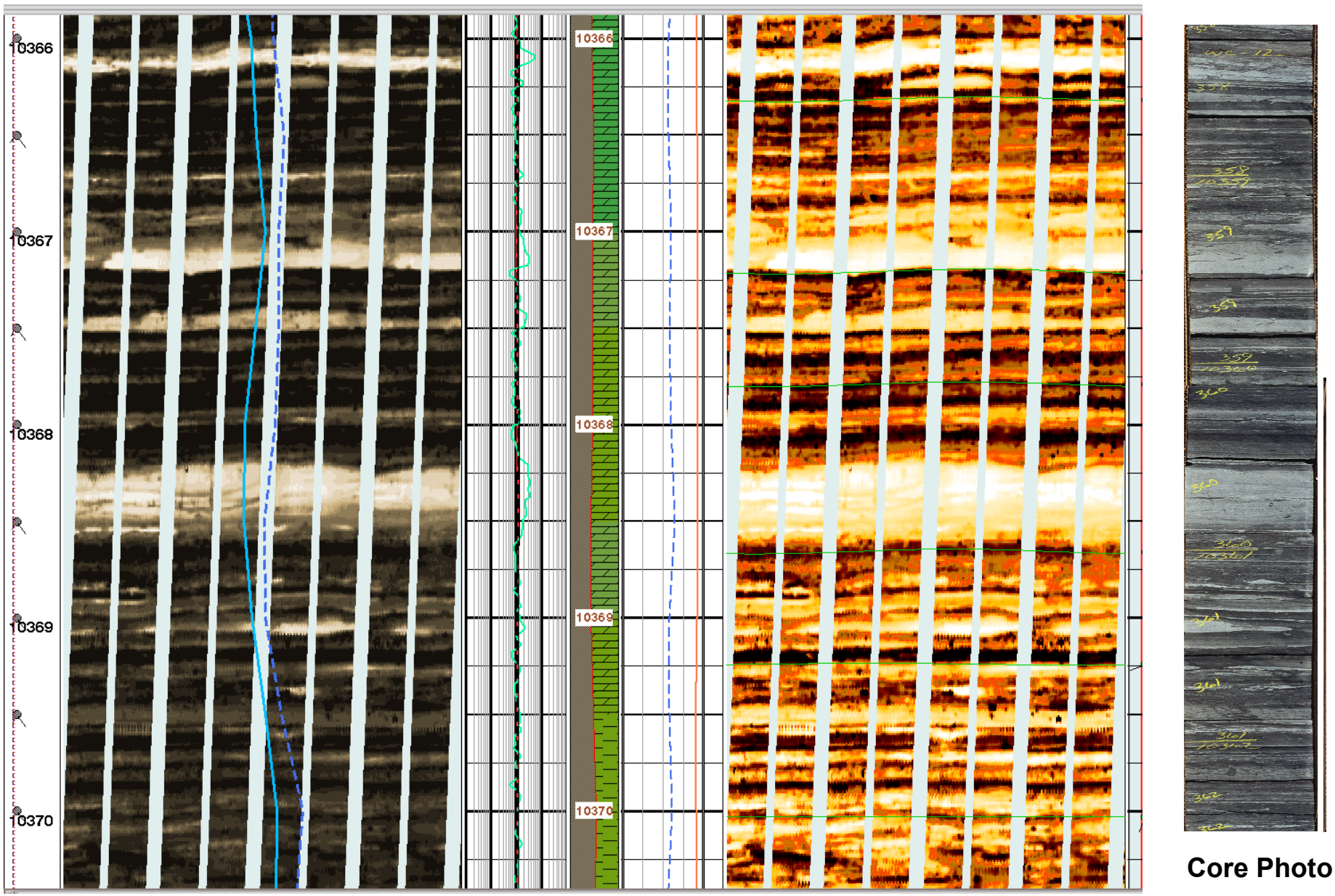

Figure 38. Comparison of FMI log and core photo in distal lower shoreface Blackhawk sandstones representing storm beds in shales.

El Paso Prod.
#3-181 Pawwinnee
(NW NW Sec. 3, T9S, R21E)

Scale: 1” = 5’

Gas Entry from Mancos “B” Turbidite Sands in Marine Gray Shale

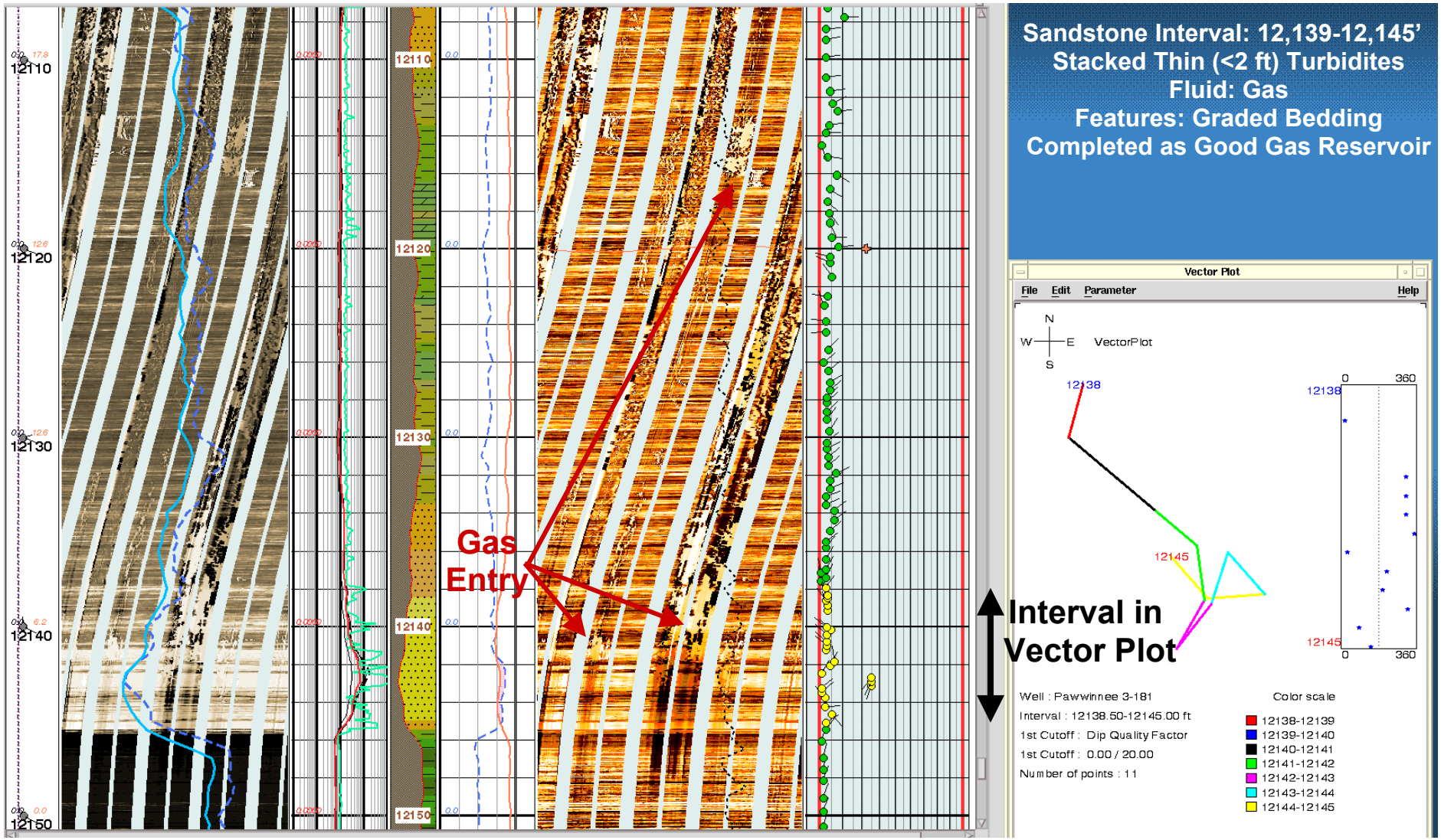

Figure 39. Part of the FMI log showing gas entry from turbidites(?) in the Mancos "B" Sandstone in the Pawwinnee 3-181 well.

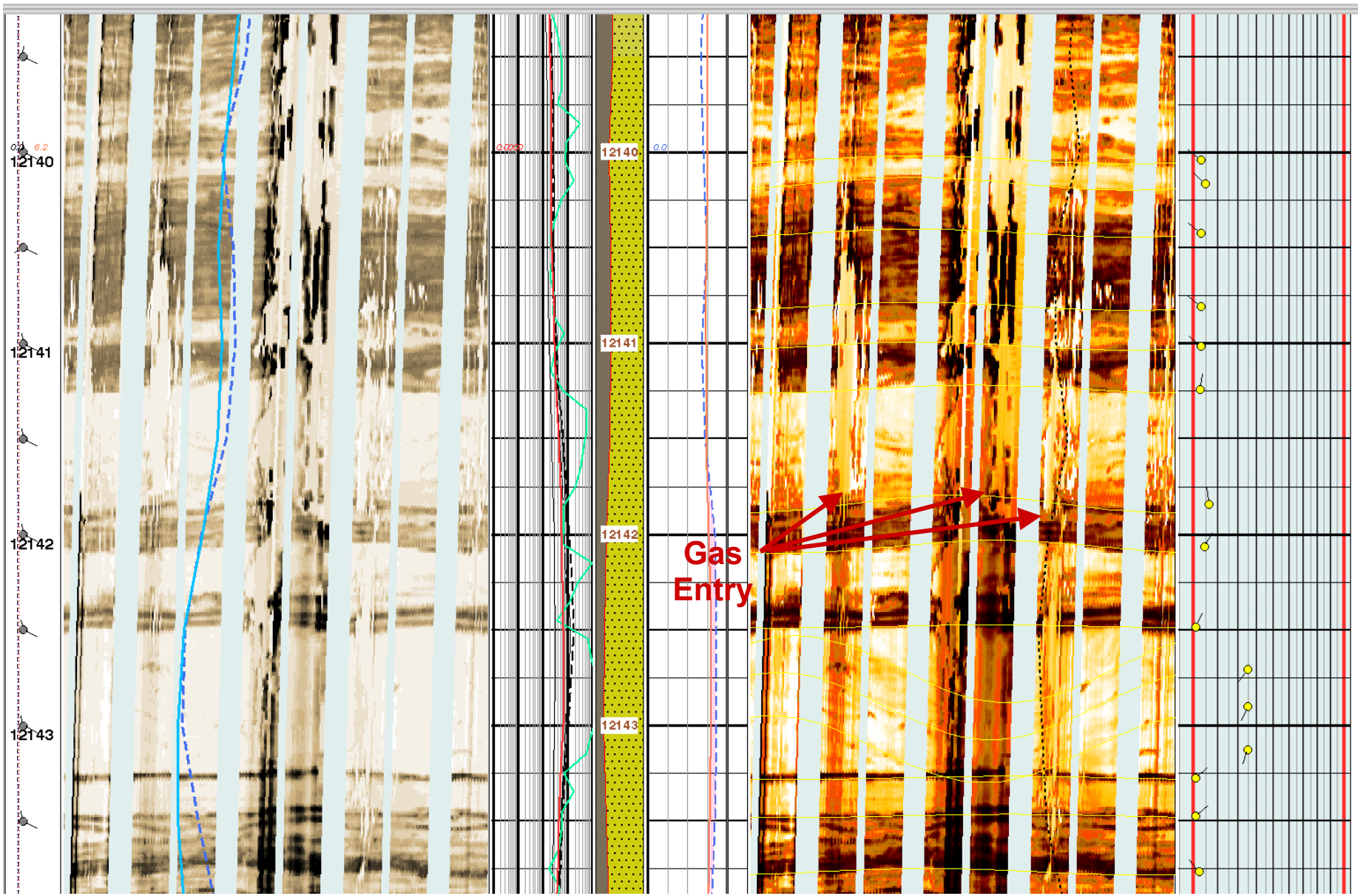

Figure 40. Closer view of gas entry from what are interpreted as thin turbidites in part of the productive Mancos "B" Sandstone.

El Paso Prod.
#3-181 Pawwinnee

Scale: 1” = 1’

More Turbidite Sands with Minor Gas Entry, but no Fractures. Note Anomalous West Dip

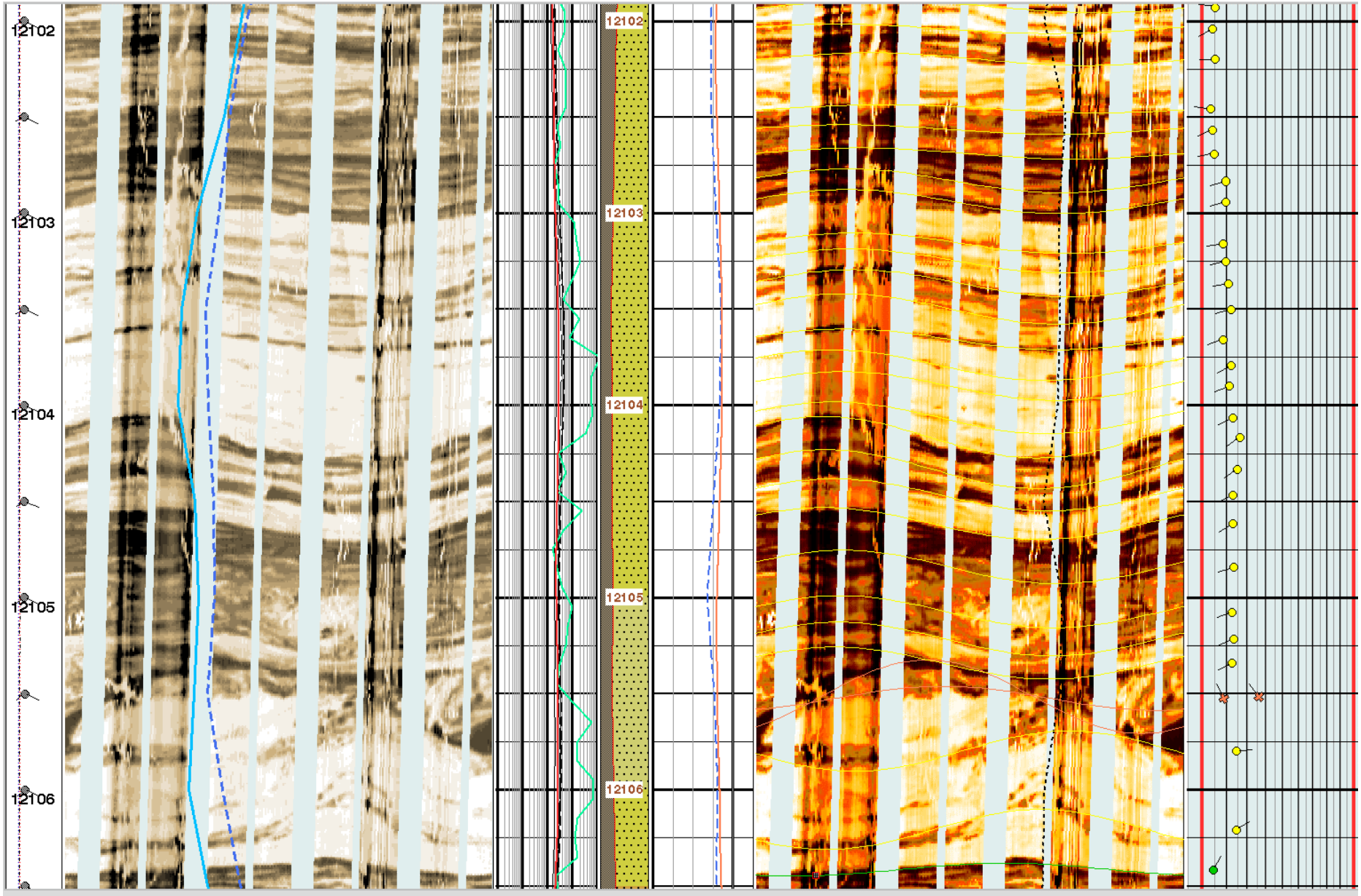

Figure 41. Part of the FMI log across another of the 3 sandstone intervals in the Mancos "B" completed for >2 MMCFGPD.

El Paso Prod.
#3-181 Pawwinnee

Scale: 1” = 1’

Gas Entry from Deep Marine Shales, but no Fractures (not perforated)

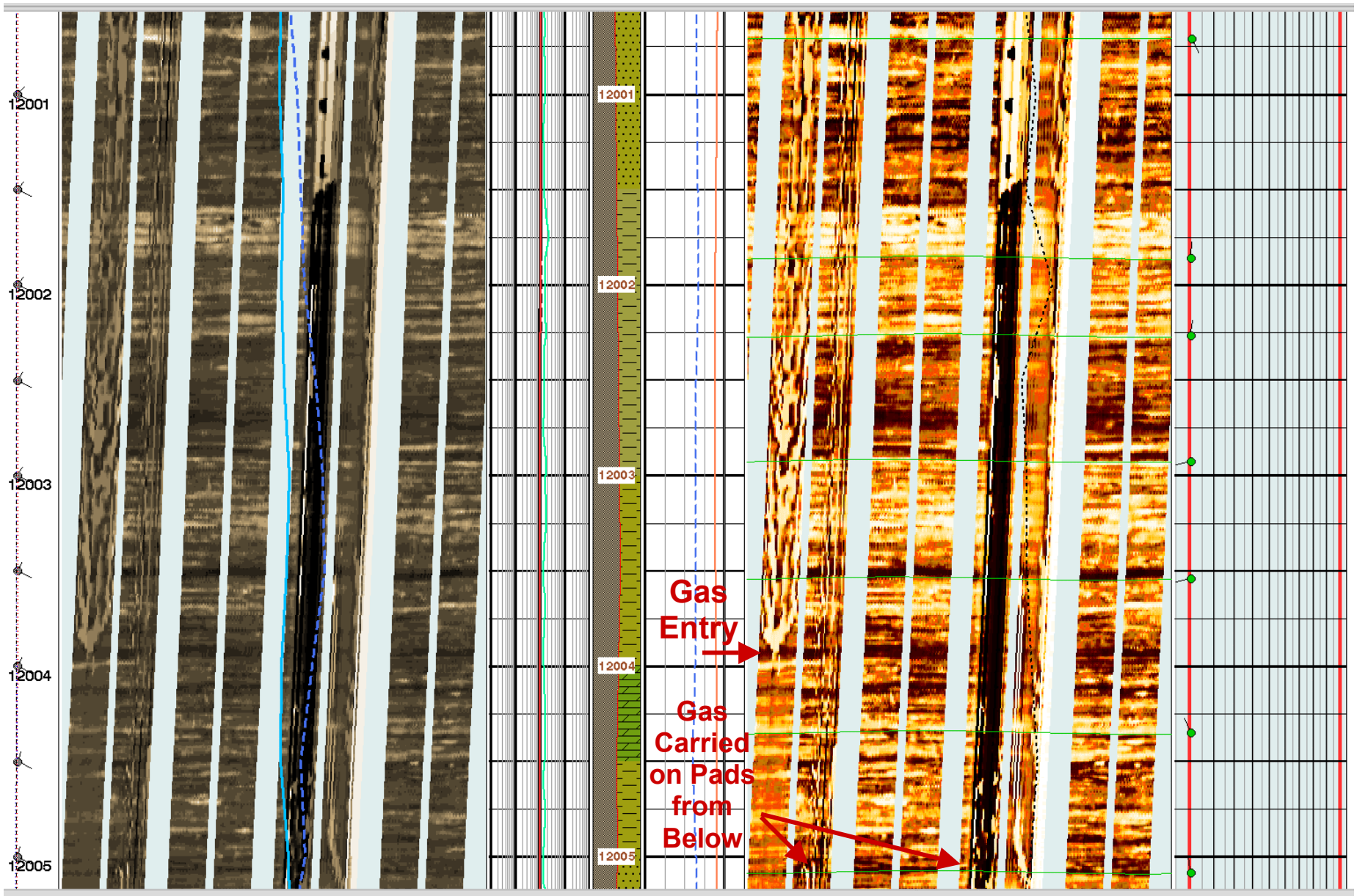

Figure 42. Part of the FMI log showing common gas entry from non-sandy, unfractured dark-gray marine shales of the Mancos Shale.

El Paso Prod.
#3-181 Pawwinnee

Scale: 1” = 5’

Gas Entry from Sands in the Mancos Shale.
Some Fractures (not perforated)

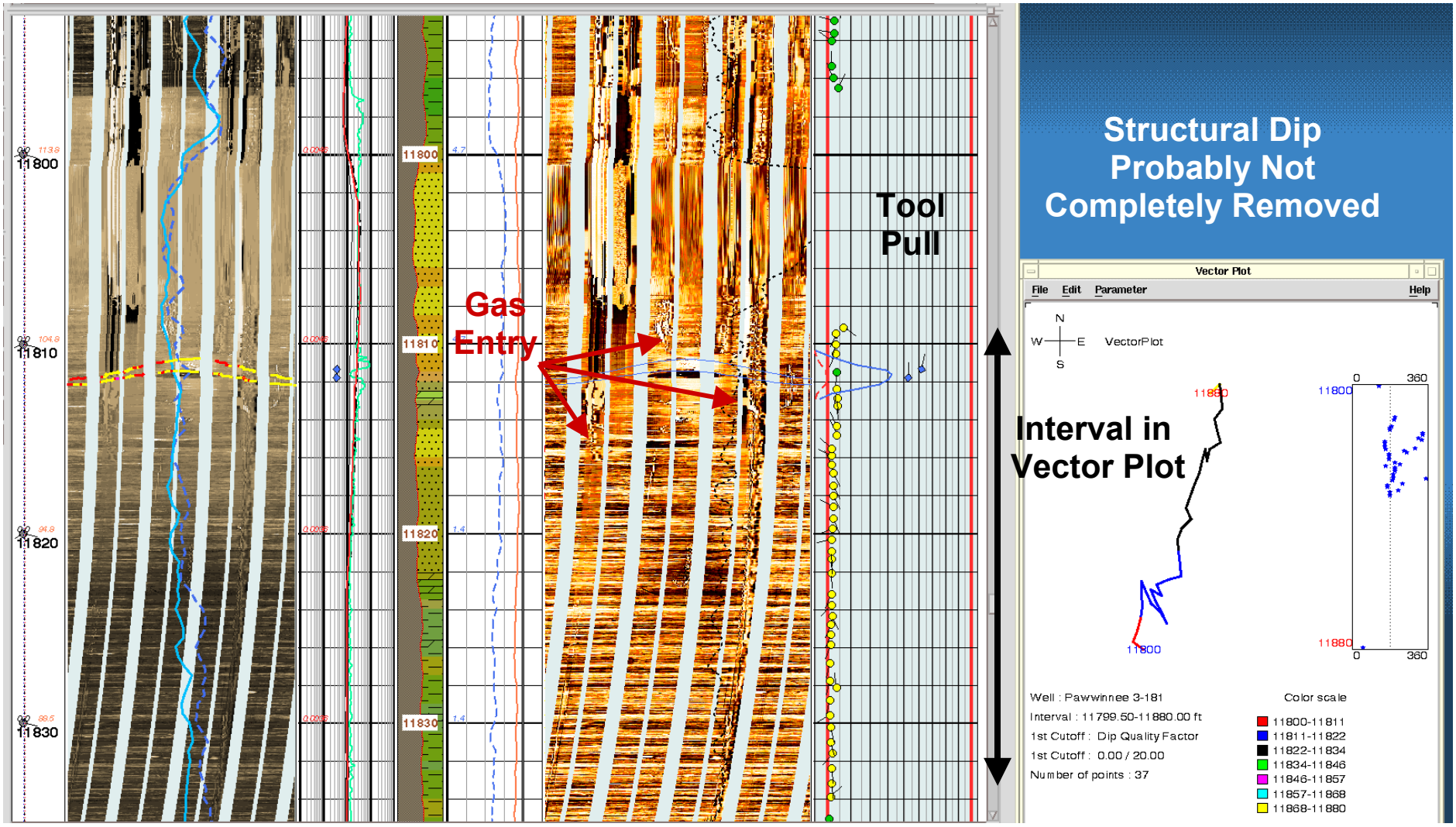

Figure 43. Part of the FMI log across a somewhat sandy part of the Mancos Shale with natural fractures and common gas entry.

El Paso Prod.
#3-181 Pawwinnee

Scale: 1” = 1’

Gas Entry from Sands in the Mancos Shale

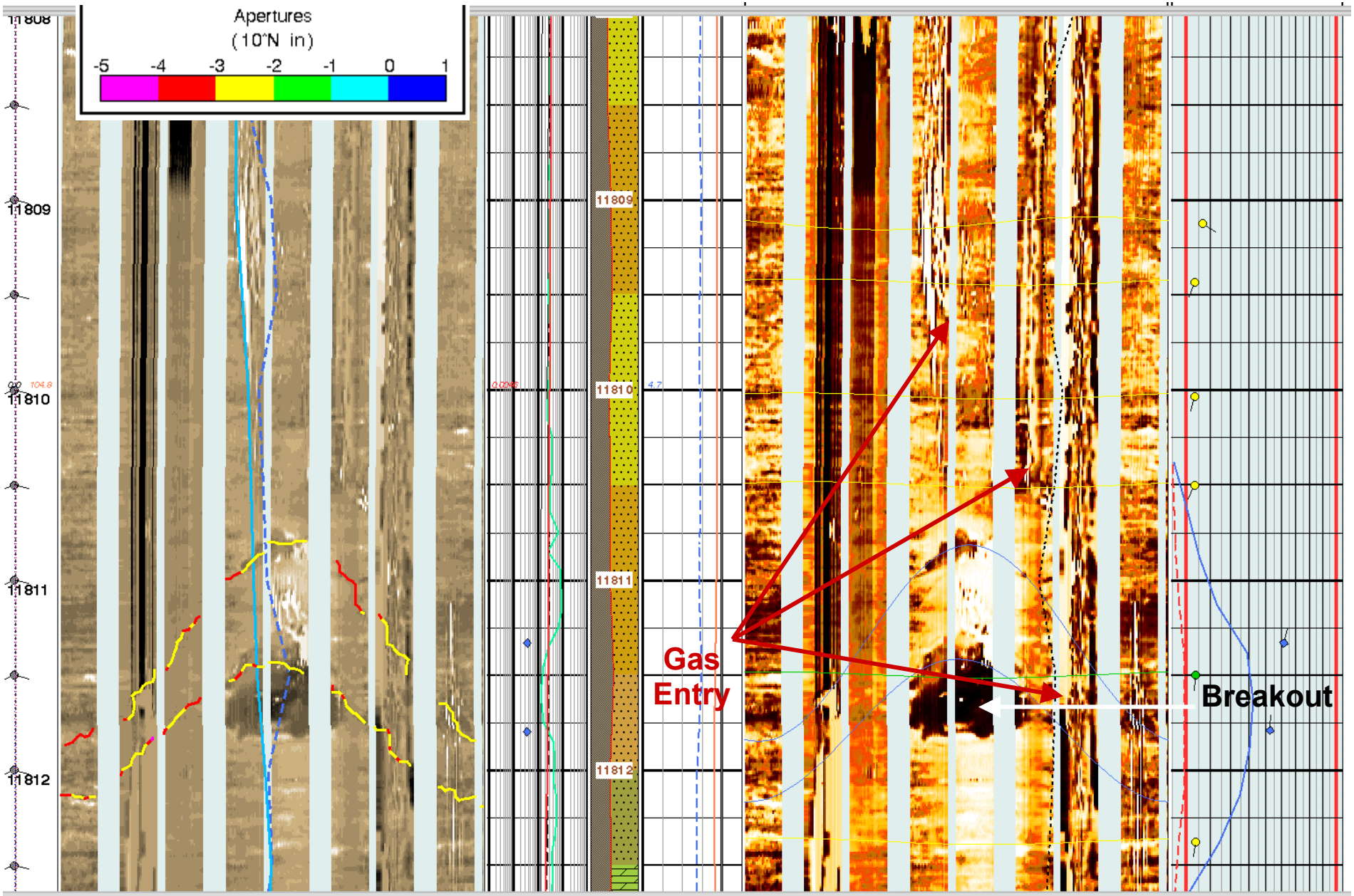

Figure 44. Closer view of part of the FMI log across the same interval in Figure 43 showing common gas entry and some fractures.

El Paso Prod.
#3-181 Pawwinnee

Scale: 1” = 5’

Gas Entry from Lower Shoreface Sandstones in the basal Blackhawk “D” Interval Not Perforated

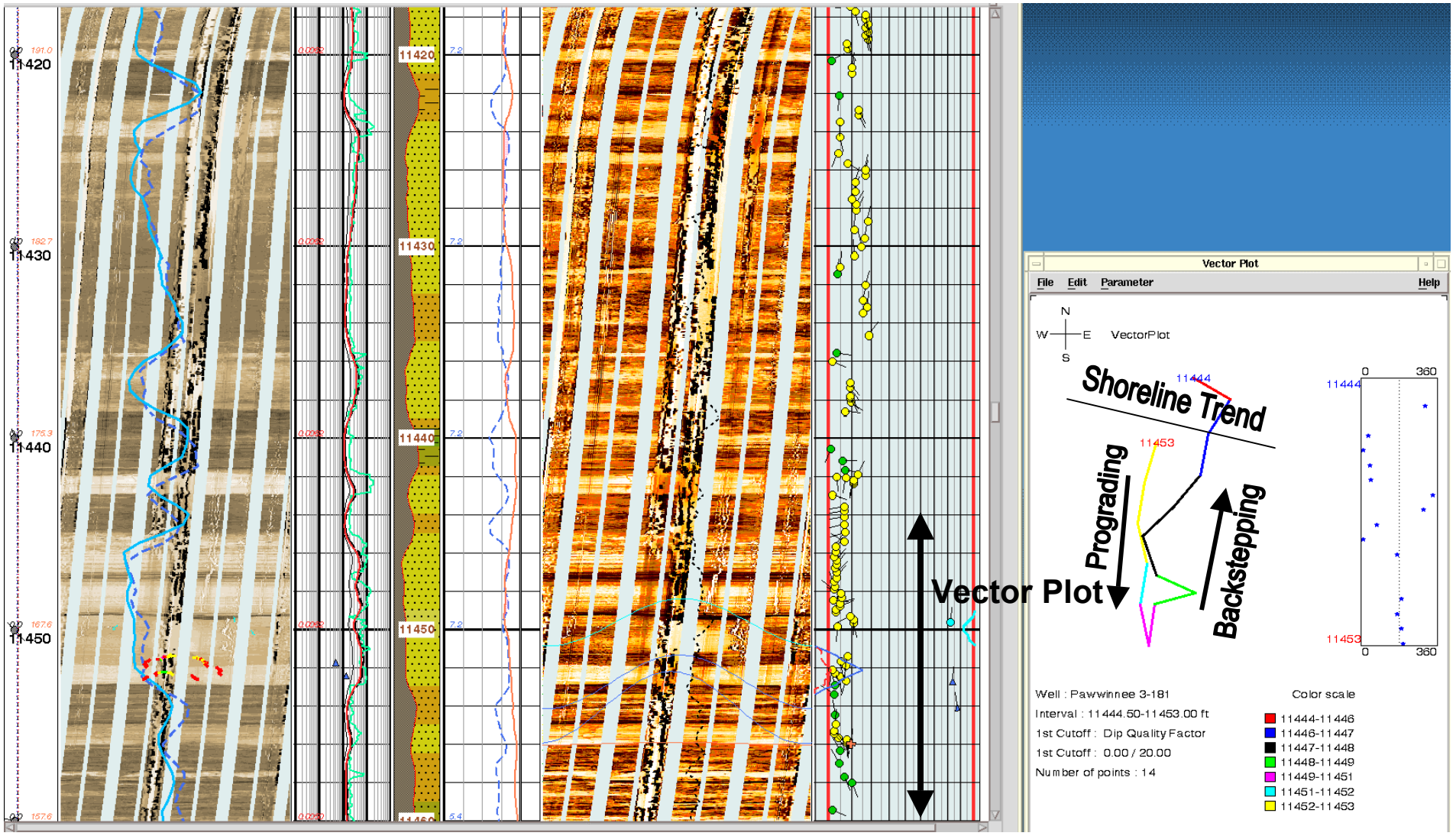

Figure 45. Part of the FMI log across the Blackhawk "D" Interval showing lower to middle shoreface sands yielding gas entry.

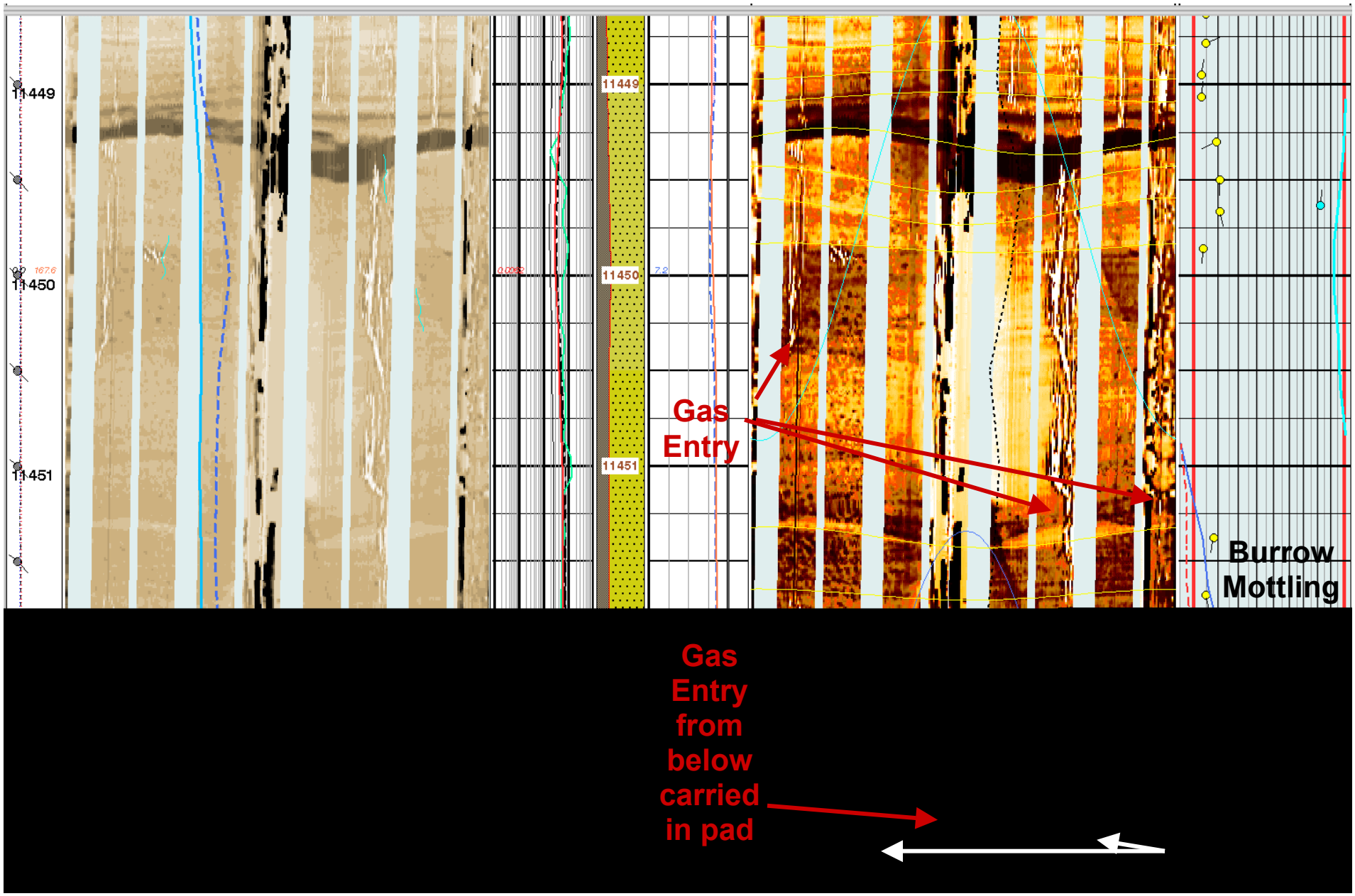

Figure 46. Closer view of the FMI log in the Blackhawk "D" showing some fractures and gas entry from burrowed and bedded sandstones.

El Paso Prod.
#3-181 Pawwinnee

Scale: 1” = 5’

Upper Shoreface Sandstones in the Blackhawk “B” Interval Perforated in 2004

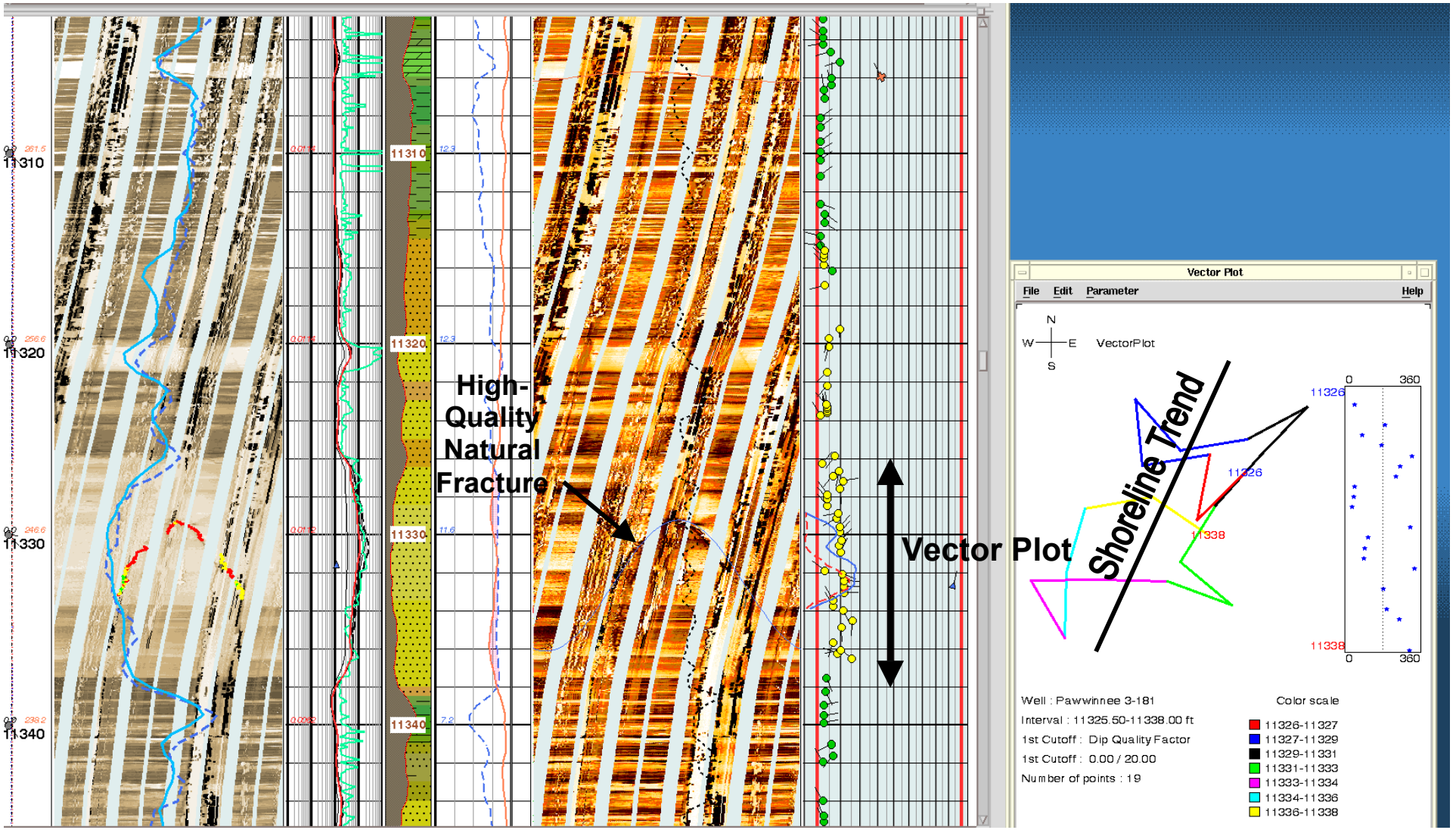

Figure 47. Part of the FMI log across upper shoreface sandstone intervals in the Blackhawk "B" Interval, which also proved productive.

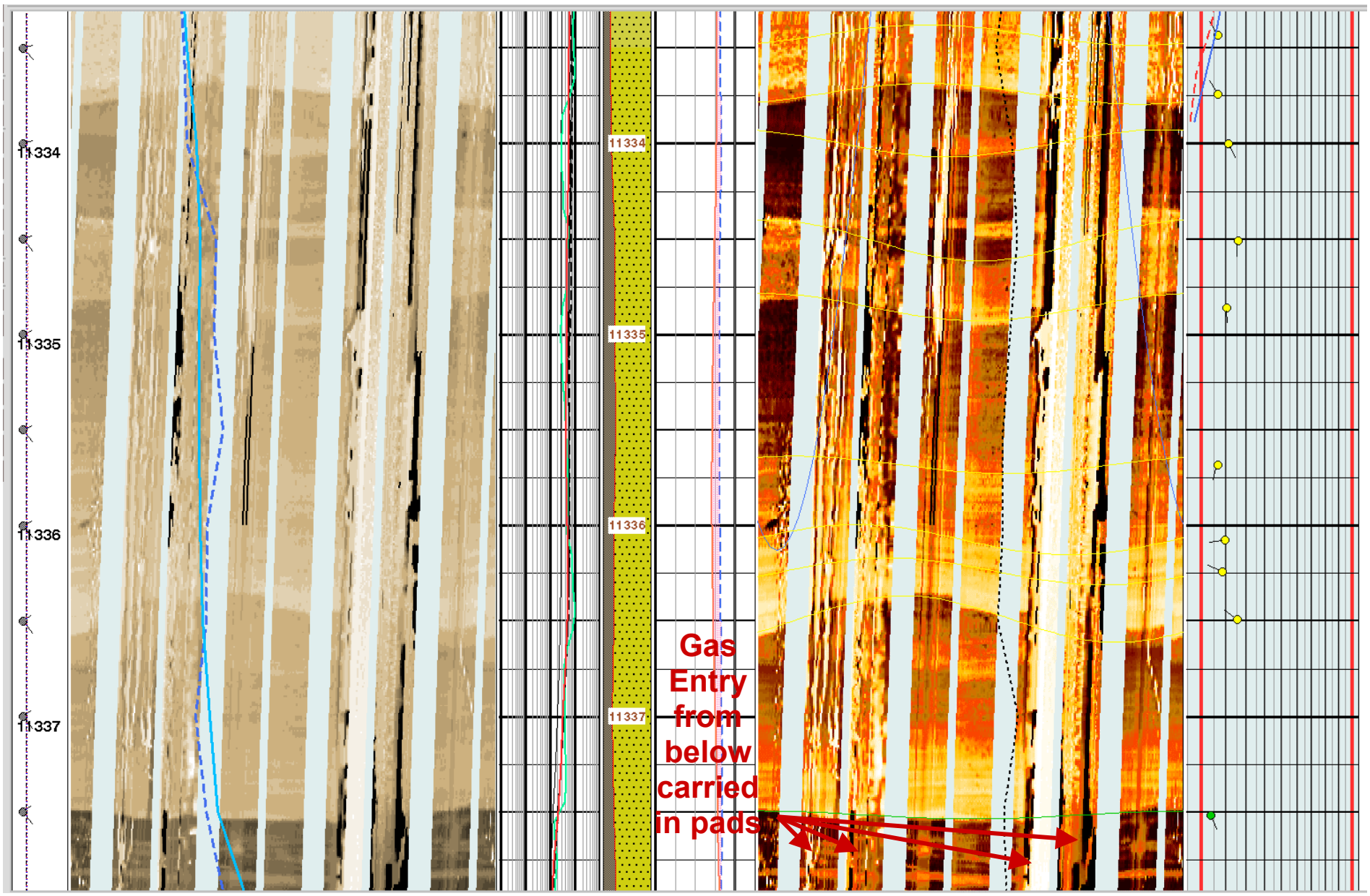

Figure 48. Closer view of the FMI log in the Blackhawk "B" showing gas entry from below and crossbedding.

Partial Explanation for Complex Bedding Patterns in Upper Shoreface Sandstones

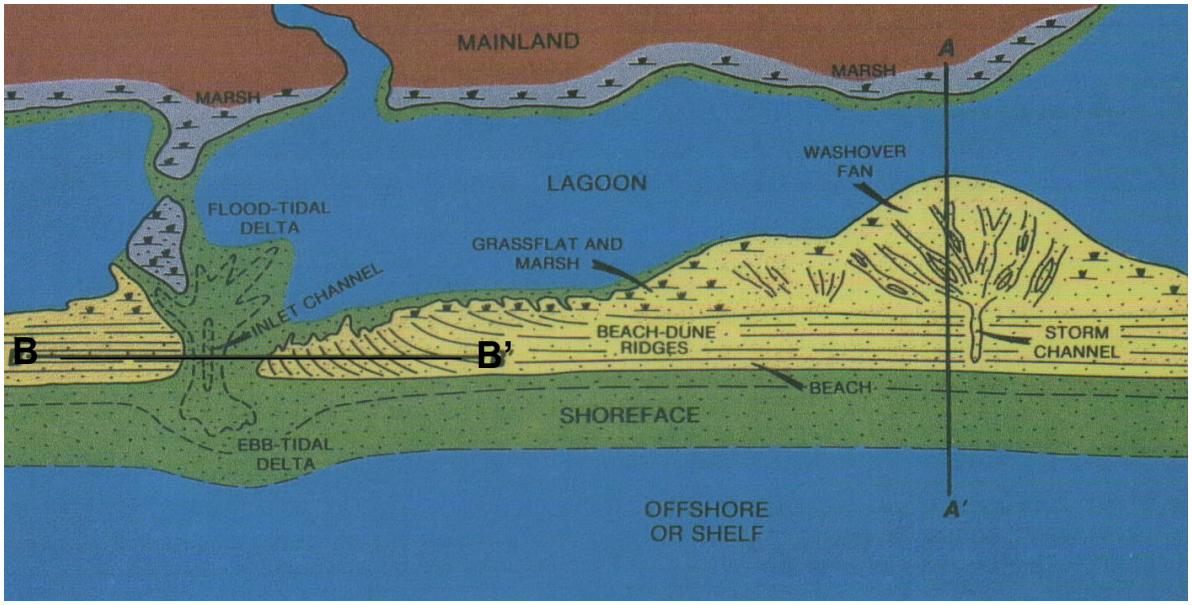

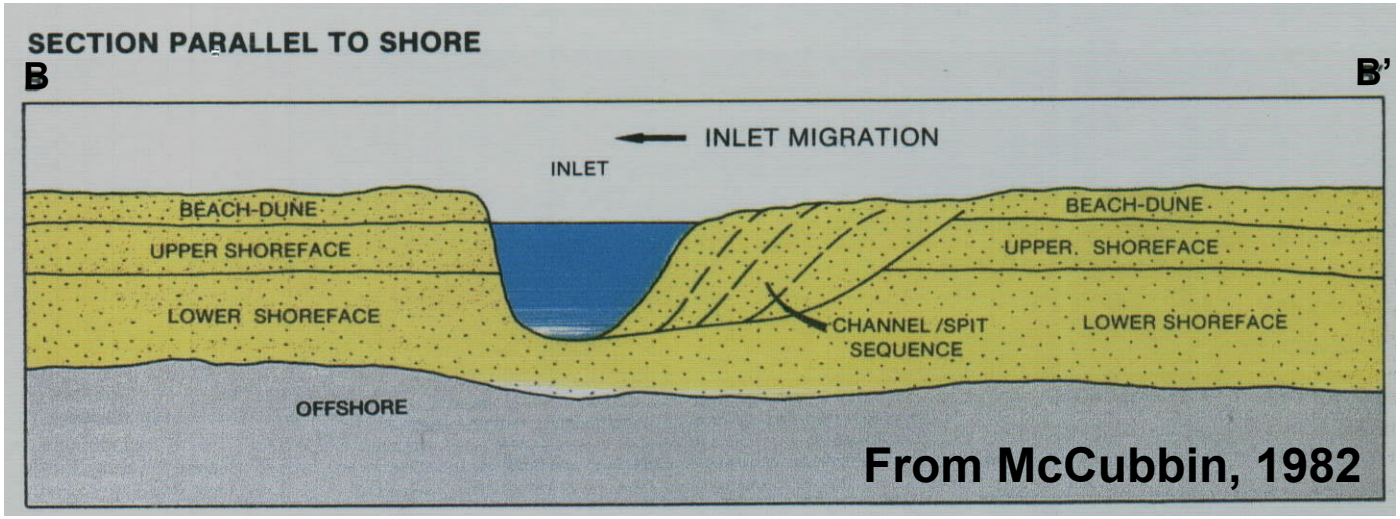

Figure 49. Schematic cross-section B-B' showing why bedding features in upper shoreface bar sands can be so complex. Adapted from McCubbin, 1982.

El Paso Prod.
#3-181 Pawwinnee
Scale: 1” = 5’

Middle Shoreface Sandstones in the Blackhawk “A” Interval Perforated in 2004

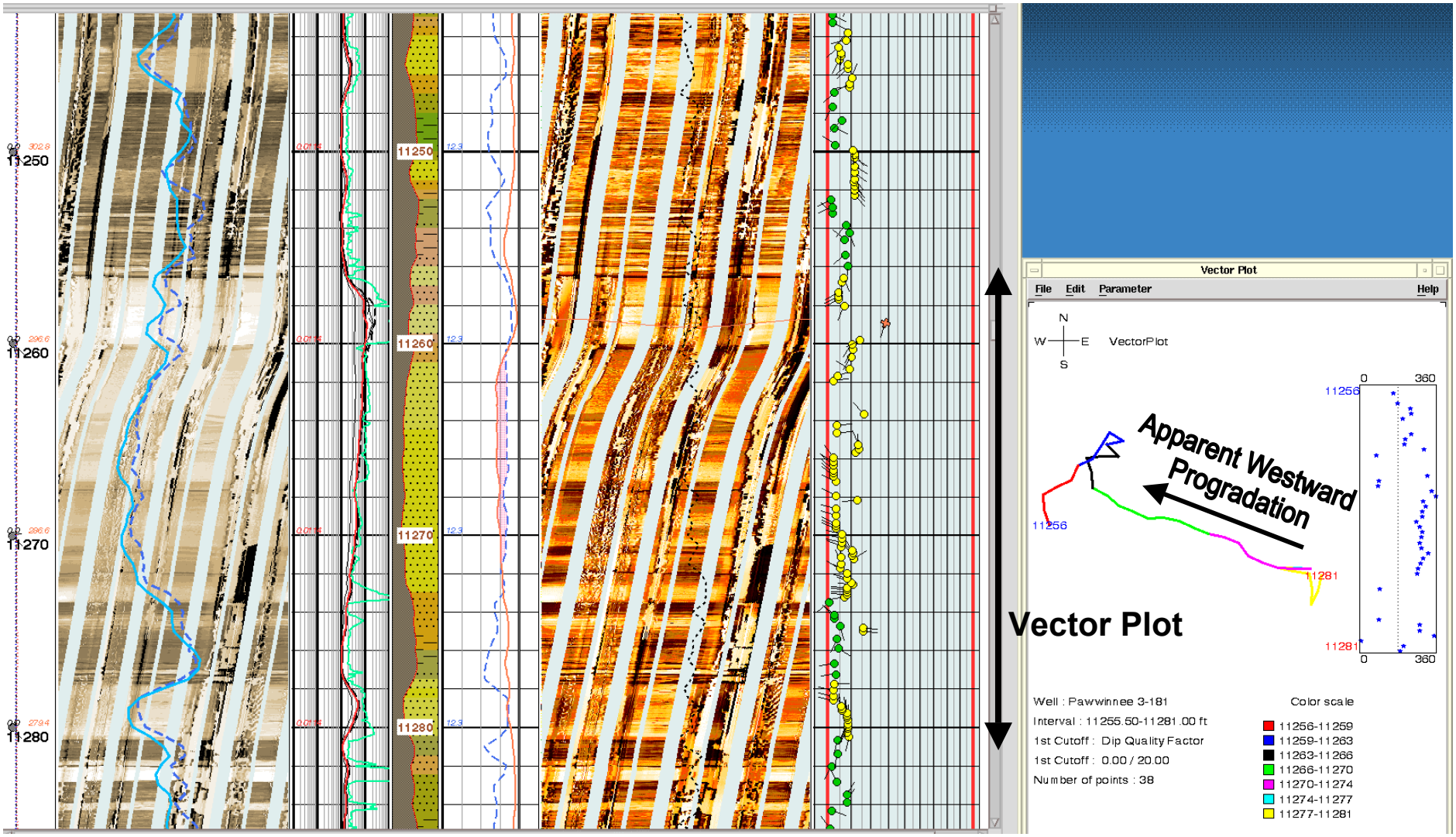

Figure 50. Part of the FMI log across the Blackhawk "A" Sandstone about 6 miles updip from the burrowed sands seen in the 807-10 well.

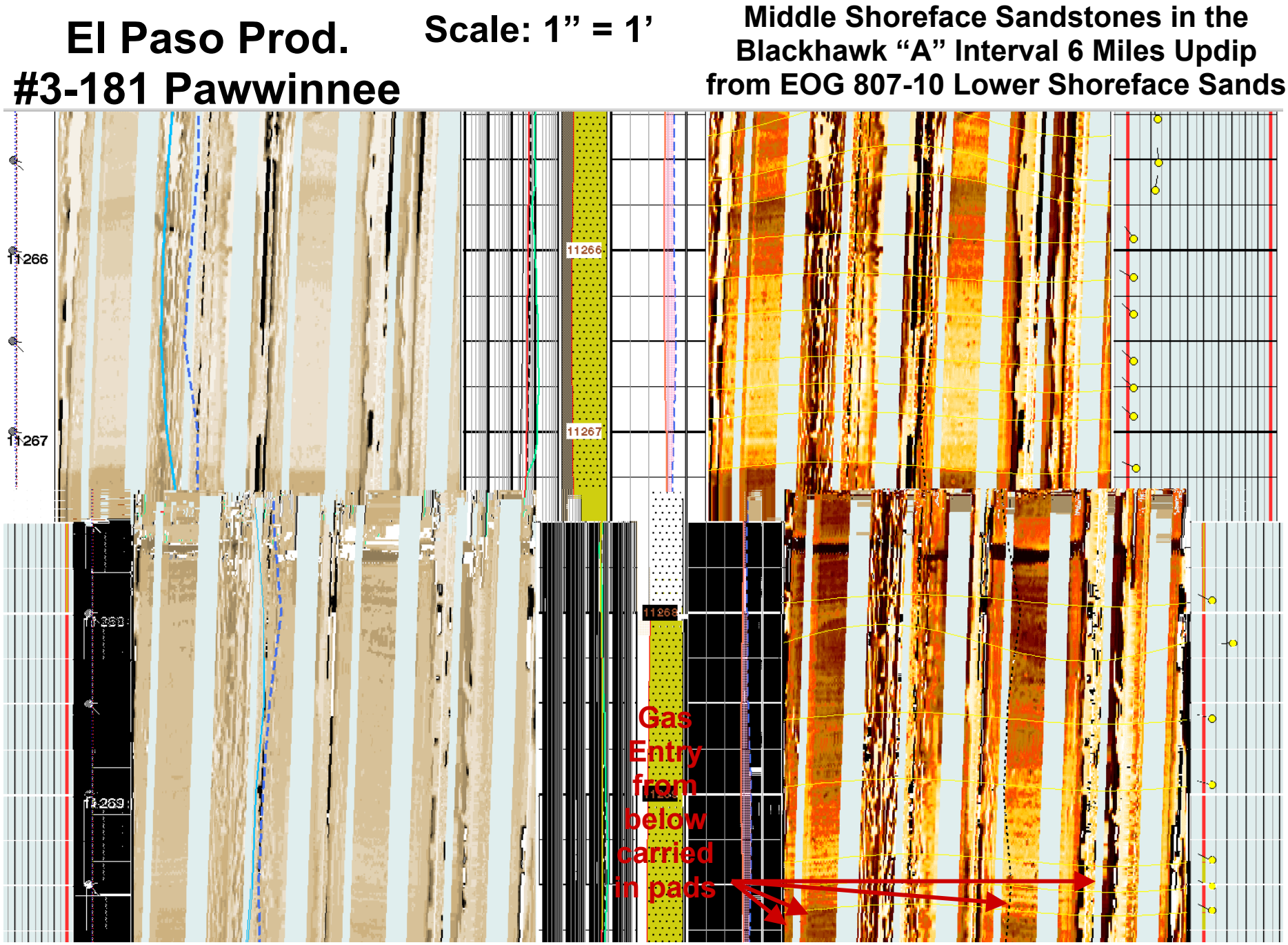

Figure 51. Closer view of the FMI log in the Blackhawk "A" Sand showing good crossbedding and few burrows updip from the 807-10 well.

Schematic Stratigraphic Section of the Mesaverde Group, Northeastern Uinta Basin

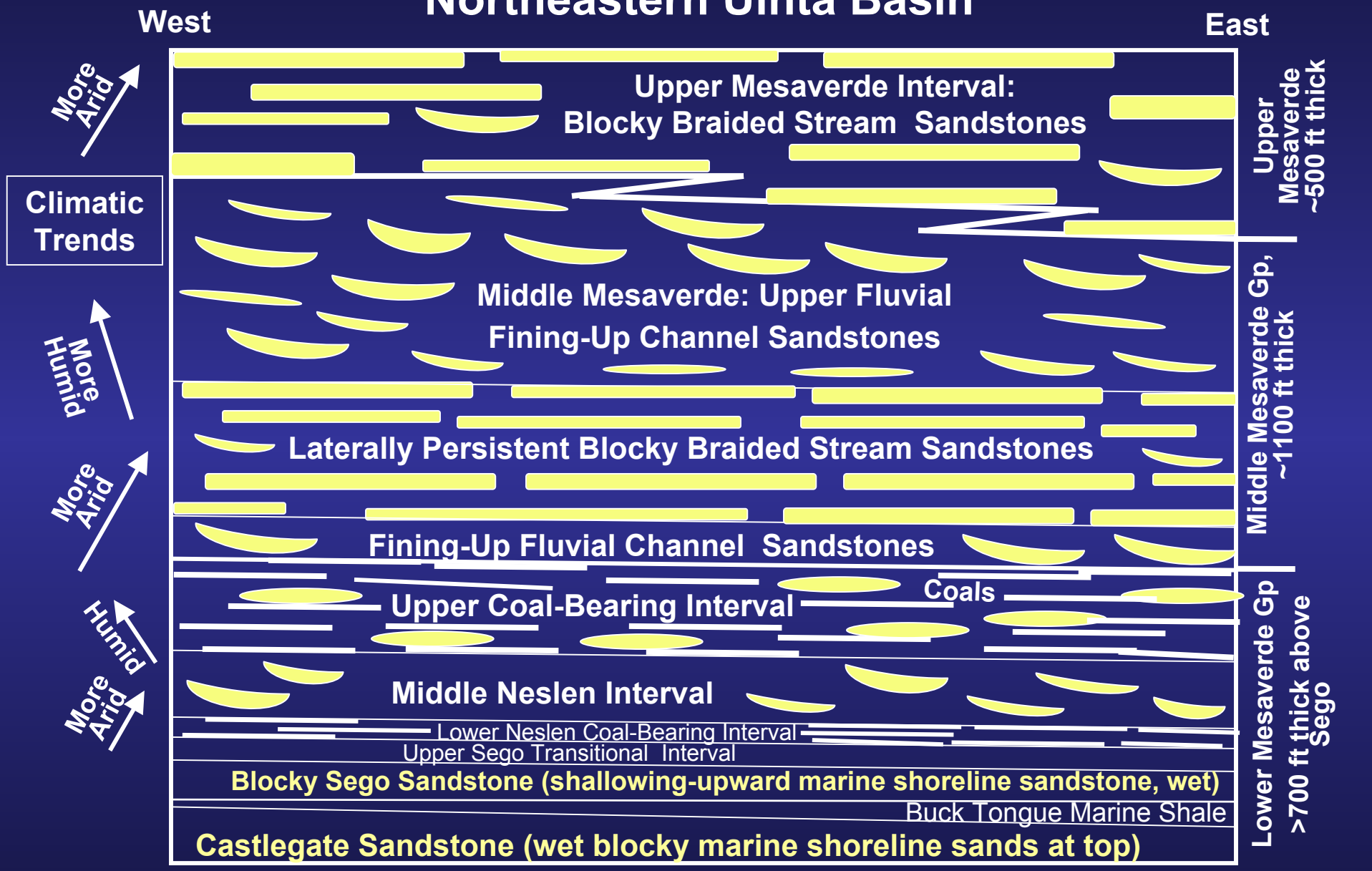

Figure 52. Schematic stratigraphic section showing idealized post-Castlegate sand-body geometries in the Mesaverde Group.

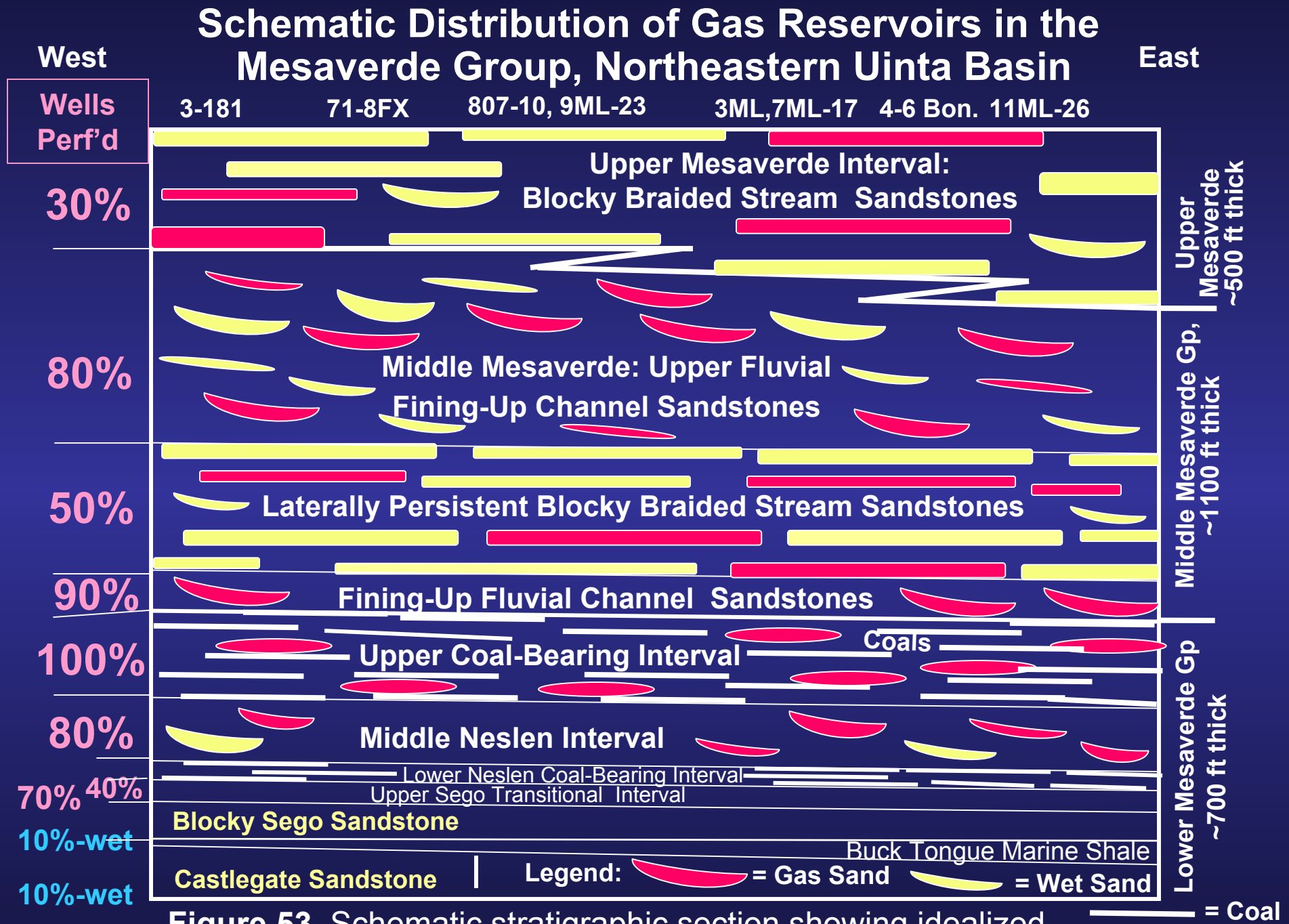

Figure 53. Schematic stratigraphic section showing idealized distribution of gas-bearing sandstones in the Mesaverde Group.

Use of Vector Plots for Defining Depositional Trends

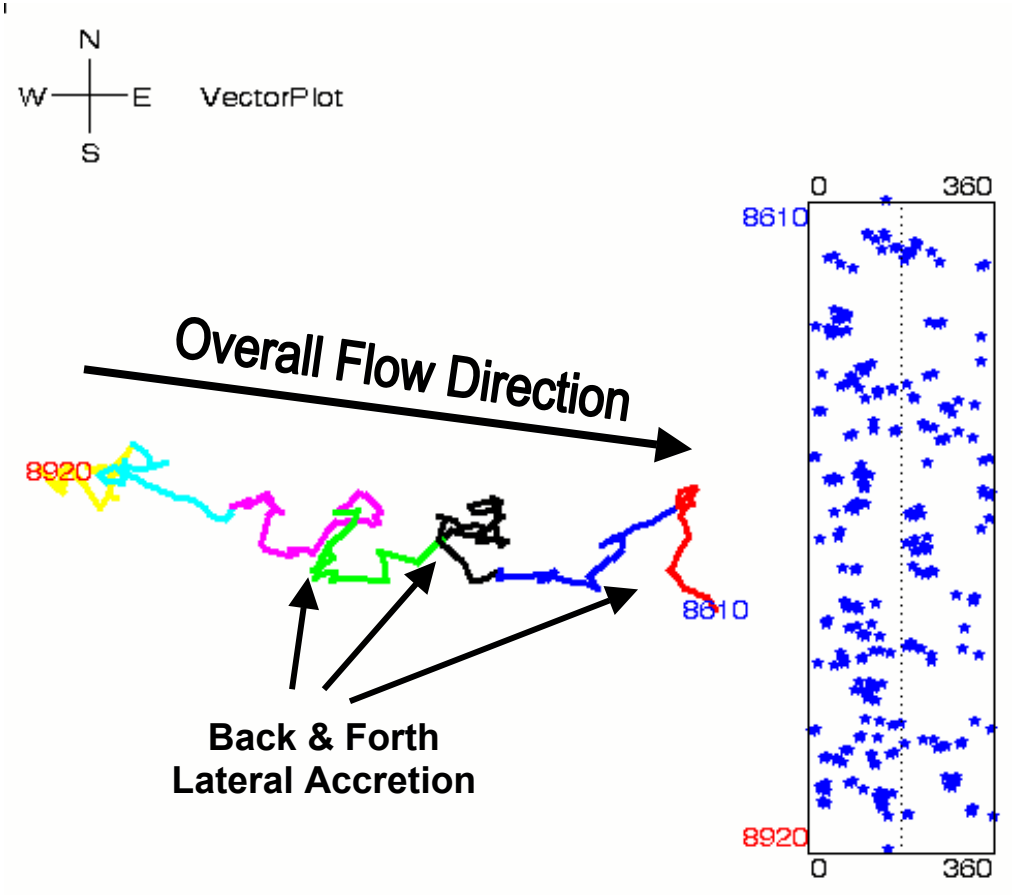

Plots can cover Correlative Intervals up to Hundreds of Feet Thick
Useful for Defining Regional Flow Patterns
Can Provide Insight into Shoreline Trends
Can Reveal Reversal of Flow Trends or Backstepping Shoreline Facies that set up Stratigraphic Traps

Well : STAGECOACH UNIT 71-8FX
Interval : 8609.50- 8920.00 ft
1st Cutoff : Dip Quality Factor
1st Cutoff : 0.00 / 20.00
Number of points : 314

Color scale
- 8610-8654
- 8654-8698
- 8698-8743
- 8743-8787
- 8787-8831
- 8831-8876
- 8876-8920

Stagecoach Unit 71-8FX, 8510-8920 ft
Middle Mesaverde Braided Stream Interval

Figure 54. Example of a vector plot for the whole Braided Stream Interval in the 71-8FX showing generalized fluid flow toward the east.

Use of Vector Plots for Defining Depositional Trends

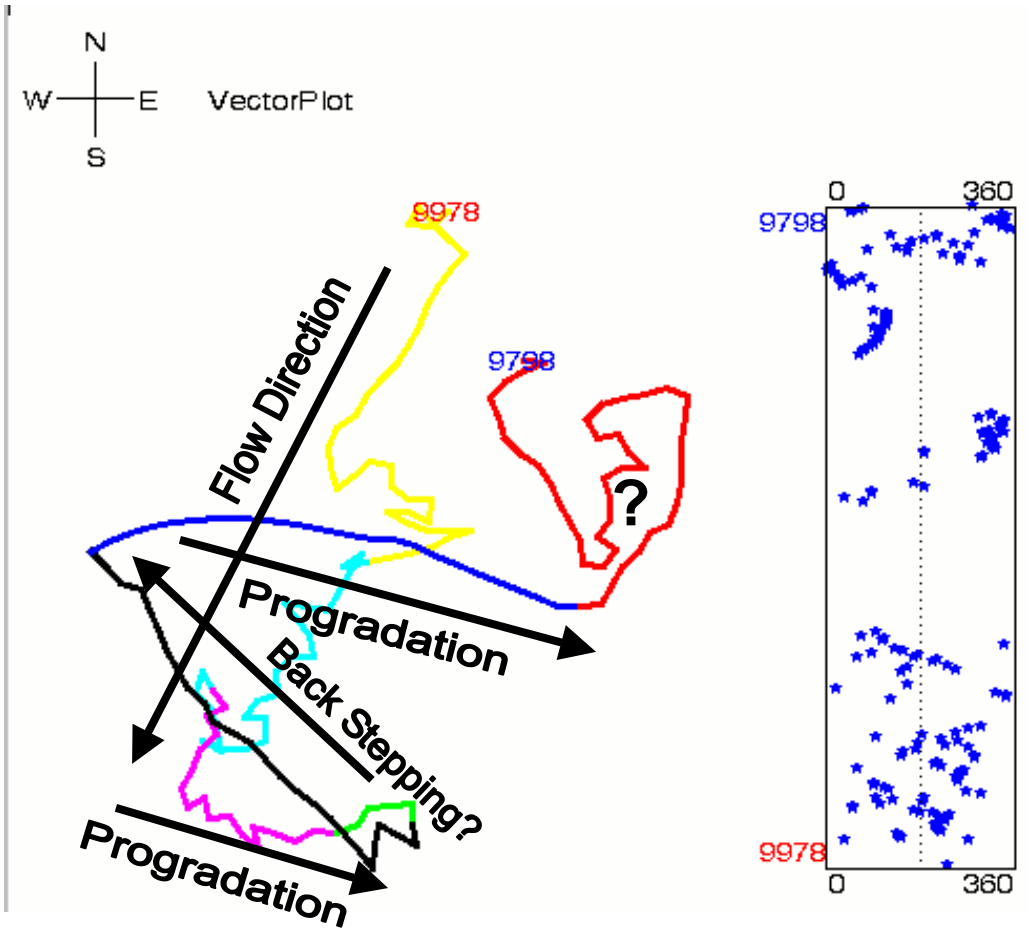

Stagecoach Unit 71-8FX, 9797-9978 ft
Lower Mesaverde Lower Neslen Interval

Vector Plots Covering Diverse Environments Create Confusing Patterns
Most Useful for Single Environmental Packages
Can Provide Insight into Transgressions and Regressions in Coastal Deposits
Plots from Multiple Wells Posted on a Map can Reveal Anomalous Areas

Well : STAGECOACH UNIT 71-8FX
Interval : 9797.50- 9978.00 ft
1st Cutoff : Dip Quality Factor
1st Cutoff : 0.00 / 20.00
Number of points : 175

Color scale
9798-9823
9823-9849
9849-9875
9875-9901
9901-9926
9926-9952
9952-9978

Figure 55. Example of a complex vector plot for the Lower Neslen Interval in the 71-8FX showing multiple depositional environments.

Middle Mesaverde Upper Fluvial Interval Vectors Plotted on Isopach Map

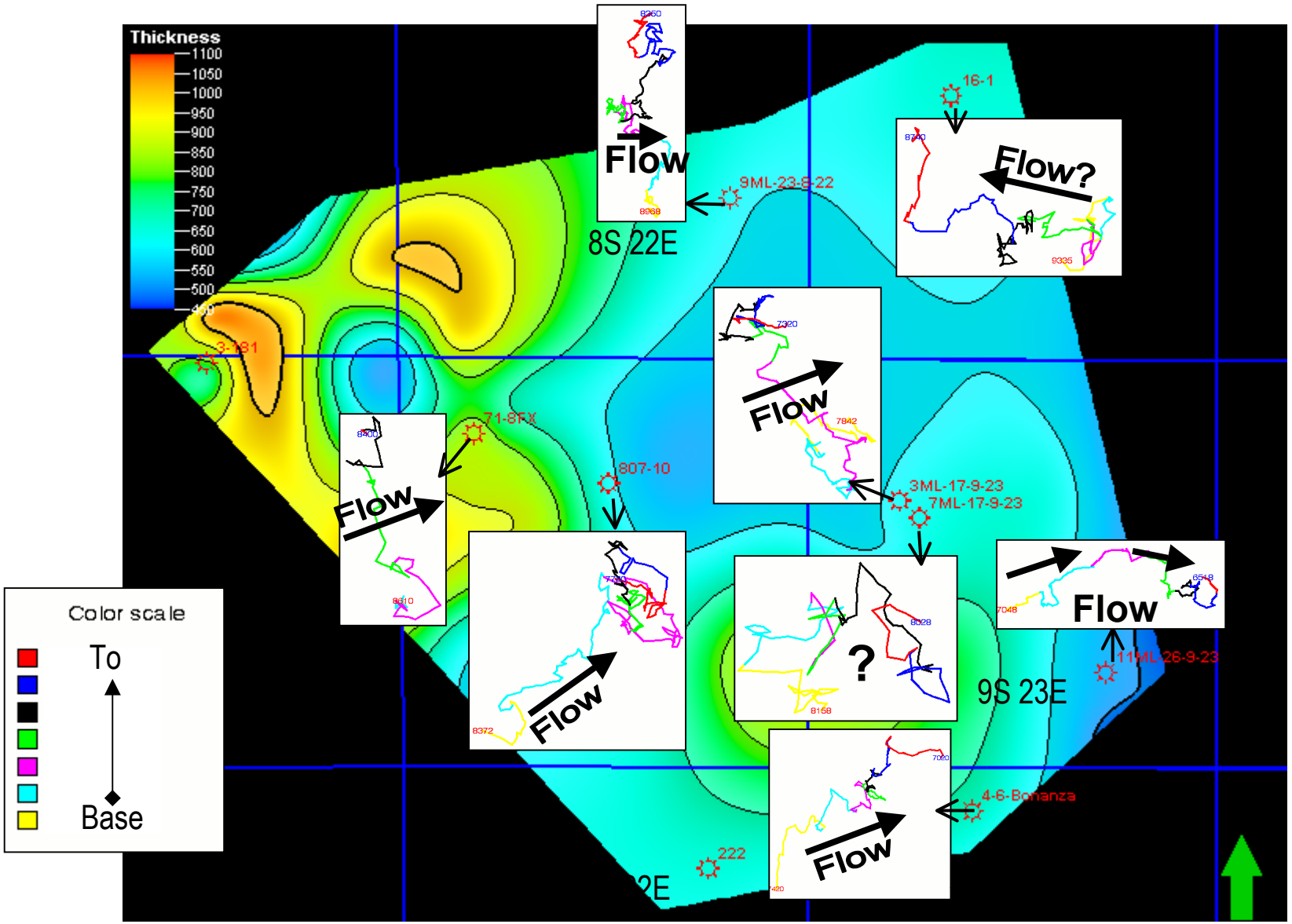

Figure 56. Vector plots for the Upper Fluvial Interval showing dominant flow directions to the northeast in most study wells.

Upper Cretaceous Paleogeography ~75 Million Years Ago

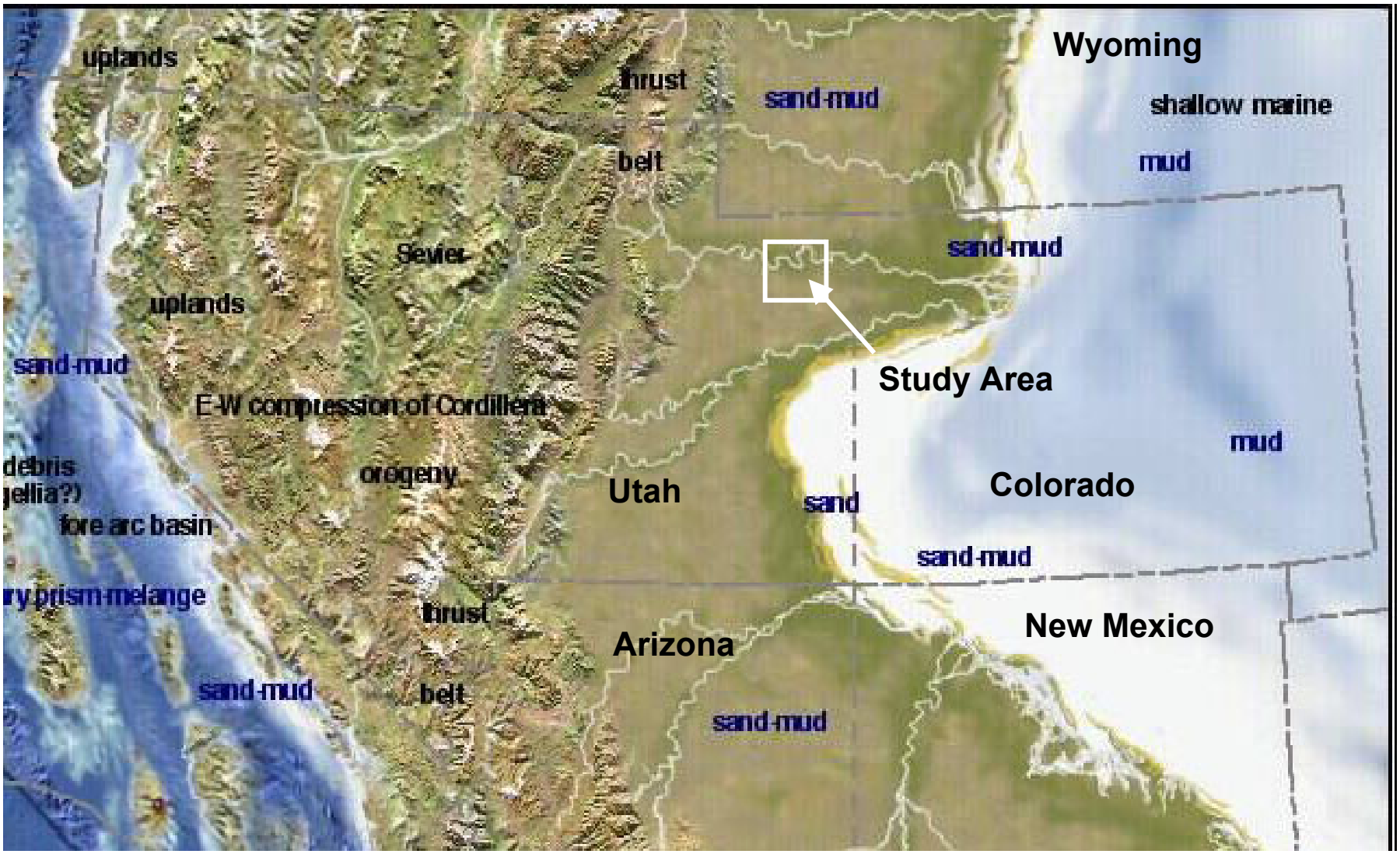

From Blakey, 1997, at http://jan.ucc.nau.edu/~rcb7/paleogeogrwus.html

Figure 57. Paleogeographic reconstruction of the western U.S. during Late Cretaceous time about 75 million years ago. Study area is shown.

Middle Mesaverde Braided Stream Interval Vectors Plotted on Isopach Map

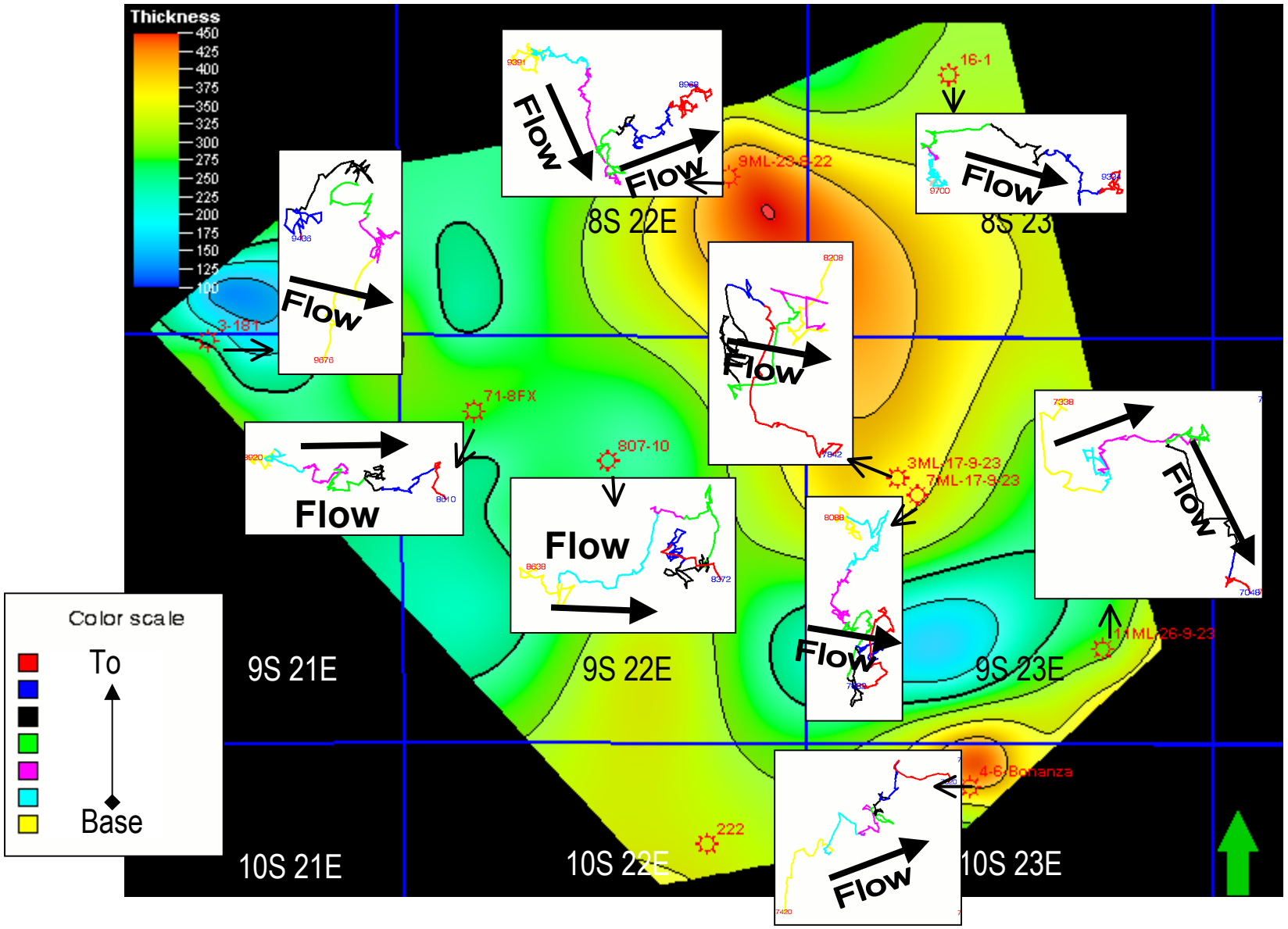

Figure 58. Vector plots for the Braided Stream Interval showing dominant flow directions to the east in most study wells.

Lower Mesaverde Upper Coaly Interval Vectors Plotted on Isopach Map

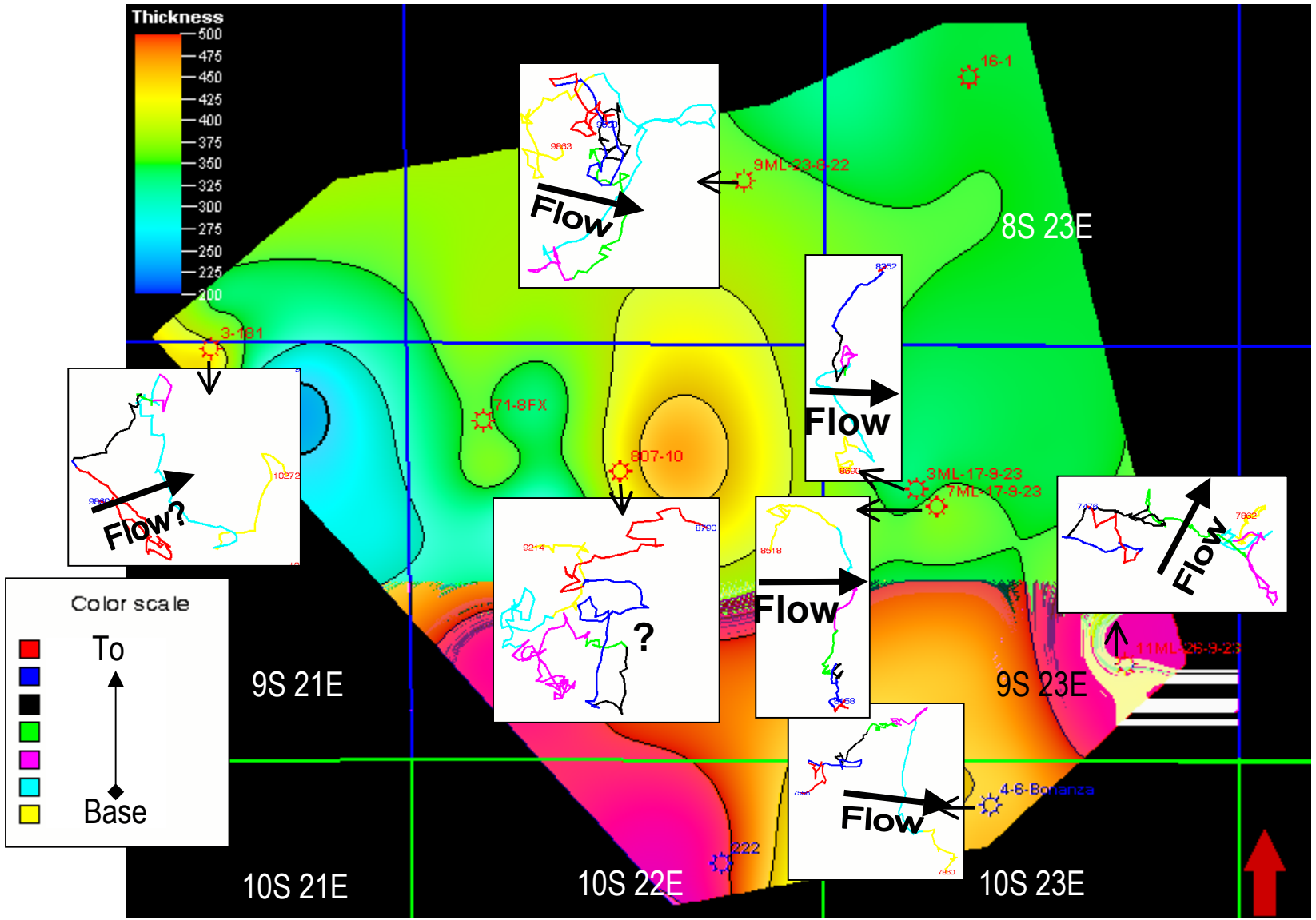

Figure 59. Vector plots for the Upper Coaly Interval showing variable fluid flow directions in the rivers present in the study area.

Shoreline Trends on Blocky Sego Sandstone Plotted on Isopach Map

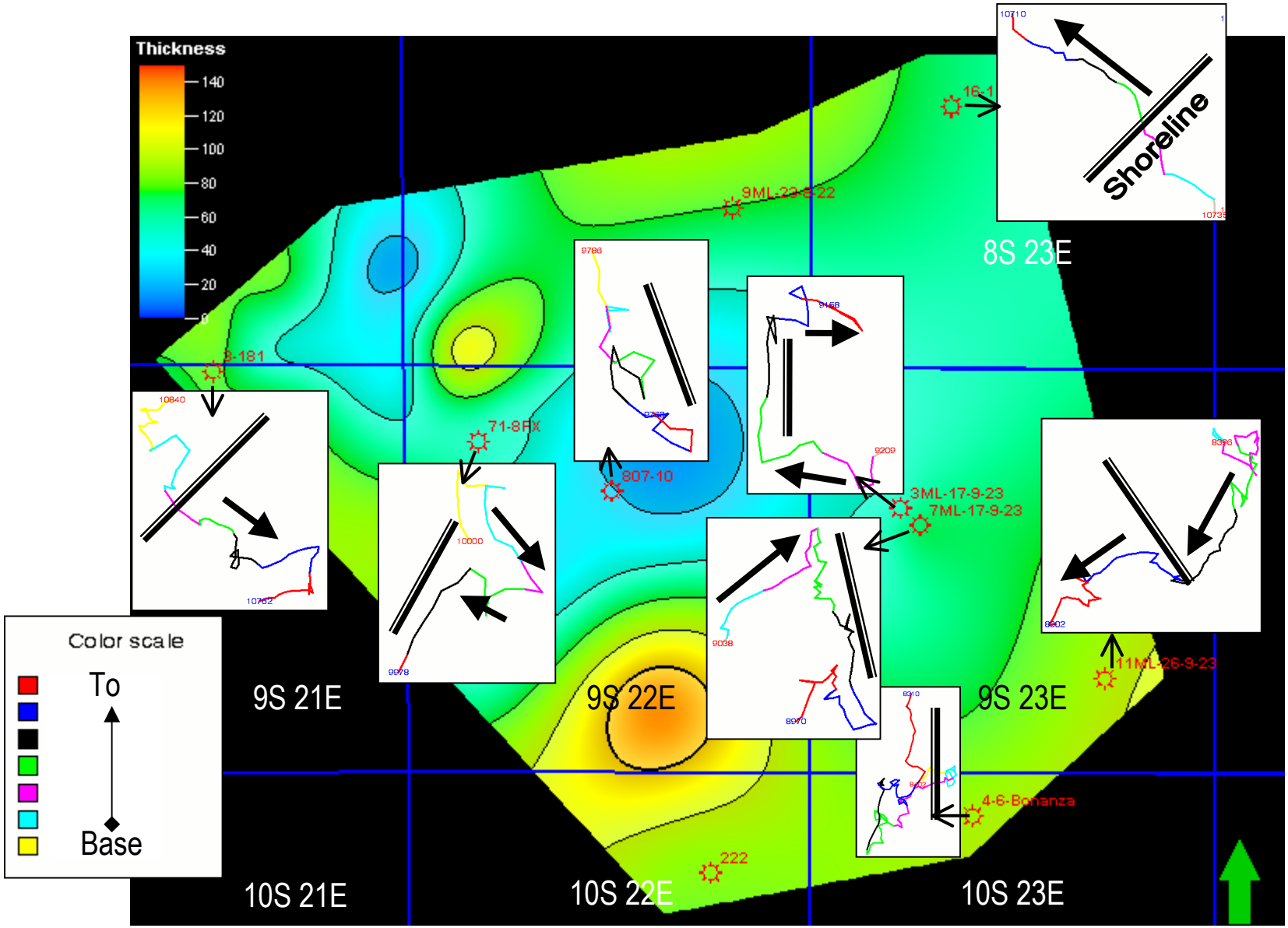

Figure 60. Shoreline trends (parallel black lines), progradation (east-pointing arrows), and backstepping in the Blocky Sego Sandstone.

Castlegate Sandstone Vector Plots on Isopach Map

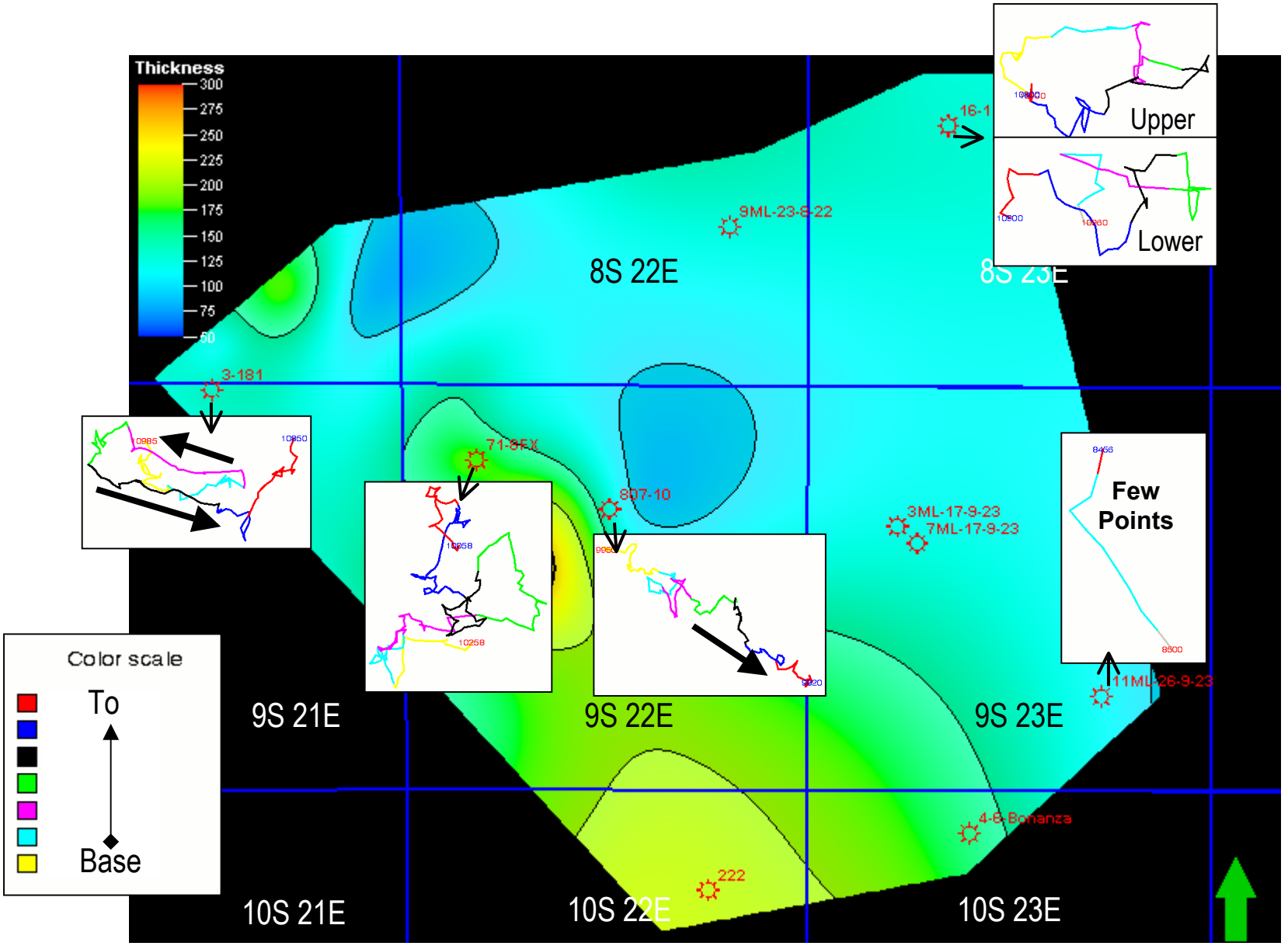

Figure 61. Vector plots for the Castlegate Sandstone showing diverse patterns due to multiple marine and non-marine environments.

Using Image Logs to Define Fracture Trends

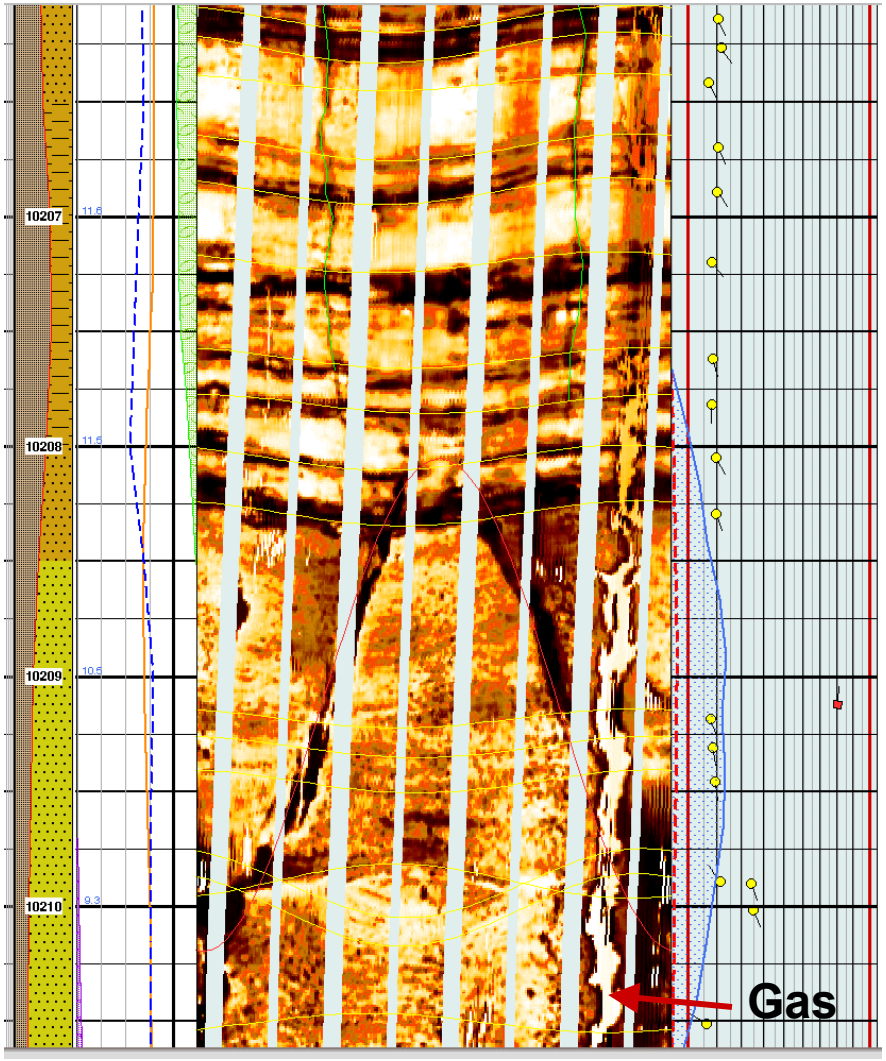

9ML-23-8-22, 10,206-10,210 ft
Open Fracture in Lower Neslen SS

Image Logs Reveal Open Fractures with Apertures Down to a few Microns
Aperture Width can be Calculated
Fracture Orientation and Dip can be Quantified
Fracture Abundance and Porosity can be Quantified and Corrected for Well Bore Drift

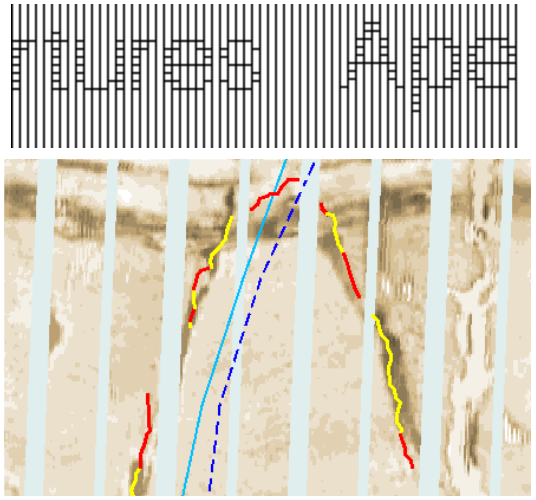

Figure 62. Use of image logs to define fracture trends with an example of a natural fracture in the Lower Neslen, 9ML-23-8-22 well.

Fracture Orientation and Abundance in the Upper Mesaverde Interval

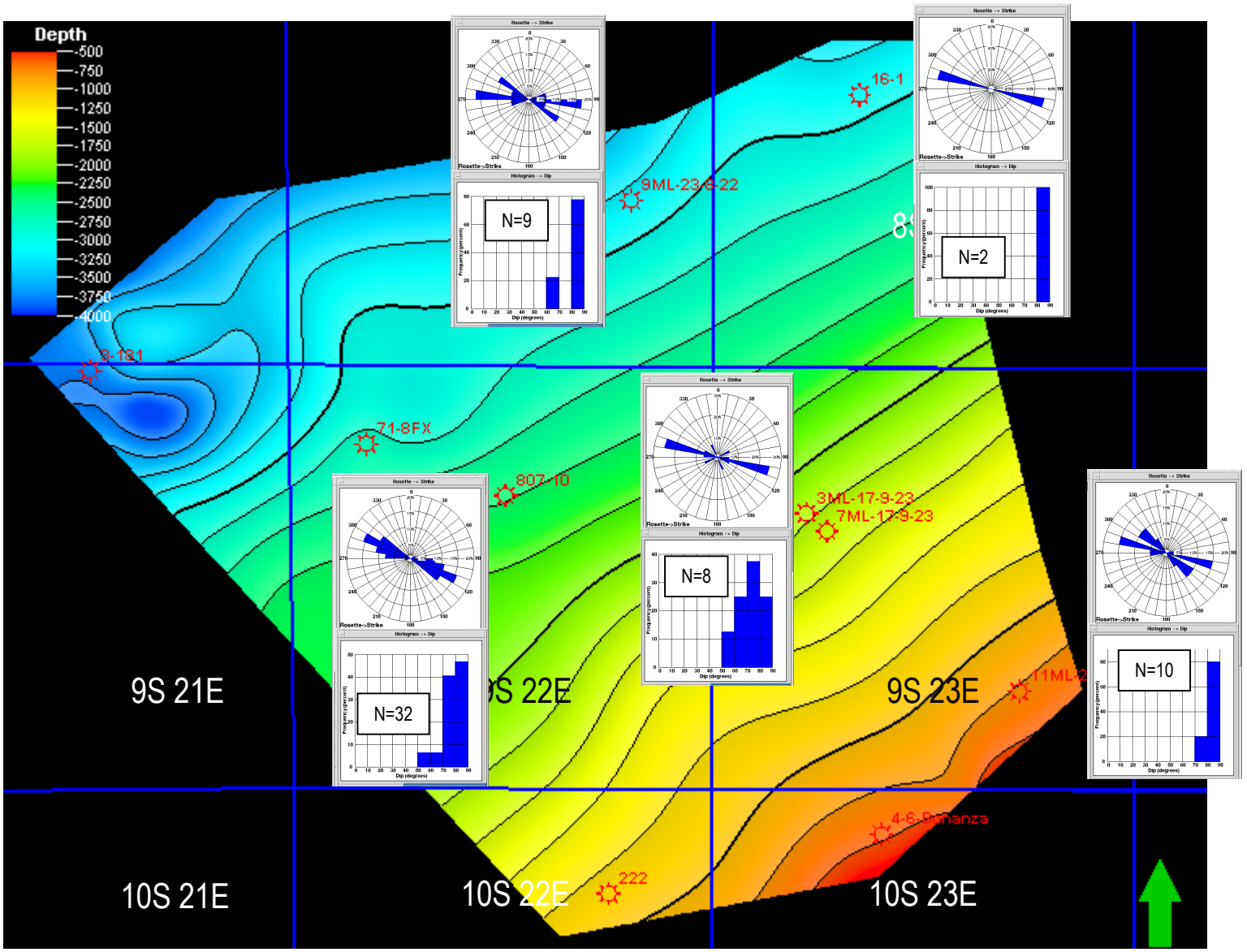

Figure 63. Rose diagrams and dip histograms for fractures in the Upper Mesaverde Interval in the study wells with images across this interval.

Fracture Orientation and Abundance in the Middle Mesaverde Upper Fluvial Interval

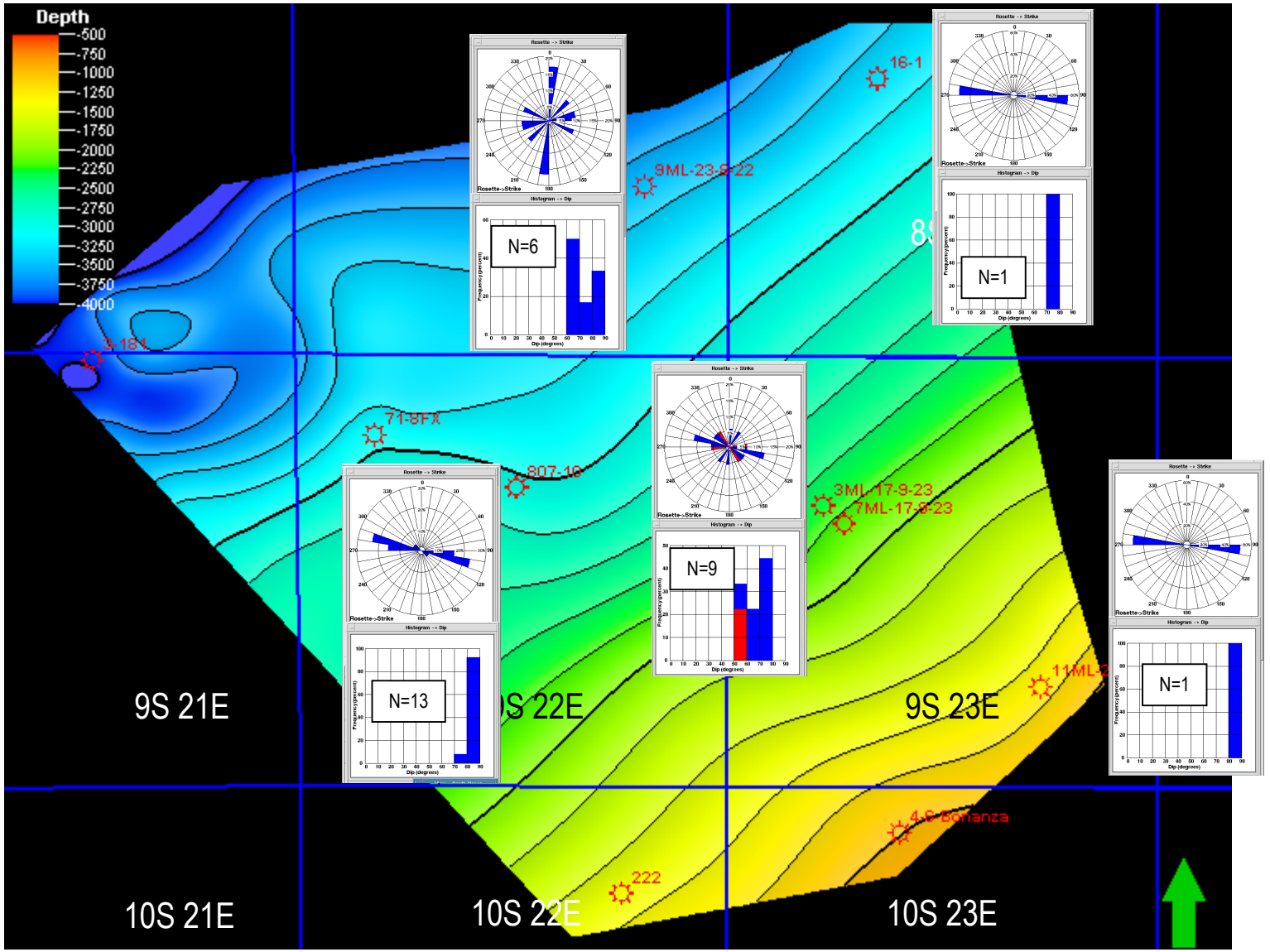

Figure 64. Rose diagrams and dip histograms for fractures in the Upper Fluvial Interval in the study wells with images across this interval.

Fracture Orientation and Abundance in the Middle Mesaverde Braided Stream Interval

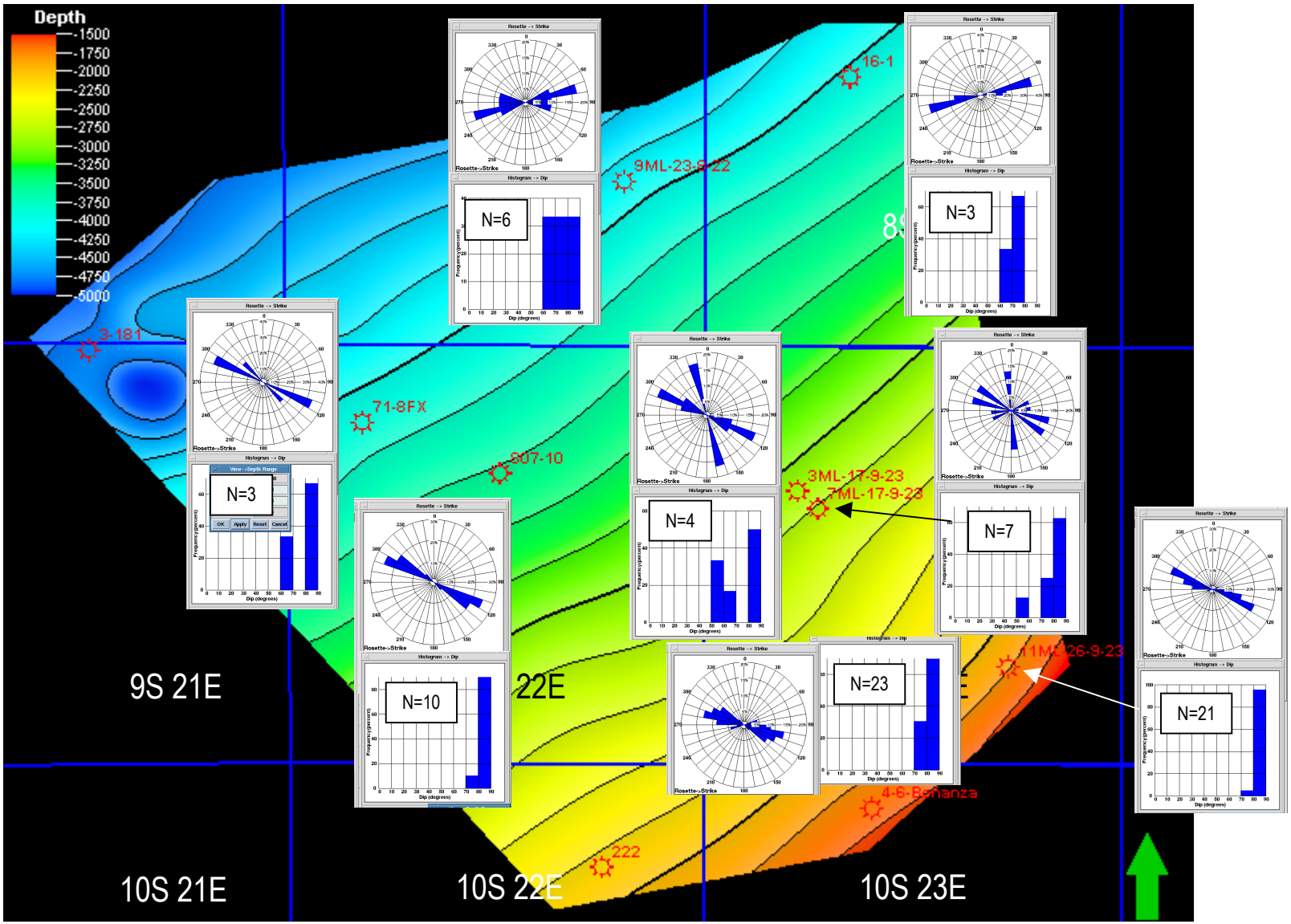

Figure 65. Rose diagrams and dip histograms for fractures in the Braided Stream Interval in the study wells with images across this interval.

Fracture Orientation and Abundance in the Middle Mesaverde Lower Fluvial Interval

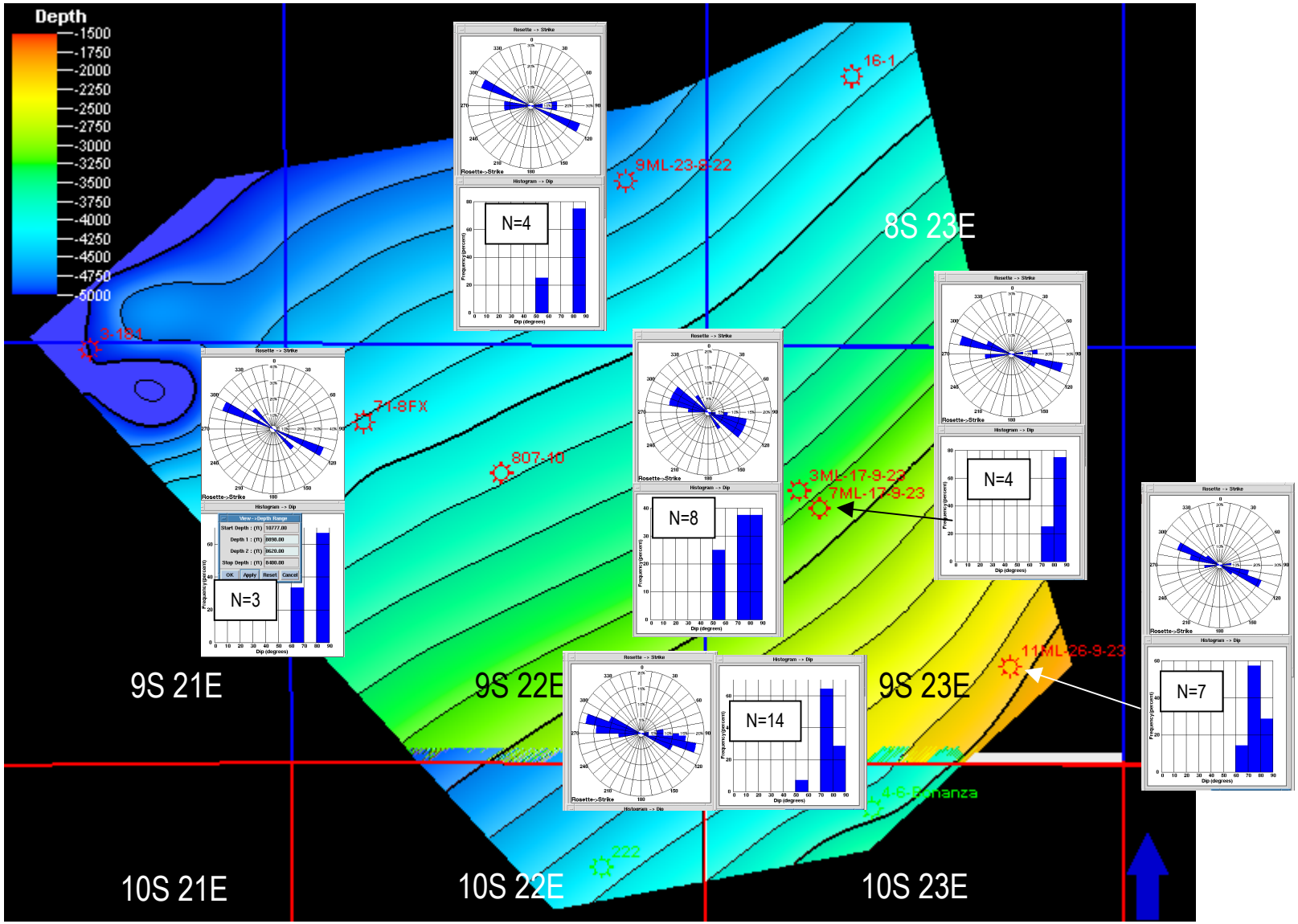

Figure 66. Rose diagrams and dip histograms for fractures in the Lower Fluvial Interval in the study wells with images across this interval.

Fracture Orientation and Abundance in the Lower Mesaverde Upper Coaly Interval

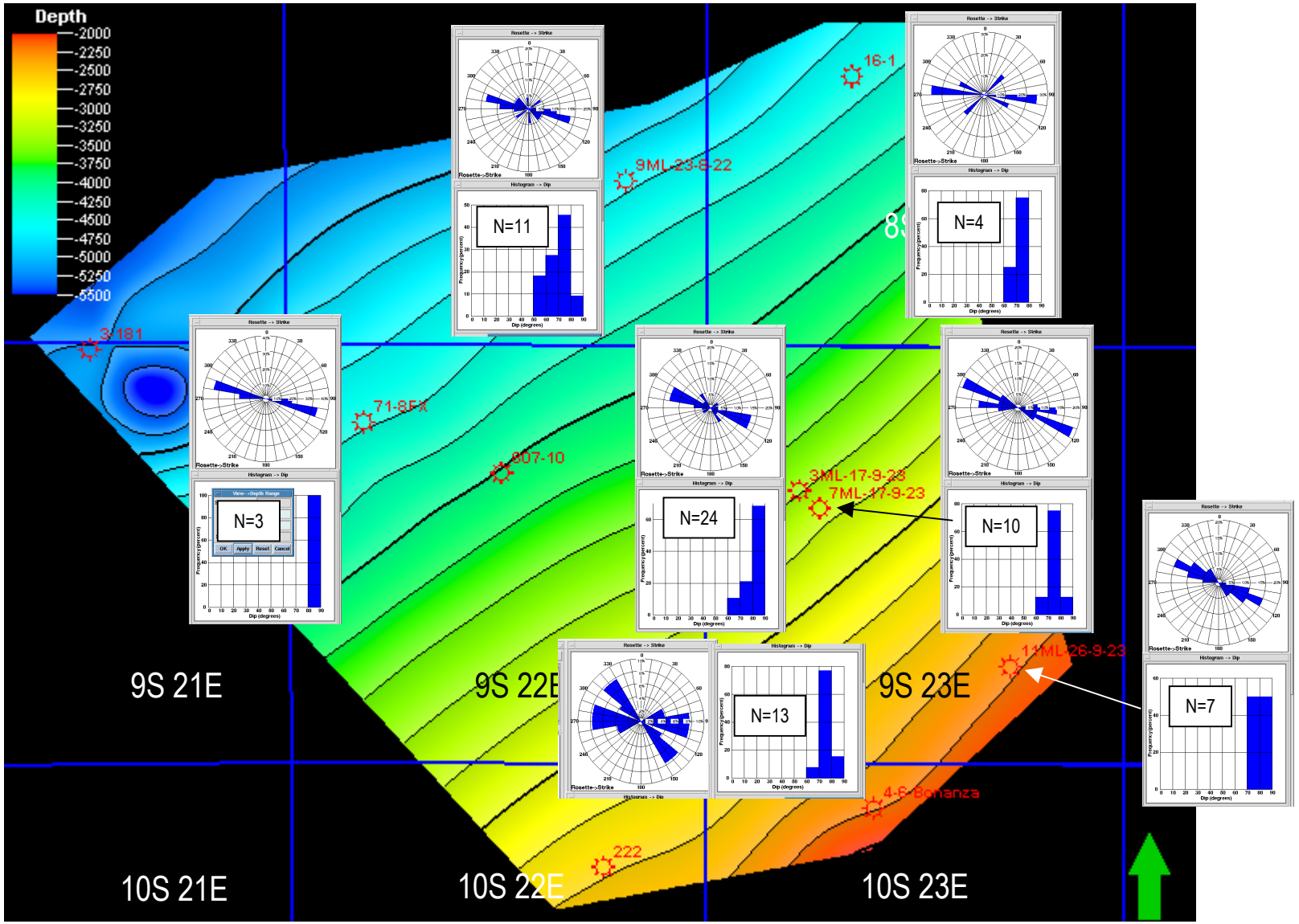

Figure 67. Rose diagrams and dip histograms for fractures in the Upper Coaly Interval in the study wells with images across this interval.

Fracture Orientation and Abundance in the Lower Mesaverde Middle Neslen Interval

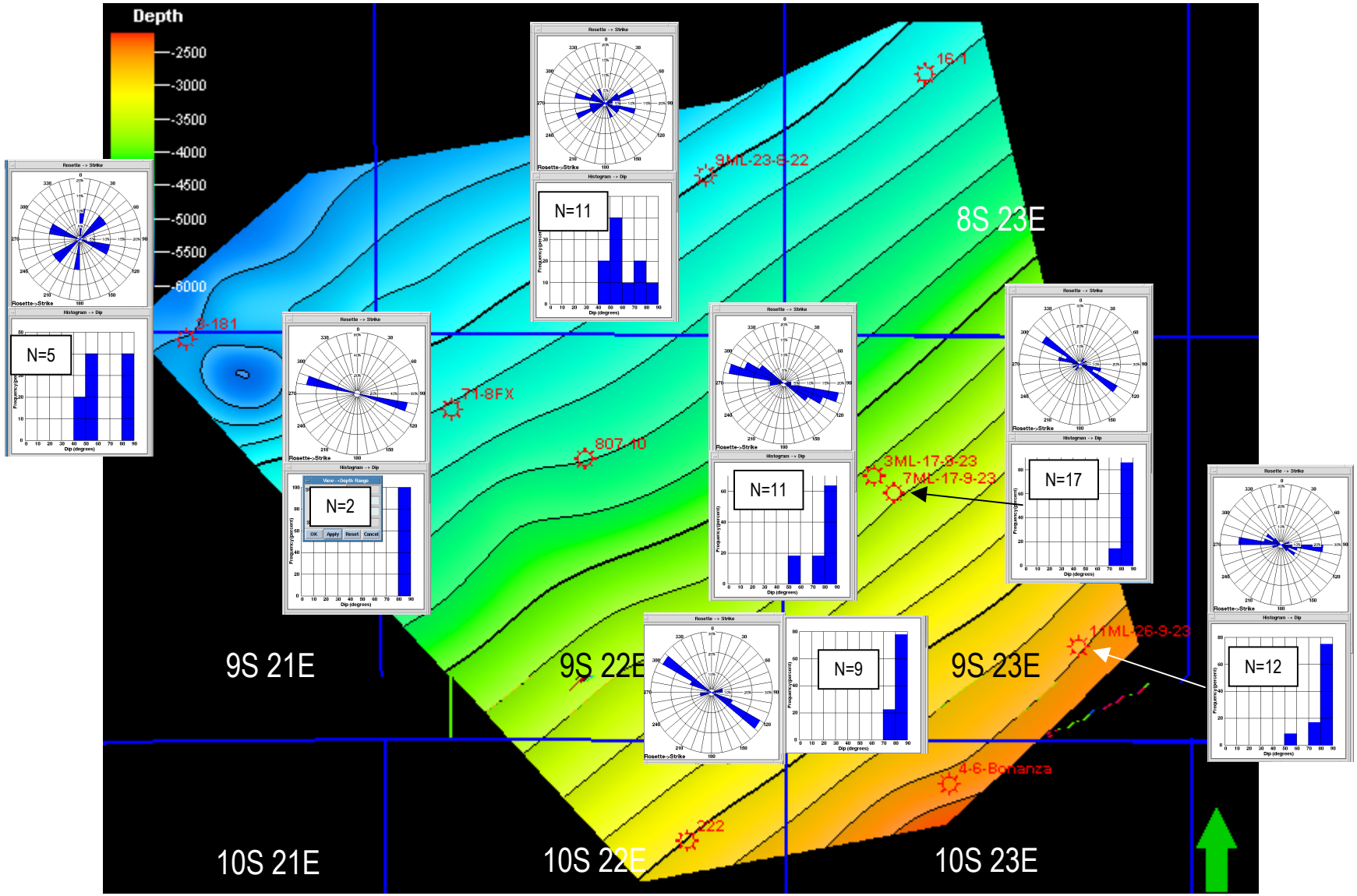

Figure 68. Rose diagrams and dip histograms for fractures in the Middle Neslen Interval in the study wells with images across this interval.

Fracture Orientation and Abundance in the Lower Mesaverde Lower Neslen Interval

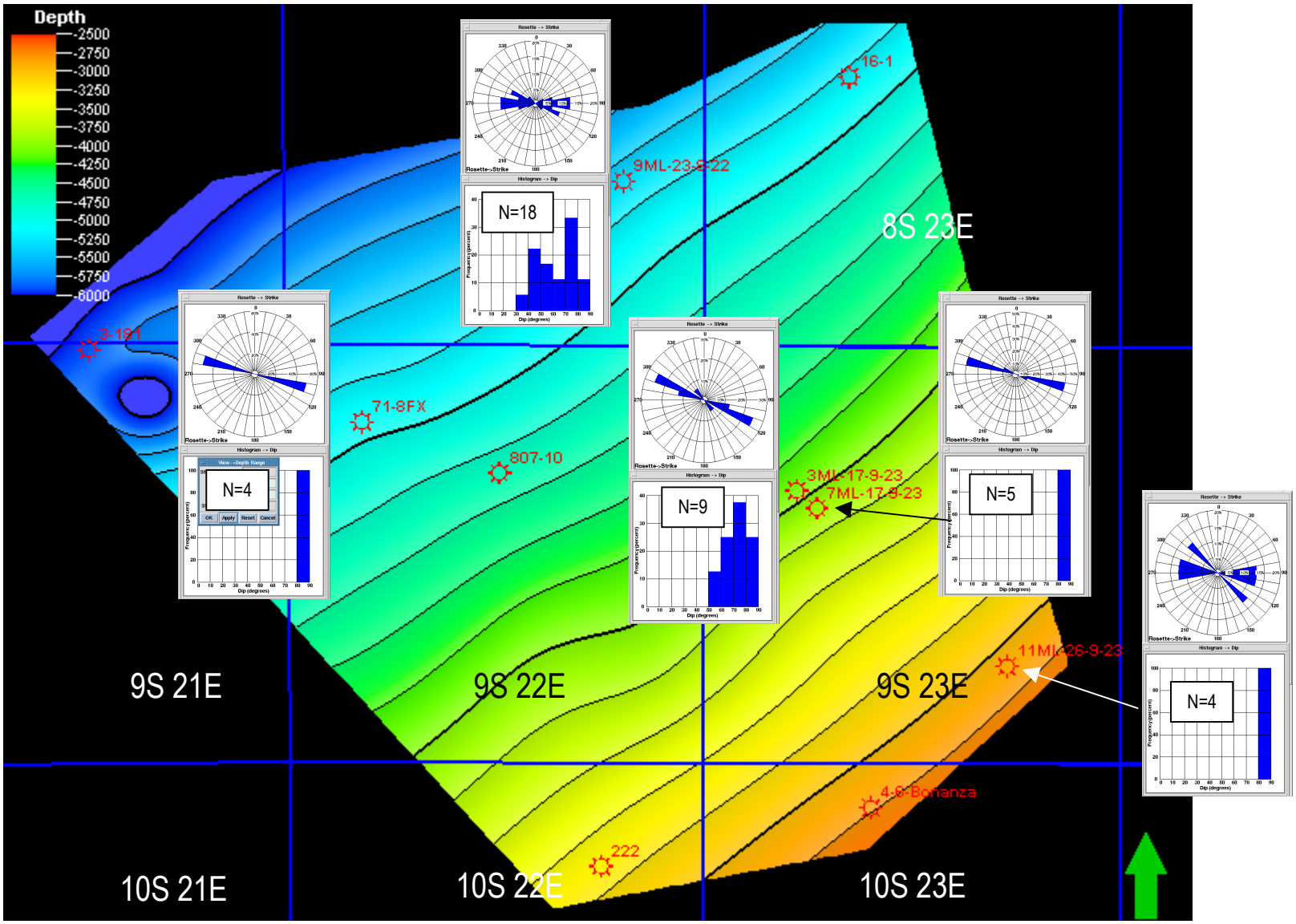

Figure 69. Rose diagrams and dip histograms for fractures in the Lower Nelsen Interval in the study wells with images across this interval.

Fracture Orientation and Abundance in the Blocky Sego Sandstone Interval

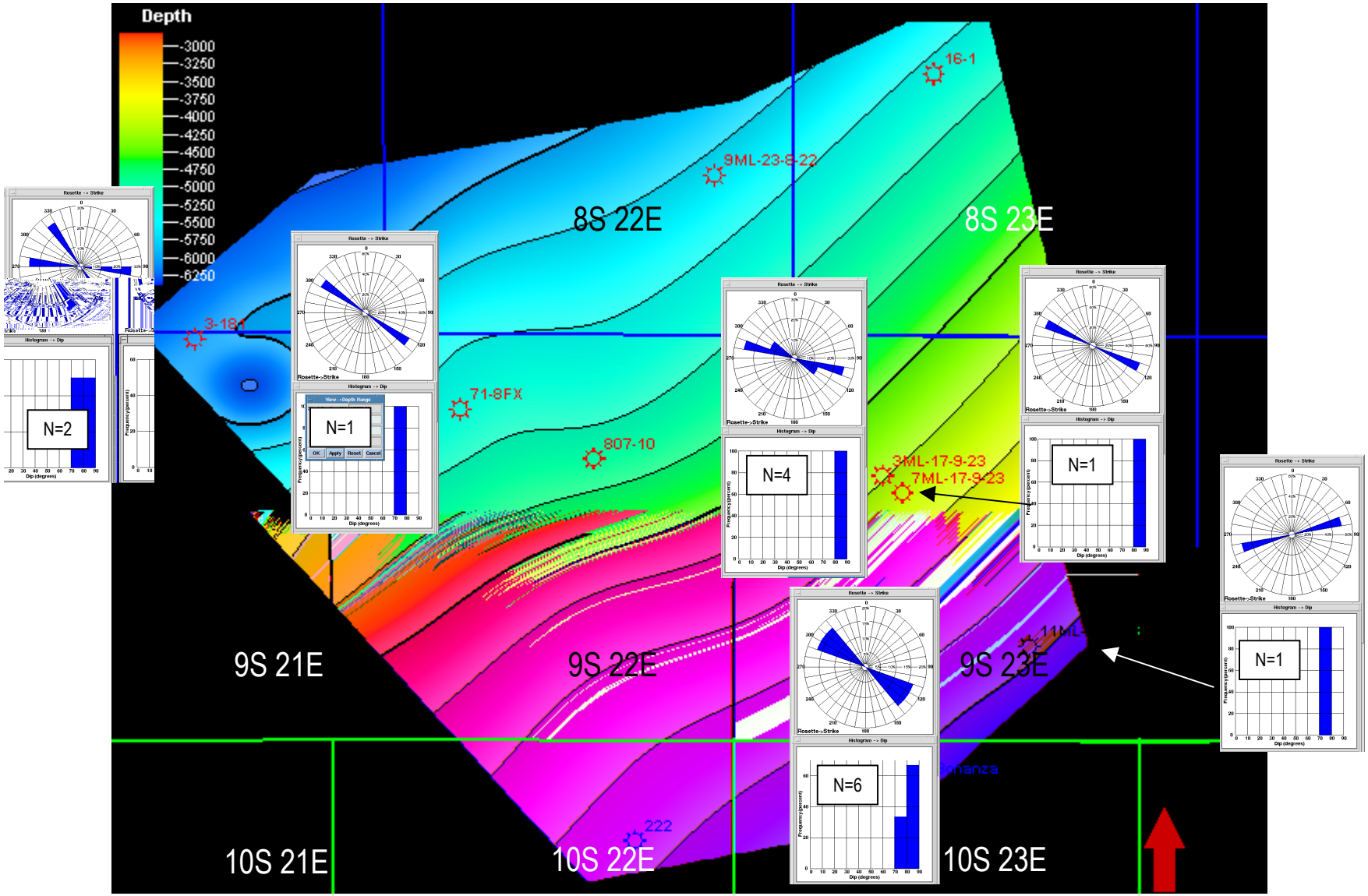

Figure 70. Rose diagrams and dip histograms for fractures in the "Blocky" Sego shoreline sand in the wells with images across this interval.

Defining Gas Reservoirs with Image Logs

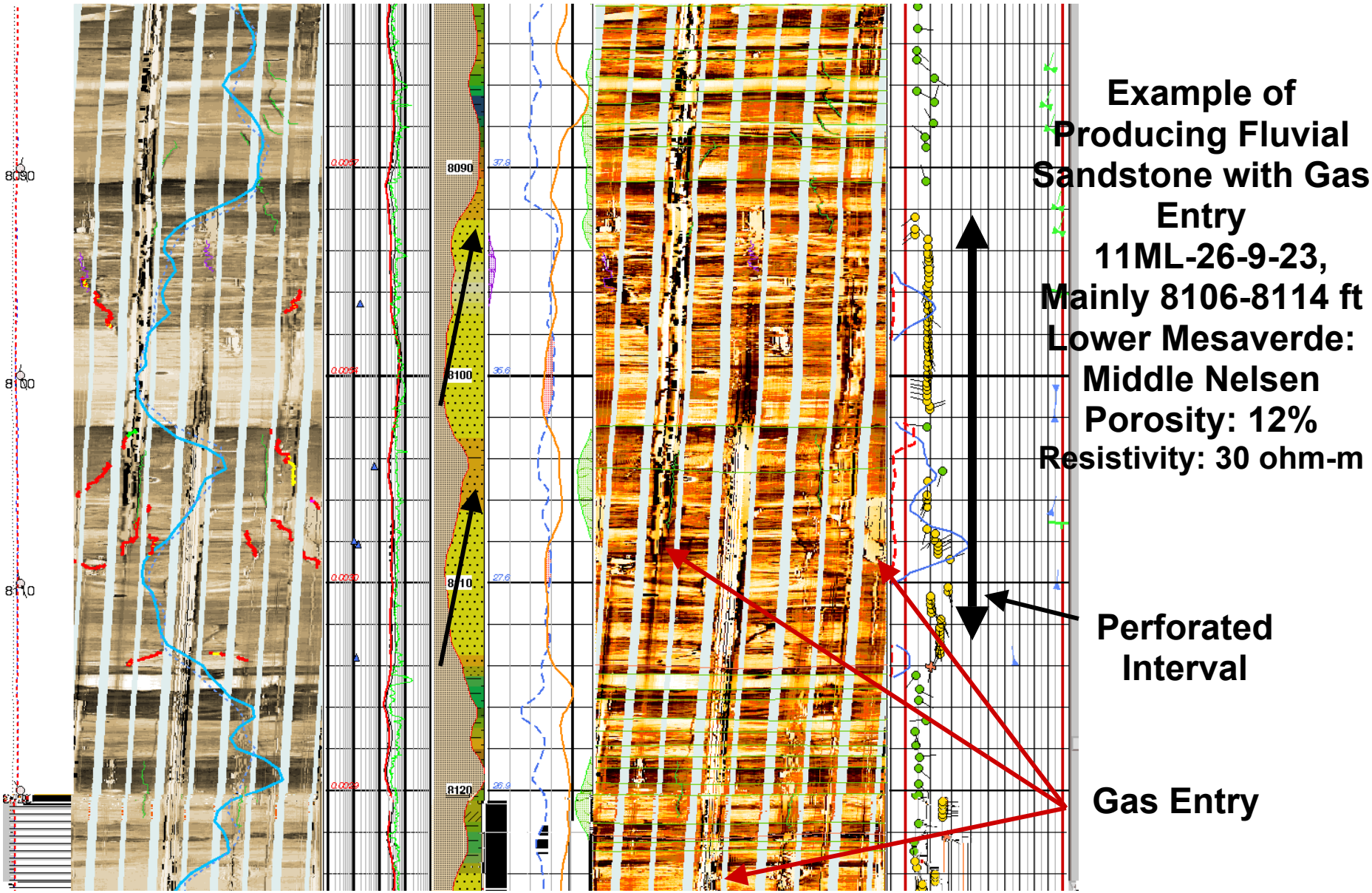

Figure 71. Gas-producing fluvial channel sandstones in the Middle Neslen Interval in the 11ML-26 well with good gas entry on some pads.

Example of Productive Fluvial Channel Sandstone, Upper Fluvial Interval, Middle Mesaverde

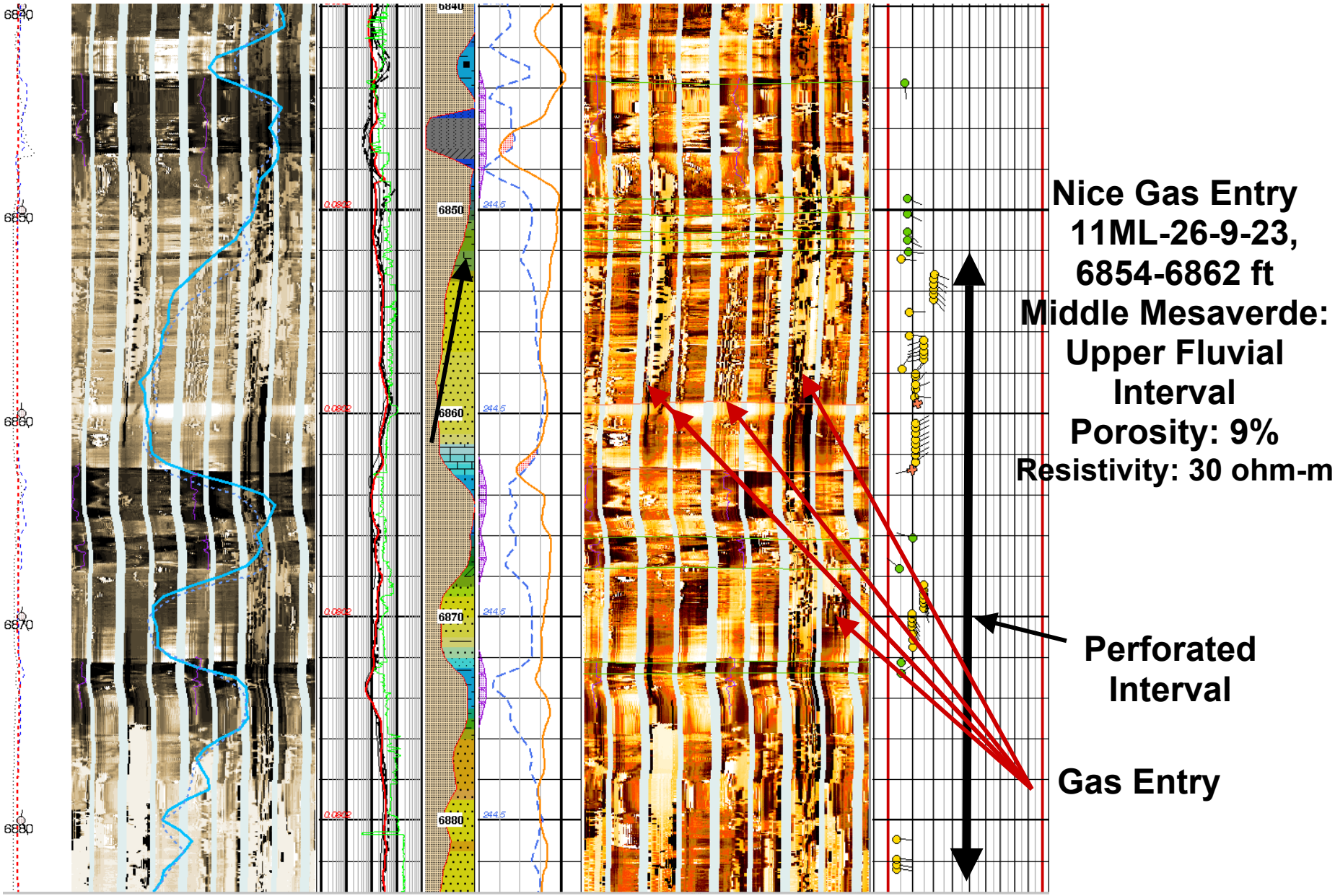

Figure 72. Gas-producing fluvial channel sandstones in the Middle Mesaverde in the 11ML-26 well with good gas entry on some pads.

Example of Productive Fluvial Channel Sandstone, Upper Fluvial Interval, Middle Mesaverde

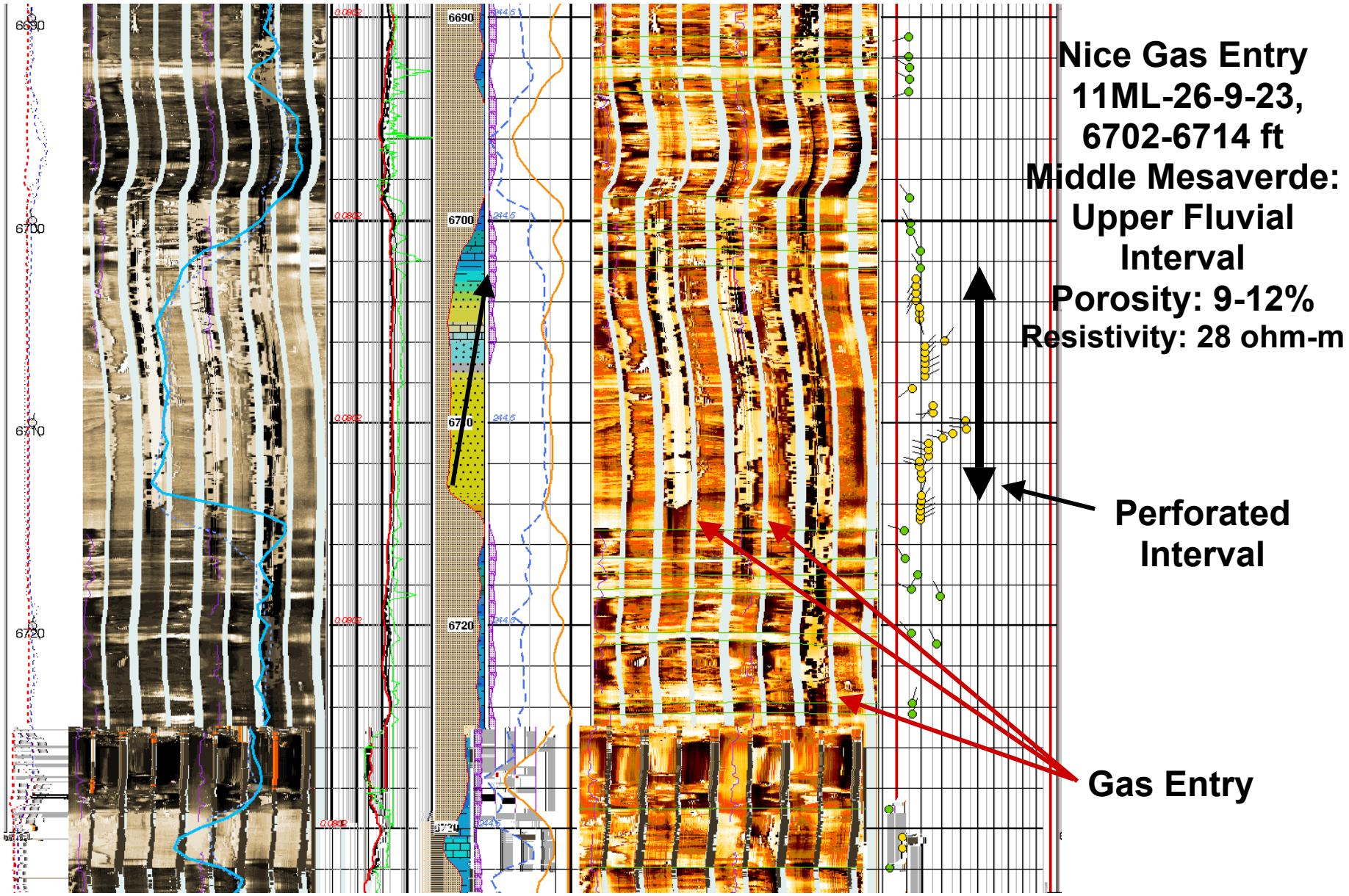

Figure 73. Gas-producing fluvial channel sandstones in the Middle Mesaverde in the 11ML-26 well with good gas entry on some pads.

Example of Possible "Regurgitated" Gas from a Braided Stream Sandstone, Upper Mesaverde

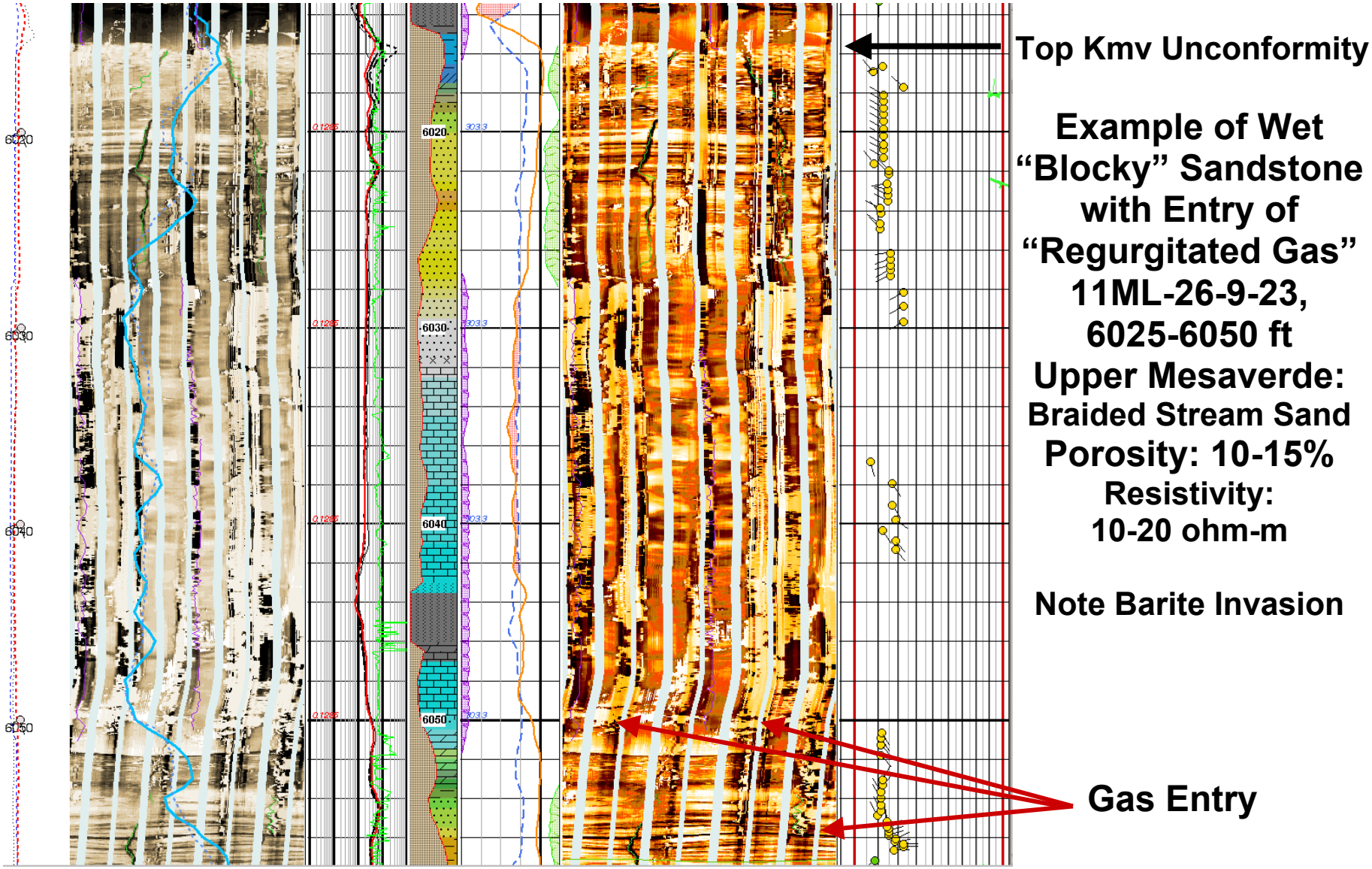

Figure 74. Example of diffuse "regurgitated" gas coming from an invaded interval in the Upper Mesaverde in the 11ML-26 well.

Example of Possible “Regurgitated” Gas from a Fluvial Channel Sandstone, Upper Mesaverde

False Dolomite Lithology due to Barite Invasion in Drilling Mud

“Regurgitated” Gas Entry
11ML-26-9-23, 6334-6346 ft
Upper Mesaverde Fluvial Sandstone
Porosity: 10%
Resistivity: 10 ohm-m

Gas Entry

Figure 75. Closer view of diffuse “regurgitated” gas coming from the same invaded interval in the Upper Mesaverde in the 11ML-26 well.

Example of Possible "Regurgitated" Gas from a Fluvial Channel Sandstone, Upper Mesaverde

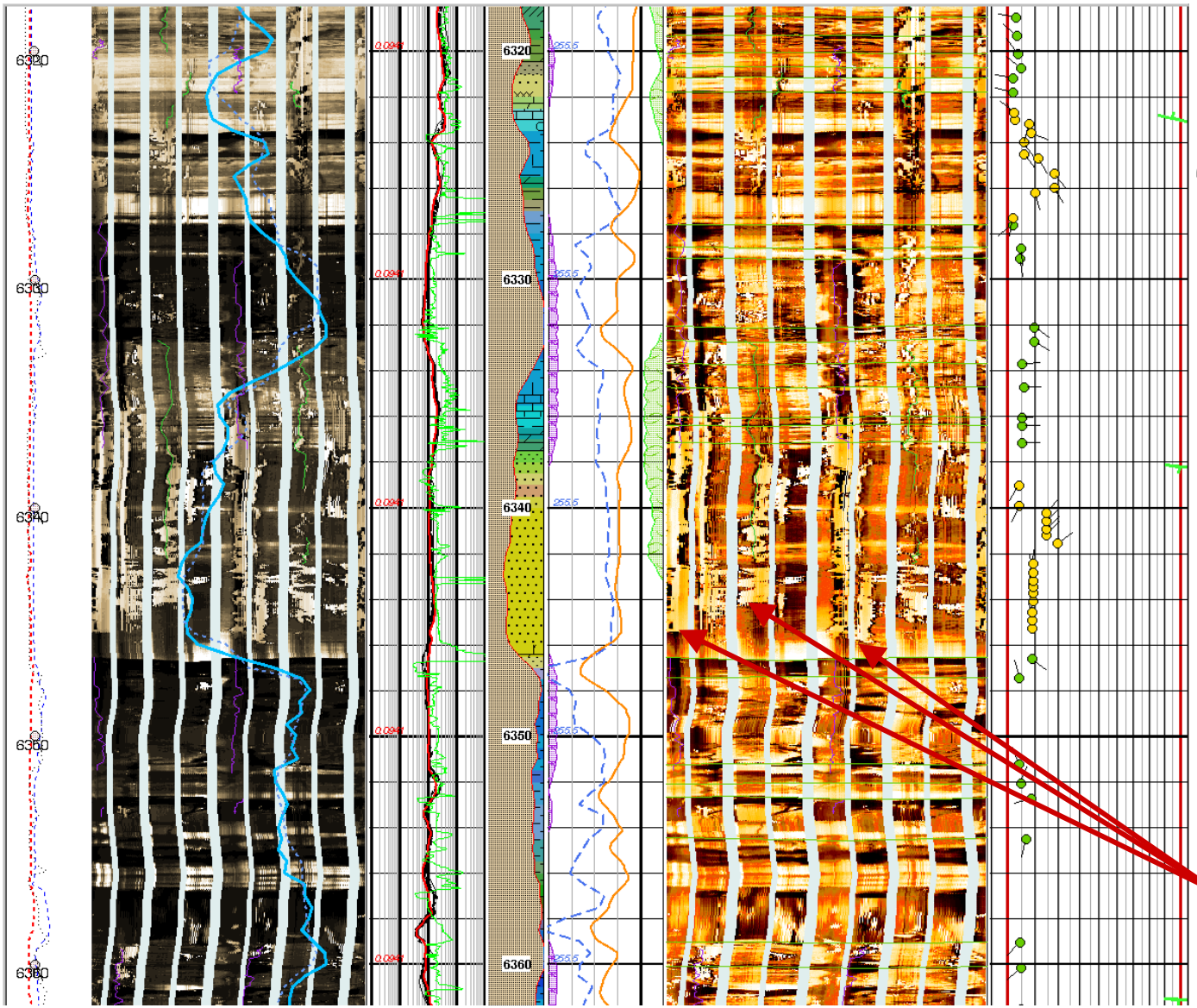

Figure 76. Another example of diffuse "regurgitated" gas coming from an invaded interval in the Upper Mesaverde in the 11ML-26 well.

Nature of the Mesaverde/Wasatch Contact on an Image Log, 11ML-26-9-23 Well

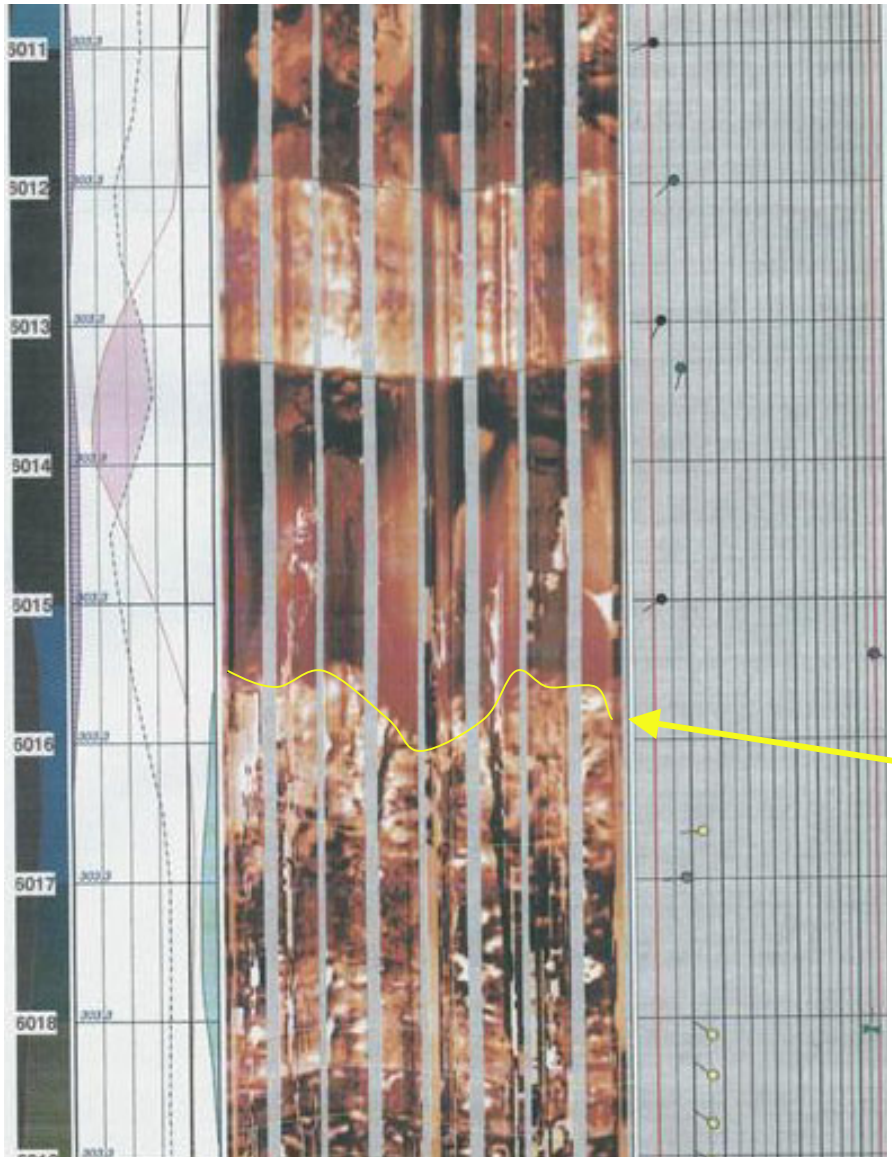

Figure 77. Image log across what is interpreted to be the contact between rooted uppermost Mesaverde in the 11ML-26 well and shales of the Wasatch Formation.

Nature of the Mesaverde/Wasatch Contact on Another Image Log, Westport Tribal 36-148 Well

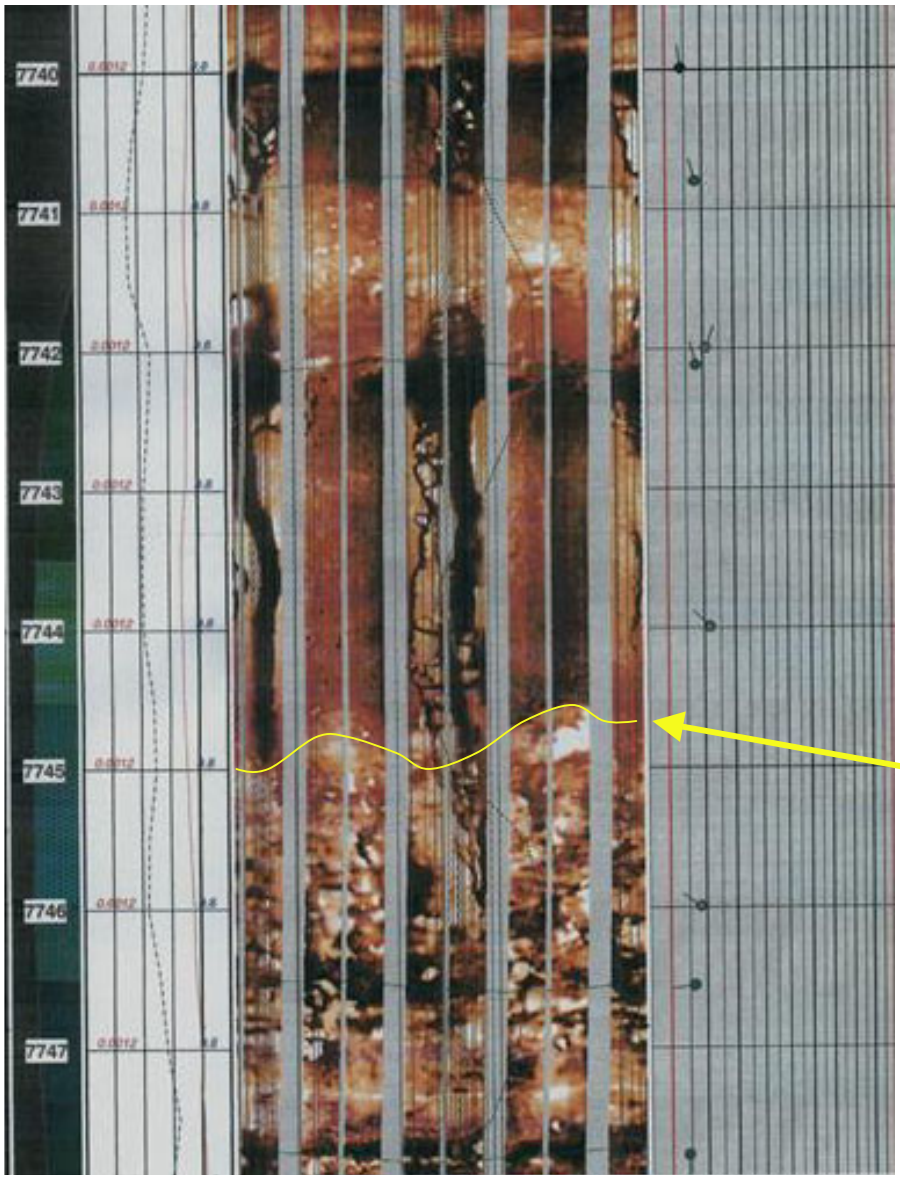

Figure 78. Image log showing another example of the interpreted contact between uppermost Mesaverde rocks and shales of the Wasatch Formation in the 36-148 Tribal well.